Electronic Supplementary Material (ESI) for ChemComm.
This journal is © The Royal Society of Chemistry 2022

SUPPLEMENTARY INFORMATION

Cyanine-Flavonol Hybrids as NIR-Light Activatable Carbon Monoxide Donors in Methanol and Aqueous Solutions

Qiuyun Yang,[a,b] Lucie Muchová,[c] Lenka Štacková,[a,b] Peter Štacko,[a,b] Vladimir Šindelář,[a,b] Libor Vítek,[c] Petr Klán*[a,b]

[a] Department of Chemistry, Faculty of Science, Masaryk University, Kamenice 5, Brno, Czech Republic
[b] RECETOX, Faculty of Science, Masaryk University, Kamenice 5, Brno, Czech Republic
[c] Institute of Medical Biochemistry and Laboratory Diagnostics General Faculty Hospital and 1st Faculty of Medicine Charles University, Na Bojišti 3, Praha 2, Czech Republic
* Email: klan@sci.muni.cz

Contents

Materials and Methods

Reagents and solvents of the highest purity available were used as purchased, or they were purified/dried using standard methods when necessary. UV-vis spectra and the molar absorption coefficients were measured on a UV−vis spectrometer with matched 1.0 cm quartz cuvettes. The molar absorption coefficients were determined from the absorption spectra (the average values were obtained from 4 independent measurements with solutions of different concentrations). Emission spectra were measured on an automated luminescence spectrometer in 1.0 cm quartz fluorescence cuvettes at 23 ± 1 °C. The corresponding optical filters were used to avoid the second harmonic excitation/emission bands induced by the grating. Sample concentrations with the absorbance ~ 0.1 at the absorption maxima were used. Each sample was measured ten times, and the spectra were averaged. Emission spectra were normalized. ^{1}H NMR spectra were recorded on 300 or 500 MHz instruments; ^{13}C NMR spectra were obtained on 75 or 125 MHz instruments in CD_3OD, D_2O, d_6-DMSO, or their mixtures.

General Procedure for Irradiation in UV Cuvettes. A prepared solution in the given solvent (3 mL) in a matched 1.0 cm quartz cuvette equipped with a stirring bar was stirred and irradiated with a light source of 32 LEDs (λ_{irr} = 770 nm). The reactions were monitored at the given time intervals by UV-vis spectroscopy.

Determination of CO Yields. Stock solutions of **3**−**8** were prepared in DMSO, methanol, or PBS. The given amount of a stock solution was inserted into a volumetric flask and diluted to 5 mL with methanol or PBS (pH 7.4, 10 mM, I = 100 mM) to give the final concentration of $c = 1.0 \times 10^{-5}$ M. The solutions (0.5 mL) in closed GC vials fitted with PTEE septa were irradiated with LEDs at 770 nm to complete conversion. The released CO was analyzed and quantified by a GC-headspace technique, which was calibrated using the quantitative CO release of cyclopropenone photoCORM (25−200 μL, $c \sim 1 \times 10^{-5}$ M, methanol).[1]

Quantum Yields of CO Release. Solutions of **3**−**8** in methanol (without or with different amounts of DMSO; 1000 μL, $c \sim 2 \times 10^{-5}$ M) in closed GC vials fitted with PTFE septa were irradiated by a xenon lamp equipped with a monochromator set to 750 or 755 nm. The samples were irradiated through the bottom of the vial to minimize the reflection of light. The absolute photon flux was measured by a calibrated Si-photodiode. The total amount of the released CO was quantified by GC-headspace.

Quantum Yields of Singlet Oxygen Production. Solutions of 1,3-diphenylisobenzofuran (DPBF; $c = 7.9 \times 10^{-5}$ M) and one of **3**−**8** ($c \sim 1 \times 10^{-6}$ M) or indocyanine green (ICG) as a sensitizer ($c = 1 \times 10^{-6}$ M) in methanol (without or with different amounts of DMSO) was prepared. The stirred solution (3.0 mL) in a quartz cell was irradiated using LEDs at 770 nm, and the UV−vis spectra were recorded every 1 s. The irradiation time was selected to reach ~10% conversion of DPBF. The procedure was repeated three times. The decomposition of DPBF monitored at 411 nm was fitted with a pseudo-first-order rate law, and the singlet oxygen production quantum yield Φ_Δ was calculated using ICG as the reference (Φ_Δ = 0.008[2]).

Reaction Rate Constants of Compounds 3−8 with Singlet Oxygen. The determination used a reporoom temperatureed procedure.[3] A solution containing **3**−**8** ($c = 6 \times 10^{-6}$ M) or reference compound **1a**[3] with rose bengal ($c \sim 5 \times 10^{-6}$ M) as a triplet sensitizer in methanol was stirred and irradiated at 545 nm. The decomposition of **3**−**8** was recorded at the given intervals using UV−vis absorption spectroscopy. The irradiation time was selected to reach ~10% conversion of **3**−**8** (more than 10 experimental points). The procedure was repeated three times. The bimolecular reaction rate constant (k_{so}) for **3**−**8** with singlet oxygen was calculated using the known rate constant of singlet oxygen quenching in methanol ($k_d = 9.7 \times 10^4$ s^{-1}) and the bimolecular reaction rate constant of **1a** with singlet oxygen ($k_d = 7.1 \times 10^6$ M^{-1} s^{-1}).

Quantum Yields of Decomposition. The decomposition caused by self-sensitization depends on both the concentration of one of **3**−**8** and the rate of the reaction with singlet oxygen (k_{SO}). The quantum yield of decomposition was calculated using the following equation:[3]

$$\phi_d \sim \phi_\Delta \frac{k_{SO} c_0}{k_d + k_{SO} c_0}$$

where ϕ_Δ is the quantum yields of singlet oxygen production of **3**−**8**, and k_{SO} is the bimolecular reaction rate constant of **3**−**8** with $^1O_2$, c_0 is the initial concentration of **3**−**8**, and k_d is the known rate constant of singlet oxygen quenching in methanol ($k_d = 9.7 \times 10^4\ s^{-1}$).

Cytotoxicity Determination. The human hepatoblastoma HepG2 cell line (ATTC, Manassas, VA, USA) and terminally differentiated hepatic cells derived from a human hepatic progenitor cell line HepaRG (Gibco, Waltham, MA, USA) were cultured in supplemented MEM or William´s media according to the manufacturer´s instructions in a humidified atmosphere containing 5% CO_2 at 37 °C. For toxicity assessment, cells were seeded into 96-well plates, and MTT (3-(4,5-dimethylthiazol-2-yl)-2,5-diphenyltetrazolim bromide) reduction assay was performed as described before.[4]

Fluorescence Microscopy Experiments. HepaRG cells were seeded into a 48-well plate and incubated with 100 μM of a hybrid (**3**−**8**). After incubation, cells were washed with PBS and visualized using fluorescent microscopy (Olympus IX 51 with a mercury burner U-RFL-T, Olympus, Japan) with a WIG emission filter. The fluorescence intensity of cyanine-flavonol compounds (c = 100 μmol L^{-1}) was determined using a multi-detection microplate reader (Synergy HT, BioTek, Winooski, VT, USA) at λ_{ex} = 530 nm and λ_{em}= 590 nm.

CO Determination in Cell Cultures. HepaRG cells were seeded into a 10-cm Petri dish and incubated with 10 mL of colorless supplemented MEM medium containing one of **3**−**8** (c = 50 μmol L^{-1}) in the dark or irradiated with white light (LED, I = 600 mW cm^{-2}). The medium without active compounds served as a control. After 30 min of incubation, 180 μL of the medium was injected into a deaerated septum-sealed vial containing 20 μL of 30% sulfosalicylic acid. CO released into the vial´s headspace was quantitated using gas chromatography with a reducing gas analyzer (Peak Performer 1, Peak Laboratories, Mountain View, CA, USA), as described previously.[5]

Synthesis

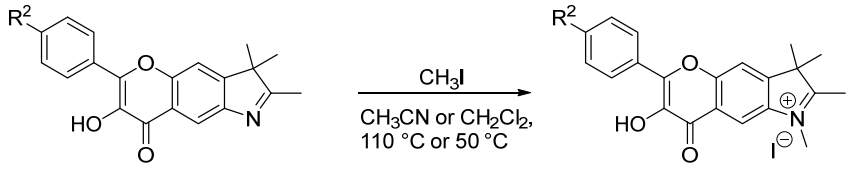

11a: $R^2 = H$

11b: $R^2 = N(CH_3)_2$

10a: $R^2 = H$

10b: $R^2 = \overset{\oplus}{N}(CH_3)_3$

10c: $R^2 = N(CH_3)_2$

Scheme S1. The preparation of **10a**–**c**.

Synthesis of Flavonols 10a–c.

The synthesis of compound **11** has been previously described.[3]

7-Hydroxy-1,2,3,3-tetramethyl-8-oxo-6-phenyl-3,8-dihydropyrano[2,3-*f*]indol-1-ium iodide (10a)

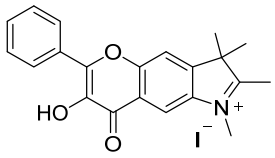

Compound **11a** (0.46 mmol, 147 mg) was dissolved in acetonitrile (15 mL) and CH_3I (5.52 mmol, 0.36 mL) was added. The mixture was heated in a glass pressure tube at 100 °C for 4 h. After cooling down to room temperature, the resulting precipitate was filtered, washed with acetonitrile (3 × 2 mL) and diethyl ether (3 × 2 mL) and dried to provide **10a**. Yield: 150 mg (71%). ^{1}H NMR (300 MHz, d_6–DMSO) δ (ppm) 8.53 (s, 1H), 8.37 (s, 1H), 8.24 (d, J = 7.3 Hz, 2H), 7.66 – 7.52 (m, 3H), 4.10 (s, 3H), 2.82 (s, 3H), 1.61 (s, 6H) (Figures S1, S2). ^{13}C NMR (125 MHz, d_6–DMSO) δ (ppm) 197.13, 172.59, 154.83, 146.49, 145.85, 139.11, 139.06, 130.89, 130.19, 128.58 (2 × C based on HSQC), 127.63 (2 × C based on HSQC (Figure S4)), 121.43, 114.63, 111.21, 54.05, 35.11, 21.93, 14.40 (Figure S3). HRMS (ESI$^+$): calcd. for $C_{21}H_{20}NO_3^+$ $[M - I]^+$ 334.1438, found 334.1439.

7-Hydroxy-1,2,3,3-tetramethyl-8-oxo-6-(4-(trimethylammonio)phenyl)-3,8-dihydropyrano[2,3-f]indol-1-ium iodide (10b)

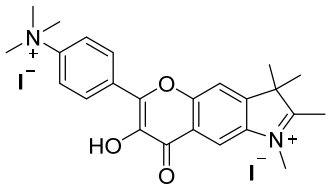

Compound **11b** (0.46 mmol, 166 mg) was dissolved in acetonitrile (15 mL) and CH_3I (11.45 mmol, 0.71 mL) was added. The mixture was heated in a glass pressure tube at 100 °C for 4 h. After cooling down to room temperature, the resulting precipitate was filtered, washed with acetonitrile (3 × 2 mL) and diethyl ether (3 × 2 mL) and dried to provide **10b**. Yield: 235 mg (79%). ^{1}H NMR (300 MHz, d_6–DMSO) δ (ppm) 8.53 (s, 1H), 8.42 (d, J = 9.3 Hz, 2H), 8.39 (s, 1H), 8.21 (d, J = 9.4 Hz, 2H), 4.10 (s, 3H), 3.68 (s, 9H), 2.82 (s, 3H), 1.62 (s, 6H) (Figures S5, S6). ^{13}C NMR (125 MHz, d_6–DMSO) δ (ppm) 197.27, 172.76, 154.88, 147.63, 146.75, 143.84, 139.91, 139.17, 132.48, 128.96 (2 × C based on HSQC (Figures S8, S9)), 121.47, 120.93(2 × C based on HSQC), 114.70, 111.28, 56.42, 54.09, 35.17, 21.93, 14.49 (Figure S7). HRMS (ESI$^+$): calcd. for $C_{24}H_{28}N_2O_3^+$ $[M - H - 2I]^+$ 391.2016, found 391.2020.

6-(4-(Dimethylamino)phenyl)-7-hydroxy-1,2,3,3-tetramethyl-8-oxo-3,8-dihydropyrano[2,3-f]indol-1-ium iodide (10c)

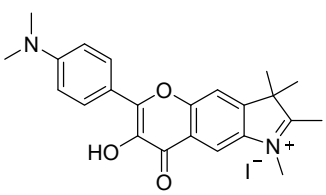

Compound **11b** (0.5 mmol, 181 mg) was dissolved in acetonitrile (15 mL) and CH_3I (5 mmol, 0.31 mL) was added. The mixture was heated in a glass pressure tube at 50 °C for 30 h. After cooling down to room temperature, the resulting precipitate was filtered, washed with acetonitrile (3 × 2 mL) and diethyl ether (3 × 2 mL) and dried to provide **10c**. Yield: 130 mg (69%). ^{1}H NMR (300 MHz, d_6–DMSO) δ (ppm) 8.47 (s, 1H), 8.31 (s, 1H), 8.17 (d, J = 9.1 Hz, 2H), 6.98 (d, J = 9.0 Hz, 2H), 4.09 (s, 3H), 3.06 (s, 6H),

2.81 (s, 3H), 1.61 (s, 6H) (Figures S10, S11). ^{13}C NMR (125 MHz, d_6–DMSO) δ (ppm) 196.82, 171.29, 154.46, 151.19, 147.52, 145.83, 138.85, 137.22, 128.97 (2 × C based on HSQC (Figures S13, S14)), 121.58, 117.34, 114.26, 111.39 (2 × C based on HSQC), 110.97, 54.00, 40.31(overlap with solvent), 35.06, 21.93, 14.34 (Figure S12). HRMS (ESI$^+$): calcd. for $C_{23}H_{25}N_2O_3^+$ [M – I]$^+$ 377.1860, found 377.1863.

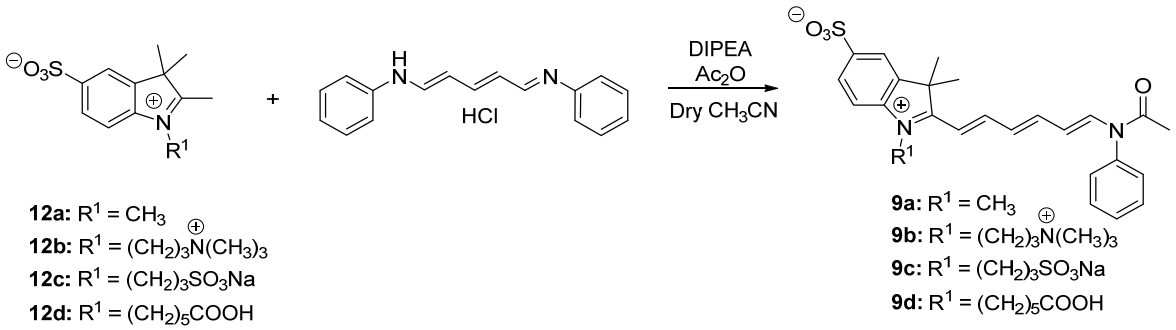

12a: $R^1 = CH_3$
12b: $R^1 = (CH_2)_3\overset{\oplus}{N}(CH_3)_3$
12c: $R^1 = (CH_2)_3SO_3Na$
12d: $R^1 = (CH_2)_5COOH$

9a: $R^1 = CH_3$
9b: $R^1 = (CH_2)_3\overset{\oplus}{N}(CH_3)_3$
9c: $R^1 = (CH_2)_3SO_3Na$
9d: $R^1 = (CH_2)_5COOH$

Scheme S2. The preparation of **9a**−**d**.

General Synthesis Procedure of Cyanine-Flavonol Compounds 3−8.
Compound **12** was prepared according to literature.[6]

2-((1*E*,3*E*,5*E*,7*E*)-7-(7-Hydroxy-1,3,3-trimethyl-8-oxo-6-(4-(trimethylammonio)phenyl)-3,8-dihydropyrano[2,3-*f*]indol-2(1*H*)-ylidene)hepta-1,3,5-trien-1-yl)-1,3,3-trimethyl-3*H*-indol-1-ium-5-sulfonate iodide (3)

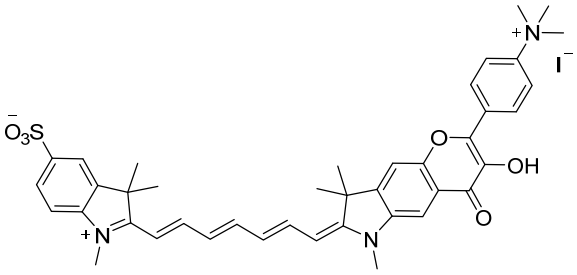

N-[5-(Phenylamino)-2,4-pentadienylidene]aniline monohydrochloride (1.26 mmol, 359 mg) was suspended in MeCN (4.5 mL) under N_2. *N*,*N*-diisopropylethylamine (2.65 mmol, 0.46 mL) and Ac_2O (3.78 mmol, 0.36 mL) were added at room temperature and stirred for 2 h. Then, the mixture was cooled to 0 °C. Compound **12a** (0.63 mmol, 159 mg) in AcOH/MeCN (2.3 : 1, mL) was added by a syringe pump over 30 min. The cooling bath was removed after 1 h and stirred for additional 1 h. After that, the mixture was added to THF (100 mL), filtered, and washed with diethyl ether (2 × 10 mL). The crude product **9a** was used for the next step immediately without further purification. Compounds **9a** (0.23 mmol, 105 mg) and **10b** (0.23 mmol, 150 mg) were dissolved in ethanol (3.5 mL) in a small flask, sodium acetate (0.35 mmol, 28.6 mg) was added, then the mixture was refluxed for 2 h under argon. Afterward, the heating bath was removed, and the mixture was continuously stirred at room temperature overnight. After the absorbance signature indicated the completion of the reaction, the reaction mixture was filtered and washed with *i*-propanol (3 × 2 mL), ethanol (2 × 2 mL), acetone (2 × 2 mL), methanol (2 × 1 mL), and diethyl ether (2 × 2 mL). The compound was purified via multiple precipitations by dissolving the compound in methanol (minimum amount) and diluting very slowly with diethyl ether to obtain a dark green product. Yield: 151 mg (78%). ^{1}H NMR (500 MHz, d_6–DMSO) δ (ppm) 9.71 (s, 1H), 8.36 (d, J = 9.1 Hz, 2H), 8.14 (d, J = 9.1 Hz, 2H), 8.00 – 7.91 (m, 2H), 7.81 (s, 1H), 7.78 – 7.69 (m, 3H), 7.66 (s, 1H), 7.42 (d, J = 8.2 Hz, 1H), 6.60 (t, J = 12.6 Hz, 1H), 6.53 (t, J = 12.5 Hz, 2H), 6.16 (d, J = 13.3 Hz, 1H), 3.71 (s, 3H), 3.69 (s, 9H), 3.58 (s, 3H), 1.73 (s, 6H), 1.66 (s, 6H) (Figure S15). ^{13}C NMR (125 MHz, d_6–DMSO/d_4–MeOD (1:1)): δ (ppm) 174.23, 173.26, 170.11, 157.02, 153.39, 152.95, 150.98, 148.81, 147.94, 144.88, 143.76, 143.59, 141.55, 141.38, 140.08, 133.16, 129.28 (2 × C based on HSQC (Figure S17)), 127.01, 126.52, 126.48, 122.40, 121.15 (2 × C based on HSQC), 120.19,

113.53, 111.44, 105.77, 104.59, 104.05, 56.99, 49.54, 48.92, 31.97, 31.46, 27.44, 27.01 (Figure S16). HRMS (ESI$^+$): calcd. for $C_{41}H_{44}N_3O_6S^+$ $[M - I]^+$ 706.2945, found 706.2947.

2-((1*E*,3*E*,5*E*,7*E*)-7-(7-Hydroxy-1,3,3-trimethyl-8-oxo-6-phenyl-3,8-dihydropyrano[2,3-*f*]indol-2(1*H*)-ylidene)hepta-1,3,5-trien-1-yl)-3,3-dimethyl-1-(3-(trimethylammonio)propyl)-3*H*-indol-1-ium-5-sulfonate bromide (4)

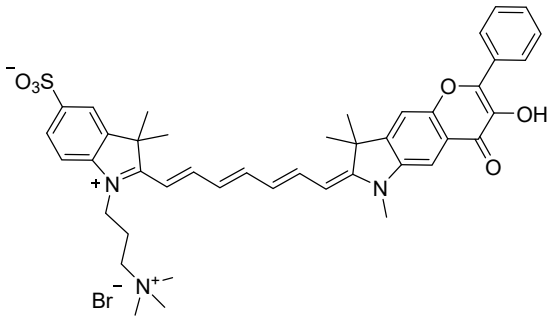

N-[5-(Phenylamino)-2,4-pentadienylidene]aniline monohydrochloride (0.63 mmol, 180 mg) was suspended in MeCN (6.6 mL) under N_2. *N*,*N*-diisopropylethylamine (1.33 mmol, 0.23 mL) and Ac_2O (1.90 mmol, 0.18 mL) were added at room temperature and stirred for 2 h. Then, the mixture was cooled to 0 °C. Compound **12b** (0.32 mmol, 132 mg) in AcOH/MeCN (2.3 : 1, mL) was added by a syringe pump over 30 min. The cooling bath was removed after 1 h and stirred for additional 1 h. After that, the mixture was added to THF (100 mL), filtered, and washed with diethyl ether (2 × 10 mL). The crude product **9b** was used for the next step immediately without further purification. Compounds **9b** (0.14 mmol, 89 mg) and **10a** (0.14 mmol, 70 mg) were dissolved in ethanol (4.5 mL) in a small flask, sodium acetate (0.39 mmol, 23.7 mg) was added, then the mixture was refluxed for 2 h under argon. Afterward, the heating bath was removed, and the mixture was continuously stirred at room temperature overnight. After the absorbance signature indicated the completion of the reaction, the reaction mixture was filtered and washed with *i*-propanol (3 × 2 mL), ethanol (2 × 2 mL), acetone (2 × 2 mL), methanol (2 × 1 mL), and diethyl ether (2 × 2 mL). The compound was purified via multiple precipitations by dissolving the compound in methanol (minimum amount) and diluting with diethyl ether to obtain a dark green product. Yield: 80 mg (68%). ^{1}H NMR (500 MHz, d_6–DMSO/d_4–MeOD (1:1)): δ (ppm) 8.22 (d, J = 7.7 Hz, 2H), 7.94 (dd, J = 14.1, 10.4 Hz, 2H), 7.88 (d, J = 13.0 Hz, 1H), 7.84 (s, 1H), 7.78 (s, 1H), 7.72 (t, J = 11.4 Hz, 2H), 7.53 (t, J = 7.2 Hz, 2H), 7.50 – 7.44 (m, 1H), 7.34 – 7.26 (m, 1H), 6.58 (t, J = 12.6 Hz, 2H), 6.35 (d, J = 13.5 Hz, 2H), 4.15 – 4.05 (m, 2H), 3.67 (s, 3H), 3.53 – 3.47 (m, 2H), 3.09 (s, 9H), 2.19 (dt, J = 16.2, 8.1 Hz, 2H), 1.74 (s, 6H), 1.67 (s, 6H) (Figure S18). ^{13}C NMR (125 MHz, d_6–DMSO/d_4-MeOD (1:1)) δ (ppm) 173.07, 171.91, 157.20, 153.95, 152.71, 152.66, 151.79, 148.40, 146.01, 144.31, 143.16, 140.98, 140.82, 139.25, 131.78, 130.40, 128.90 (2 × C based on HSQC (Figure S20)), 128.12 (2 × C based on HSQC), 127.06, 127.01, 126.98, 122.07, 120.47, 113.68, 110.19, 105.34, 105.11, 104.33, 63.57, 53.13, 49.59, 49.20, 41.11, 31.81, 27.58, 27.29, 21.36 (Figure S19). HRMS (ESI$^+$): calcd. for $C_{43}H_{48}N_3O_6S^+$ $[M - Br]^+$ 734.3258, found 734.3267.

2-((1*E*,3*E*,5*E*,7*E*)-7-(7-Hydroxy-1,3,3-trimethyl-8-oxo-6-(4-(trimethylammonio)phenyl)-3,8-dihydropyrano[2,3-*f*]indol-2(1*H*)-ylidene)hepta-1,3,5-trien-1-yl)-3,3-dimethyl-1-(3-sulfonatopropyl)-3*H*-indol-1-ium-5-sulfonate (5)

N-[5-(Phenylamino)-2,4-pentadienylidene]aniline monohydrochloride (1.3 mmol, 371 mg) was suspended in MeCN (10 mL) under N_2. *N*,*N*-diisopropylethylamine (2.74 mmol, 0.48 mL) and Ac_2O (3.91mmol, 0.37 mL) were added at room temperature and stirred for 2 h. Then, the mixture was cooled to 0 °C. Compound **12c** (0.65 mmol, 250 mg) in AcOH/MeCN (3.5 : 1.5, mL) was added by a syringe pump over 30 min. The cooling bath was removed after 1 h and stirred for additional 1 h. After that, the mixture was added to THF (240 mL), filtered, and washed with diethyl ether (2 × 10 mL). The crude

product **9c** was used for the next step immediately without further purification. Compounds **9c** (0.22 mmol, 129 mg) and **10b** (0.22 mmol, 144 mg) were dissolved in ethanol (3.5 mL) in a small flask, sodium acetate (0.44 mmol, 36.6 mg) was added, and then the mixture was refluxed under argon for 2 h. Afterward, the heating bath was removed, and the mixture was continuously stirred at room temperature overnight. After the absorbance signature indicated the completion of the reaction, the reaction mixture was filtered and washed with *i*-propanol (3 × 2 mL), ethanol (3 × 2 mL), acetone (3 × 2 mL), methanol (3 × 2 mL), and diethyl ether (2 × 2 mL). After that, the crude product was dissolved in DMSO (minimum amount), then acetone was slowly added until dark green precipitation (product) appeared. Yield: 181 mg (78%). ^{1}H NMR (500 MHz, d_6–DMSO) δ (ppm) 8.39 (d, J = 9.3 Hz, 2H), 8.18 (d, J = 9.3 Hz, 2H), 8.06 (s, 1H), 8.05 (s, 1H), 8.03 – 7.95 (m, 1H), 7.83 (s, 1H), 7.79 (s, 1H), 7.71 (s, 1H), 7.66 (d, J = 8.1 Hz, 1H), 7.48 (d, J = 8.2 Hz, 1H), 6.66 (d, J = 14.7 Hz, 1H), 6.57 (t, J = 11.9 Hz, 2H), 6.24 (d, J = 13.3 Hz, 1H), 4.31 (dd, J = 12.1, 5.3 Hz, 2H), 3.68 (s, 9H), 3.60 (s, 3H), 2.66 (t, J = 6.1 Hz, 2H), 2.02 (dd, J = 13.2, 7.5 Hz, 2H), 1.72 (s, 6H), 1.65 (s, 6H). HRMS (ESI$^+$): calcd. for $C_{43}H_{47}N_3O_9S_2Na$ $[M - I]^+$ 836.2646, found 836.2654. We tried to dissolved this compound in all common solvents, even in the presence of an acid, base, or ammounium salts but because of its not sufficient solubility, the NMR spectrum is noisy, although all signals are assigned (Figure S21).

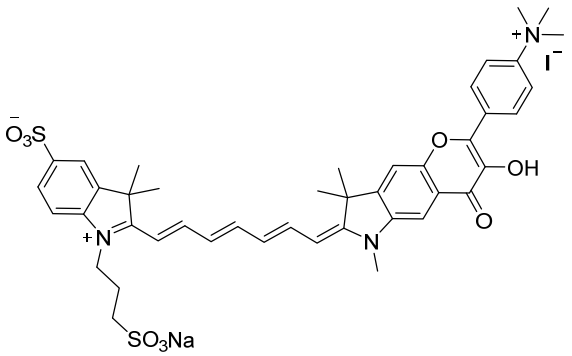

2-((1*E*,3*E*,5*E*,7*E*)-7-(7-Hydroxy-1,3,3-trimethyl-8-oxo-6-(4-(trimethylammonio)phenyl)-3,8-dihydropyrano[2,3-*f*]indol-2(1*H*)-ylidene)hepta-1,3,5-trien-1-yl)-3,3-dimethyl-1-(3-(trimethylammonio)propyl)-3*H*-indol-1-ium-5-sulfonate bromide iodide (6)

N-[5-(Phenylamino)-2,4-pentadienylidene]aniline monohydrochloride (0.63 mmol, 180 mg) was suspended in MeCN (6.6 mL) under N_2. *N*,*N*-diisopropylethylamine (1.33 mmol, 0.23 mL) and Ac_2O (1.90 mmol, 0.18 mL) were added at room temperature and stirred for 2 h. Then, the mixture was cooled to 0 °C. Compound **12b** (0.32 mmol, 132 mg) in AcOH/MeCN (2.3 : 1, mL) was added by a syringe pump over 30 min. The cooling bath was removed after 1 h and stirred for additional 1 h. After that, the mixture was added to THF (100 mL), filtered, and washed with diethyl ether (2 × 10 mL). The crude product **9b** was used for the next step immediately without further purification. Compounds **9b** (0.17 mmol, 107 mg) and **10b** (0.17 mmol, 112 mg) were dissolved in ethanol (4.5 mL) in a small flask, sodium acetate (0.35 mmol, 28.5 mg) was added, then the mixture was refluxed under argon for 2 h. Afterward, the heating bath was removed, and the mixture was continuously stirred at room temperature overnight. After the absorbance signature indicated the completion of the reaction, the reaction mixture was filtered and washed with *i*-propanol (3 × 1 mL), ethanol (2 × 2 mL), acetone (2 × 2 mL), methanol (2 × 1 mL), and diethyl ether (2 × 2 mL). After that, the crude product was dissolved in methanol/water (2 : 1), then acetone was slowly added until dark green precipitation (product) appeared or isolated using reverse-phase C18 silica gel with an acetonitrile (or methanol)/water (0.1% trifluoroacetic acid; 20 : 80) gradient as an eluting solvent. Yield: 106 mg (61%). ^{1}H NMR (500 MHz, d_6–DMSO/d_4–MeOD (1:1)): δ (ppm) 8.17 (d, J = 8.7 Hz, 2H), 8.01 (d, J = 9.2 Hz, 2H), 7.91 (s, 1H), 7.90 – 7.82 (m, 2H), 7.70 (dd, J = 8.2, 1.1 Hz, 1H), 7.67 (d, J = 6.3 Hz, 2H), 7.56 (t, J = 12.7 Hz, 1H), 7.29 (d, J = 8.3 Hz, 1H), 6.52 (t, J = 12.6 Hz, 1H), 6.40 (dd, J = 26.4, 13.2 Hz, 2H), 6.16 (d, J = 13.4 Hz, 1H), 4.08 – 4.03 (m, 2H), 3.71 (s, 3H), 3.65 (s, 9H), 3.44 (dd, J = 10.3, 6.5 Hz, 2H), 3.07 (s, 9H), 2.12 (dt, J = 15.6, 7.6 Hz, 2H),

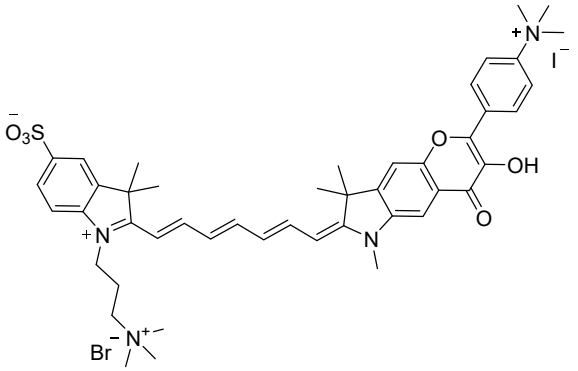

1.70 (s, 6H), 1.51 (s, 6H) (Figure S21). ^{13}C NMR (125 MHz, d_6–DMSO/d_4–MeOD (1:1)): δ (ppm) 173.33, 172.88, 171.80, 157.63, 153.99, 153.12, 152.11, 148.96, 148.13, 144.19, 143.75, 143.27, 141.20, 141.14, 140.31, 133.51, 129.59 (2 × C based on HSQC), 127.13 (2 × C based on HSQC (Figure S23)), 126.93, 122.39, 121.24 (2 × C based on HSQC), 120.56, 113.90, 110.59, 105.93, 105.28, 104.47, 63.56, 57.07, 53.16, 49.69, 49.29, 41.21, 31.89, 27.56, 27.35, 21.52 (Figure S22). HRMS (ESI$^+$): calcd. for $C_{46}H_{52}N_4O_6S^{2+}$ $[M - Br - I]^{2+}$ 396.1955, found 396.1946.

1-(5-Carboxypentyl)-2-((1*E*,3*E*,5*E*,7*E*)-7-(7-hydroxy-1,3,3-trimethyl-8-oxo-6-(4-(trimethylammonio)phenyl)-3,8-dihydropyrano[2,3-*f*]indol-2(1*H*)-ylidene)hepta-1,3,5-trien-1-yl)-3,3-dimethyl-3*H*-indol-1-ium-5-sulfonate iodide (7)

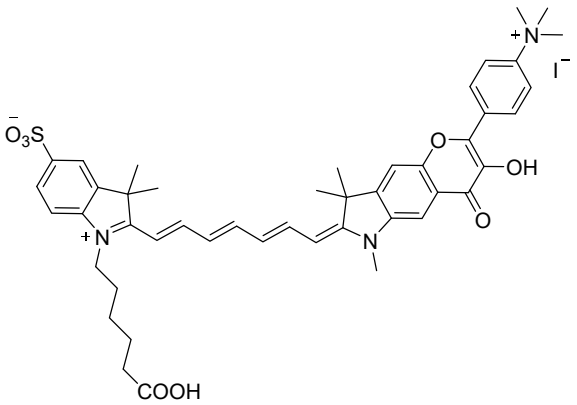

N-[5-(Phenylamino)-2,4-pentadienylidene]aniline monohydrochloride (0.63 mmol, 180 mg) was suspended in MeCN (6.6 mL) under N_2. *N*,*N*-diisopropylethylamine (1.33 mmol, 231 mg) and Ac_2O (1.90 mmol, 179 mg) were added at room temperature and stirred for 2 h. Then, the mixture was cooled to 0 °C. Compound **12d** (0.32 mmol, 119 mg) in AcOH/MeCN (2.3 : 1, mL) was added by a syringe pump over 30 min. The cooling bath was removed after 1 h and stirred for additional 1 h. After that, the mixture was added to THF (100 mL), filtered, and washed with diethyl ether (2 × 10 mL). The crude product **9d** was used for the next step immediately without further purification. Compounds **9d** (0.17 mmol, 96 mg) and **10b** (0.17 mmol, 112 mg) were dissolved in ethanol (4.5 mL) in a small flask, sodium acetate (0.35 mmol, 28.5 mg) was added, then the mixture was refluxed under argon for 2 h. Afterward, the heating bath was removed, and the mixture was continuously stirred at room temperature overnight. After the absorbance signature indicated the completion of the reaction, the reaction mixture was filtered and washed ethanol (2 × 2 mL), acetone (2 × 2 mL), methanol (2 × 2 mL), and diethyl ether (2 × 2 mL). After that, the crude product was dissolved in methanol/water (2 : 1), then acetone was slowly added until dark green precipitation (product) appeared. Yield: 116 mg (72%). ^{1}H NMR (500 MHz, d_6–DMSO) δ (ppm) 9.78 (s, 1H), 8.24 (d, J = 8.9 Hz, 2H), 8.12 (d, J = 9.1 Hz, 2H), 7.97 (s, 1H), 7.87 (t, J = 12.9 Hz, 1H), 7.81 – 7.71 (m, 3H), 7.69 (d, J = 7.7 Hz, 2H), 7.38 (d, J = 8.2 Hz, 1H), 6.53 (dt, J = 25.6, 12.8 Hz, 2H), 6.42 (d, J = 13.8 Hz, 1H), 6.22 (d, J = 13.3 Hz, 1H), 4.20 – 4.08 (m, 2H), 3.69 (s, 9H), 3.64 (s, 3H), 2.21 (t, J = 7.2 Hz, 2H), 1.75 (m, 2H), 1.72 (s, 6H), 1.60 (s, J = 9.7 Hz, 6H), 1.58 – 1.52 (m, 2H), 1.45 – 1.36 (m, 2H) (Figure S24). HRMS (ESI$^+$): calcd. for $C_{46}H_{52}N_3O_8S^+$ $[M - I]^+$ 806.3470, found 806.3476. Due to the limited solubility of **7** in all common solvents, we could not obtain a reasonable ^{13}C NMR. However, we were able to measure the HSQC (Figure S25) and HMBC (Figure S26) to see partial carbon chemical shifts that supported the anticipated structure.

2-((1*E*,3*E*,5*E*,7*E*)-7-(6-(4-(Dimethylamino)phenyl)-7-hydroxy-1,3,3-trimethyl-8-oxo-3,8-dihydropyrano[2,3-*f*]indol-2(1*H*)-ylidene)hepta-1,3,5-trien-1-yl)-3,3-dimethyl-1-(3-(trimethylammonio)propyl)-3*H*-indol-1-ium-5-sulfonate bromide (8)

N-[5-(Phenylamino)-2,4-pentadienylidene]aniline monohydrochloride (0.63 mmol, 180 mg) was suspended in MeCN (6.6 mL) under N_2. *N*,*N*-diisopropylethylamine (1.33 mmol, 0.23 mL) and Ac_2O (1.90 mmol, 0.18 mL) were added at room temperature and stirred for 2 h. Then, the mixture was cooled to 0 °C. Compound **12b** (0.32 mmol, 132 mg) in AcOH/MeCN (2.3 : 1, mL) was added by a syringe pump over 30 min. The cooling bath was removed after 1 h and stirred for additional 1 h. After that, the mixture was added to THF (100 mL), filtered, and washed with diethyl ether (2 × 10 mL). The crude

product **9b** was used for the next step immediately without further purification. Compounds **9b** (0.15 mmol, 93 mg) and **10c** (0.15 mmol, 76 mg) were dissolved in ethanol (4.5 mL) in a small flask, sodium acetate (0.30 mmol, 24.6 mg) was added, then the mixture was refluxed under N_2 for 2 h. Afterward, the heating bath was removed, and the mixture was continuously stirred at room temperature overnight. After the absorbance signature indicated the completion of the reaction, the reaction mixture was filtered and washed with ethanol (2 × 2 mL), acetone (2 × 2 mL), methanol (2 × 1 mL), and diethyl ether (2 × 2 mL). After that, the crude product was dissolved in methanol/water (2 : 1) to obtain the product as dark green. Yield: 85 mg (66%). ^{1}H NMR (500 MHz, d_6–DMSO) δ (ppm) 9.07 (s, 1H), 8.13 (d, J = 9.1 Hz, 2H), 8.04 (s, 1H), 7.93 (td, J = 13.1, 2.8 Hz, 2H), 7.86 – 7.79 (m, 2H), 7.78 (s, 1H), 7.67 (dd, J = 8.2, 1.3 Hz, 1H), 7.35 (d, J = 8.3 Hz, 1H), 6.87 (d, J = 9.2 Hz, 2H), 6.58 (dd, J = 22.4, 12.5 Hz, 2H), 6.39 (dd, J = 15.8, 14.2 Hz, 2H), 4.13 (t, J = 7.0 Hz, 2H), 3.69 (s, 4H), 3.56 – 3.47 (t, 3H), 3.10 (s, 9H), 3.04 (s, 6H), 2.16 (dt, J = 15.6, 7.6 Hz, 3H), 1.75 (s, 6H), 1.68 (s, 6H) (Figure S27). ^{13}C NMR (125 MHz, d_6–DMSO) δ (ppm) 171.40, 171.37, 171.15, 156.17, 152.38, 151.08 (2 × C based on HSQC (Figure S28)), 150.98, 146.77, 146.70, 145.60, 141.58, 140.06, 139.85, 136.83, 128.67 (2 × C based on HSQC), 125.98, 125.74 (2 × C based on HSQC), 121.42, 119.71, 117.64, 112.93, 111.26 (2 × C based on HSQC), 109.70, 104.20 (2 × C based on HSQC), 103.88, 62.50, 52.47, 48.57, 48.54, 40.60, 39.26 (HSQC, overlap with solvent signal), 31.48, 27.07, 26.92, 20.67 (Figure S29). HRMS (ESI$^+$): calcd. for $C_{45}H_{53}N_4O_6S^+$ $[M - Br]^+$ 777.3680, found 777.3685.

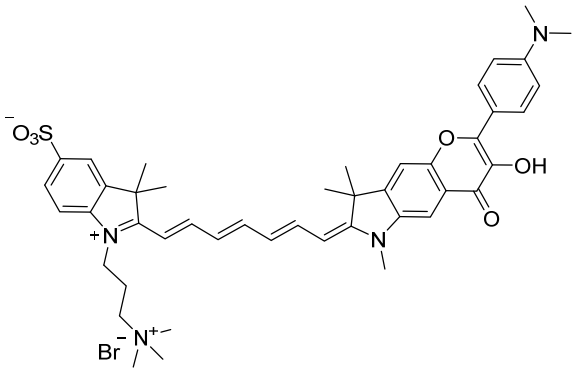

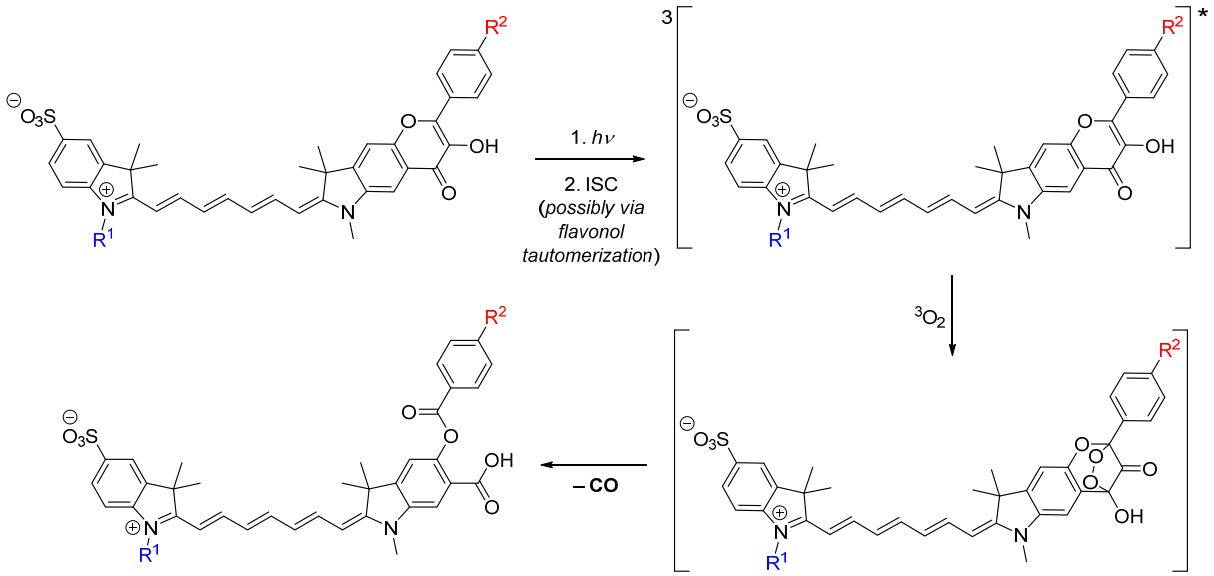

Scheme S3. Proposed mechanism of the CO release.

NMR Spectra

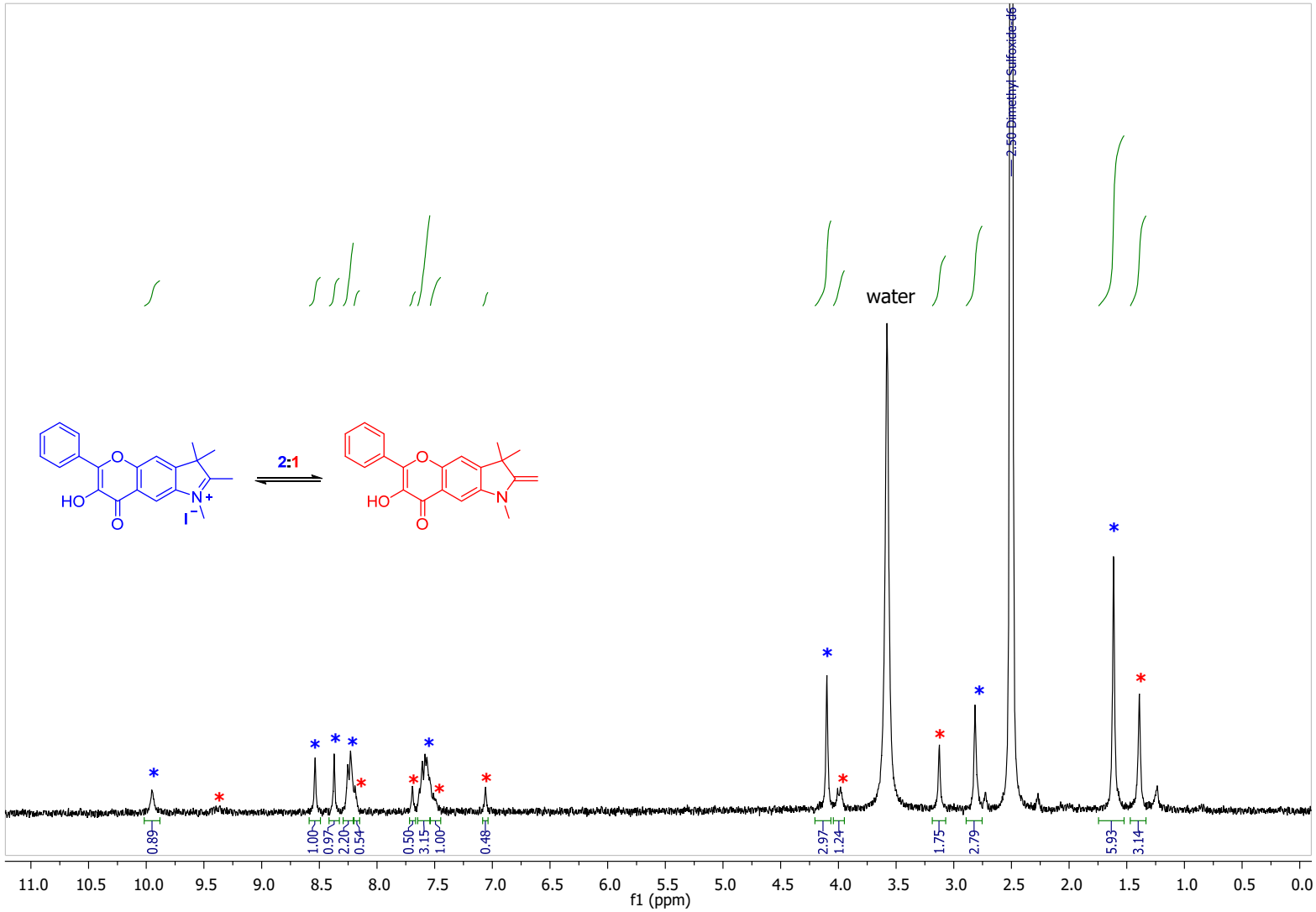

Figure S1. ^{1}H NMR (300 MHz, d_6–DMSO): **10a** (blue) and its tautomer (red).

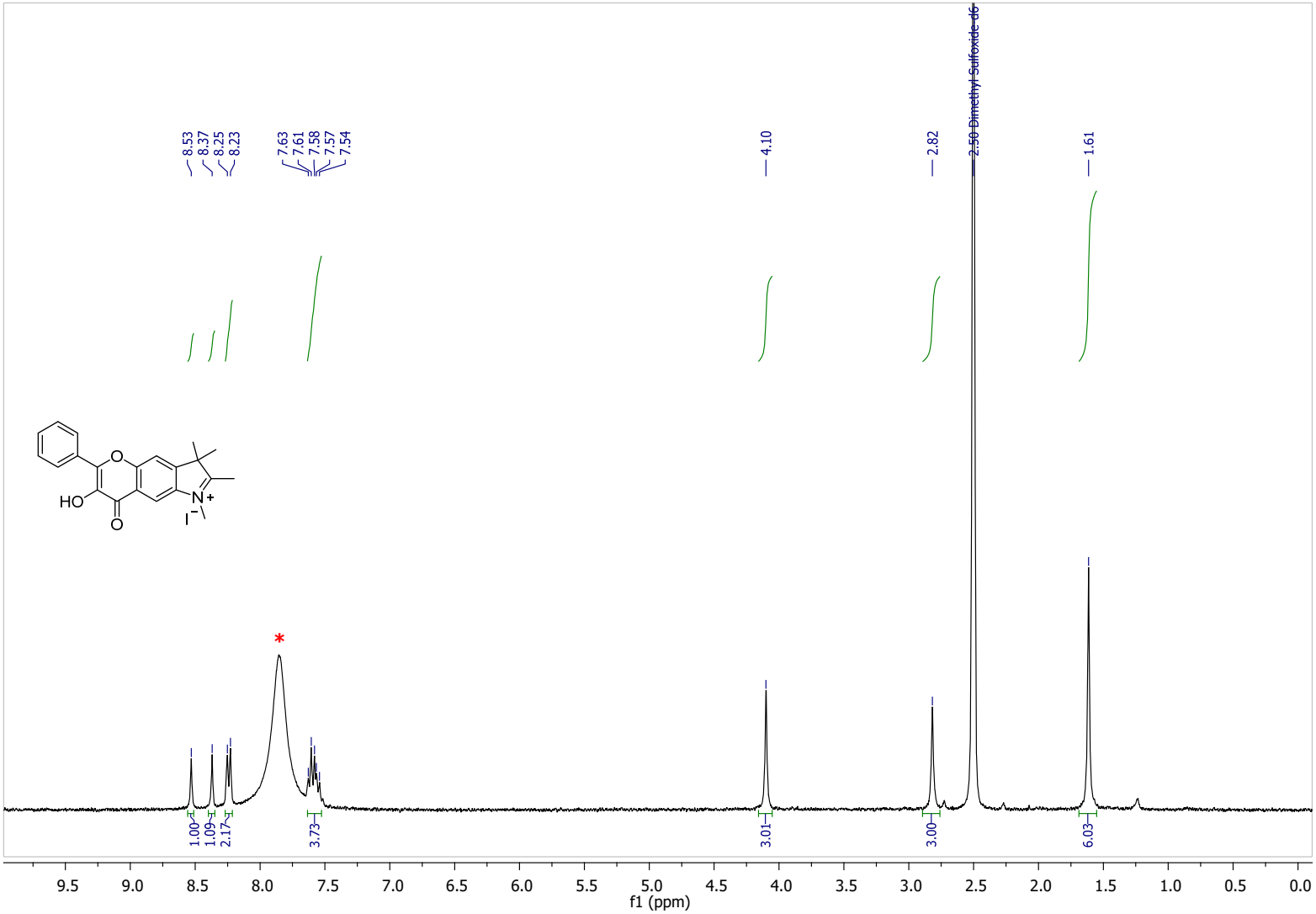

Figure S2. ^{1}H NMR (300 MHz, d_6–DMSO + 1µL H_2SO_4): **10a**. Asterisk denotes H_2SO_4.

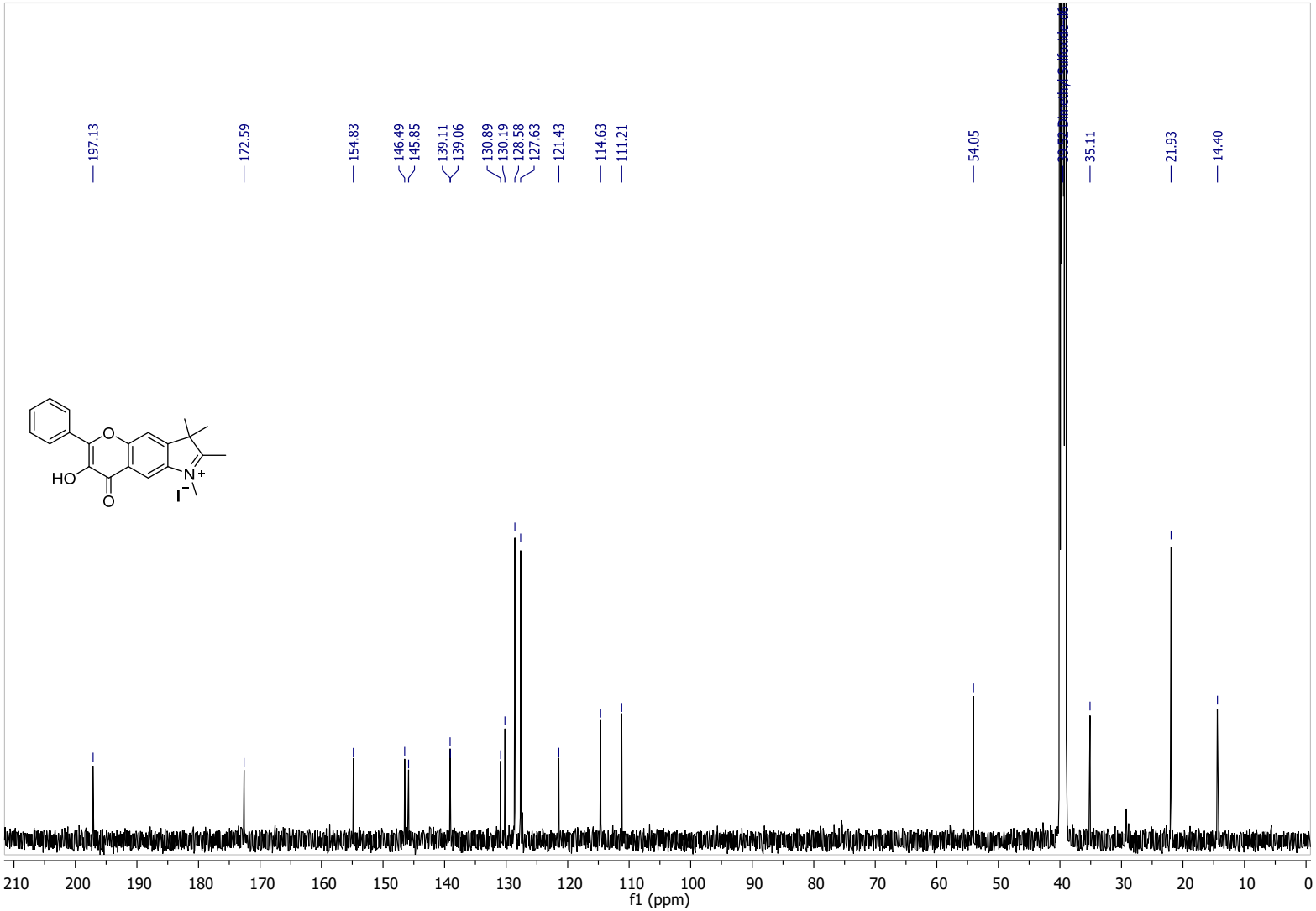

Figure S3. ^{13}C NMR (125 MHz, d_6–DMSO): **10a**.

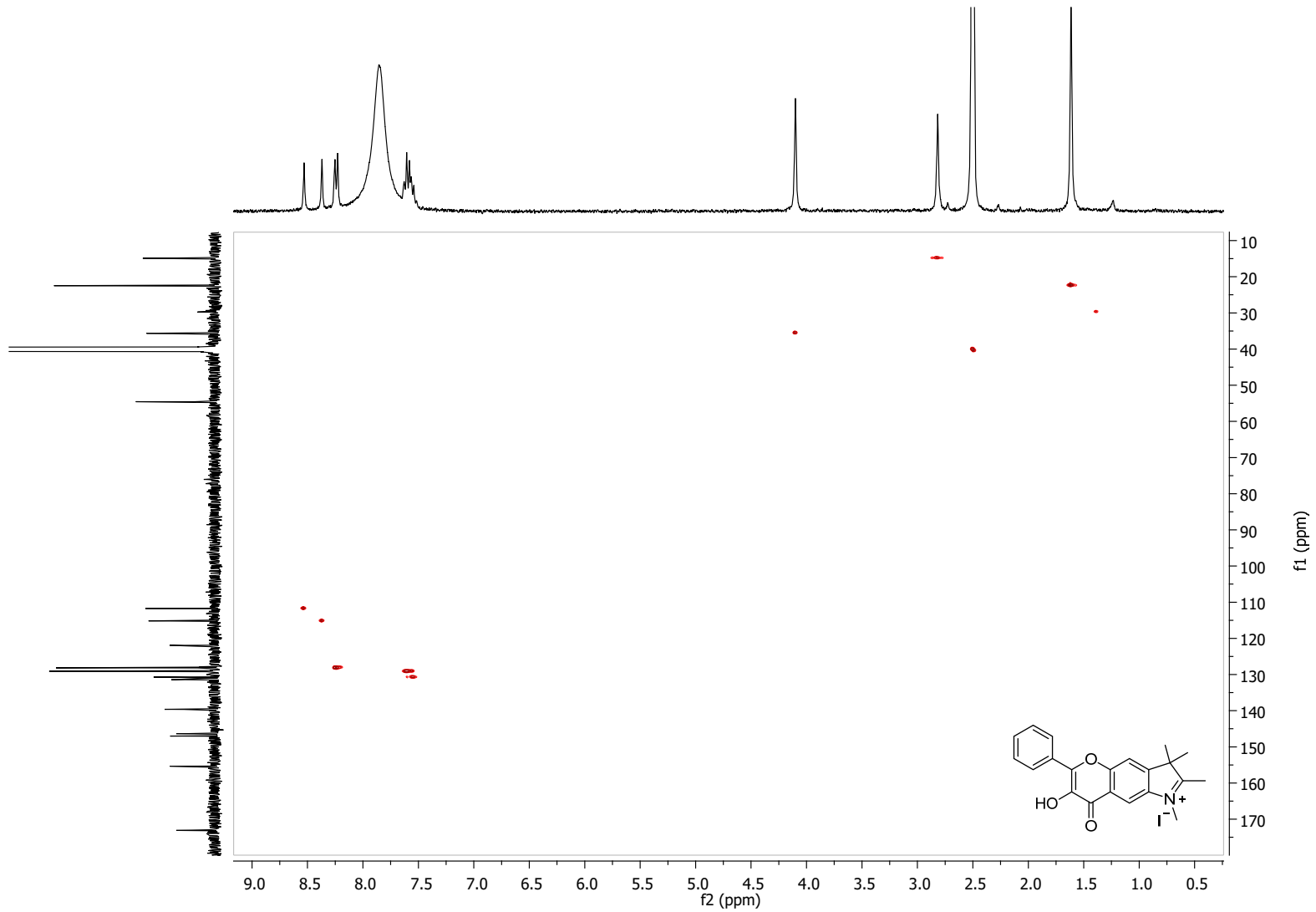

Figure S4. $^{1}H–^{13}C$ HSQC (500 MHz, d_6–DMSO): **10a**.

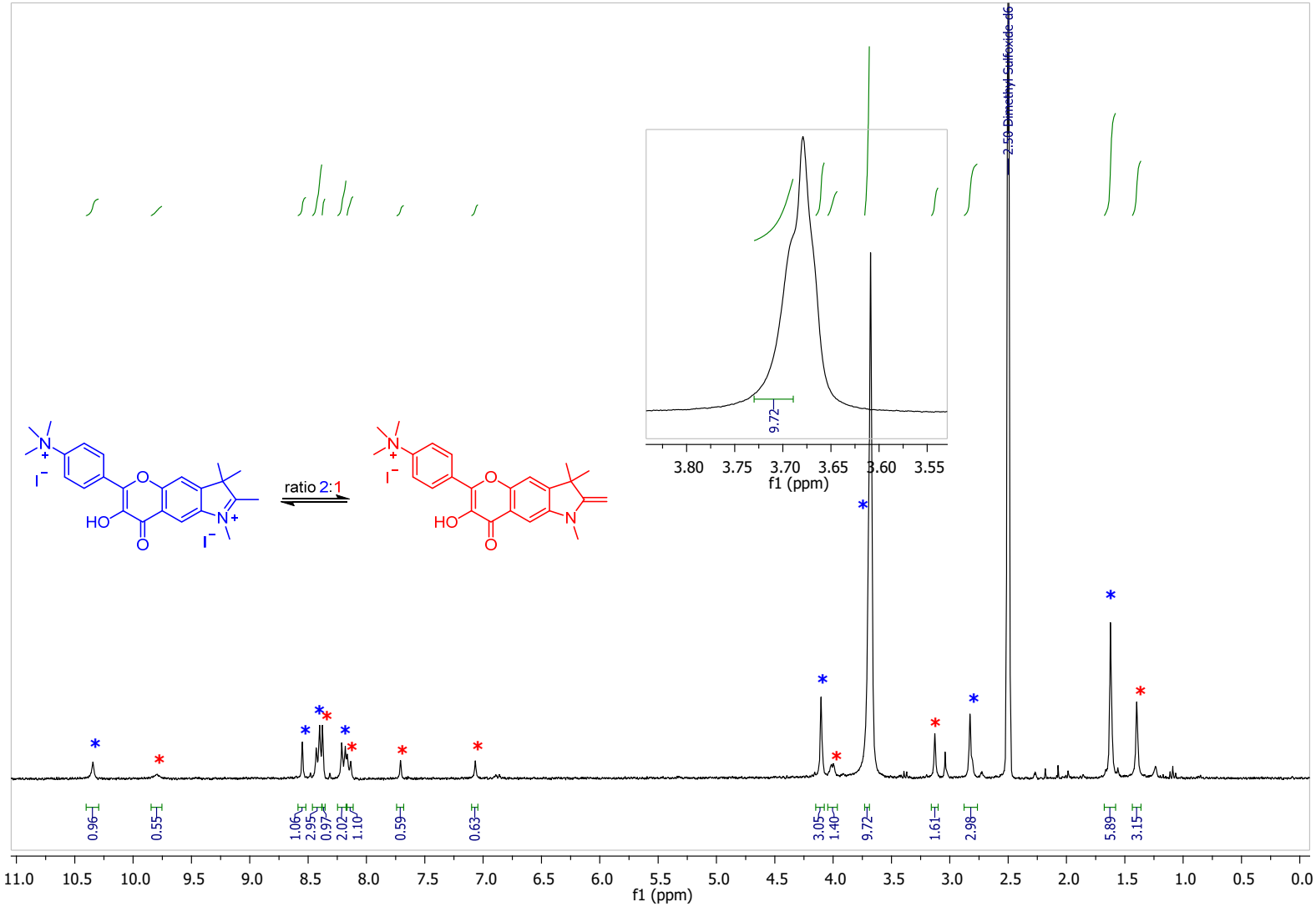

Figure S5. ^{1}H NMR (300 MHz, d_6–DMSO): **10b** (blue) and its tautomer (red).

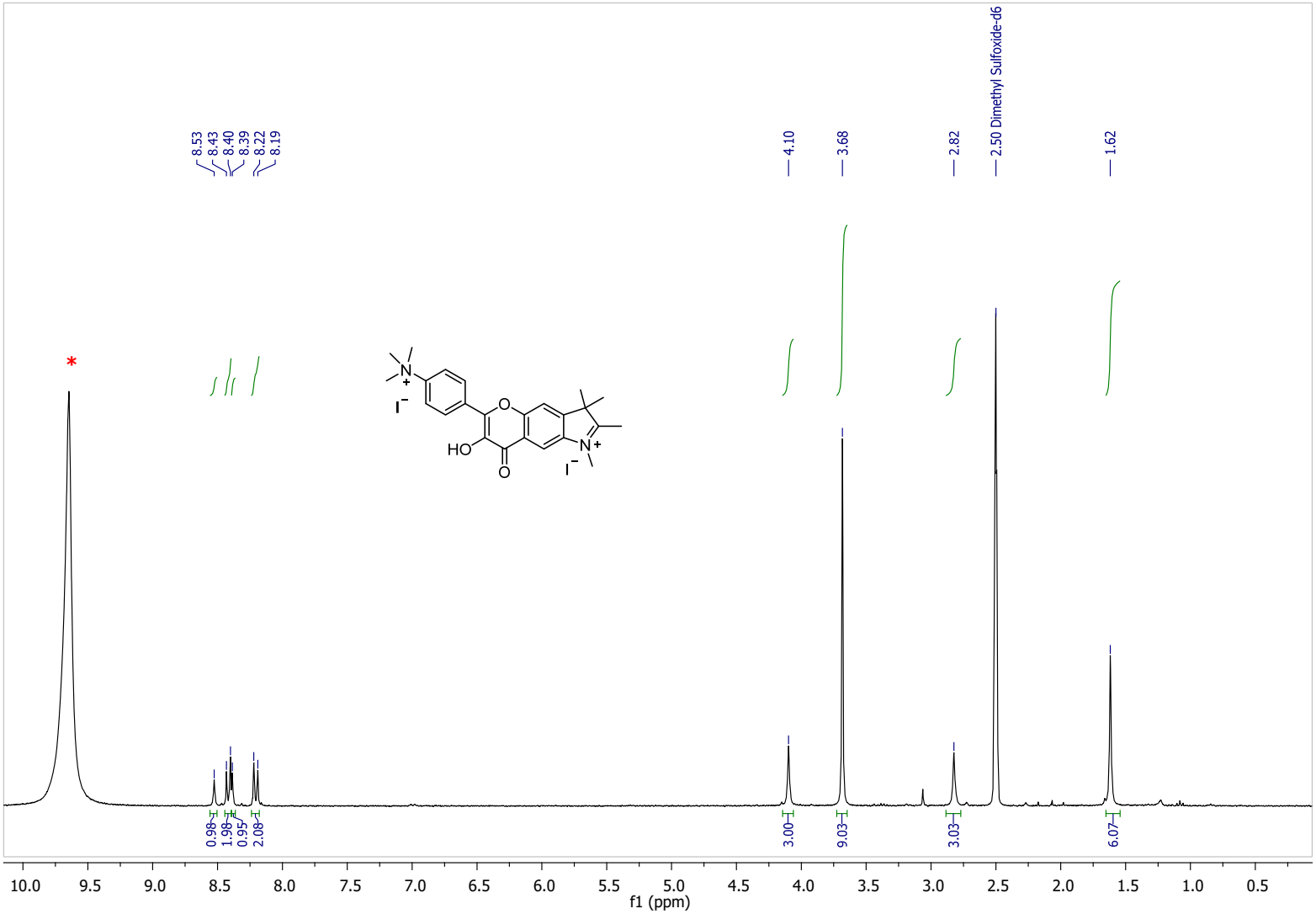

Figure S6. ^{1}H NMR (300 MHz, d_6–DMSO + 2 μL H_2SO_4): **10b**. Asterisk denotes H_2SO_4.

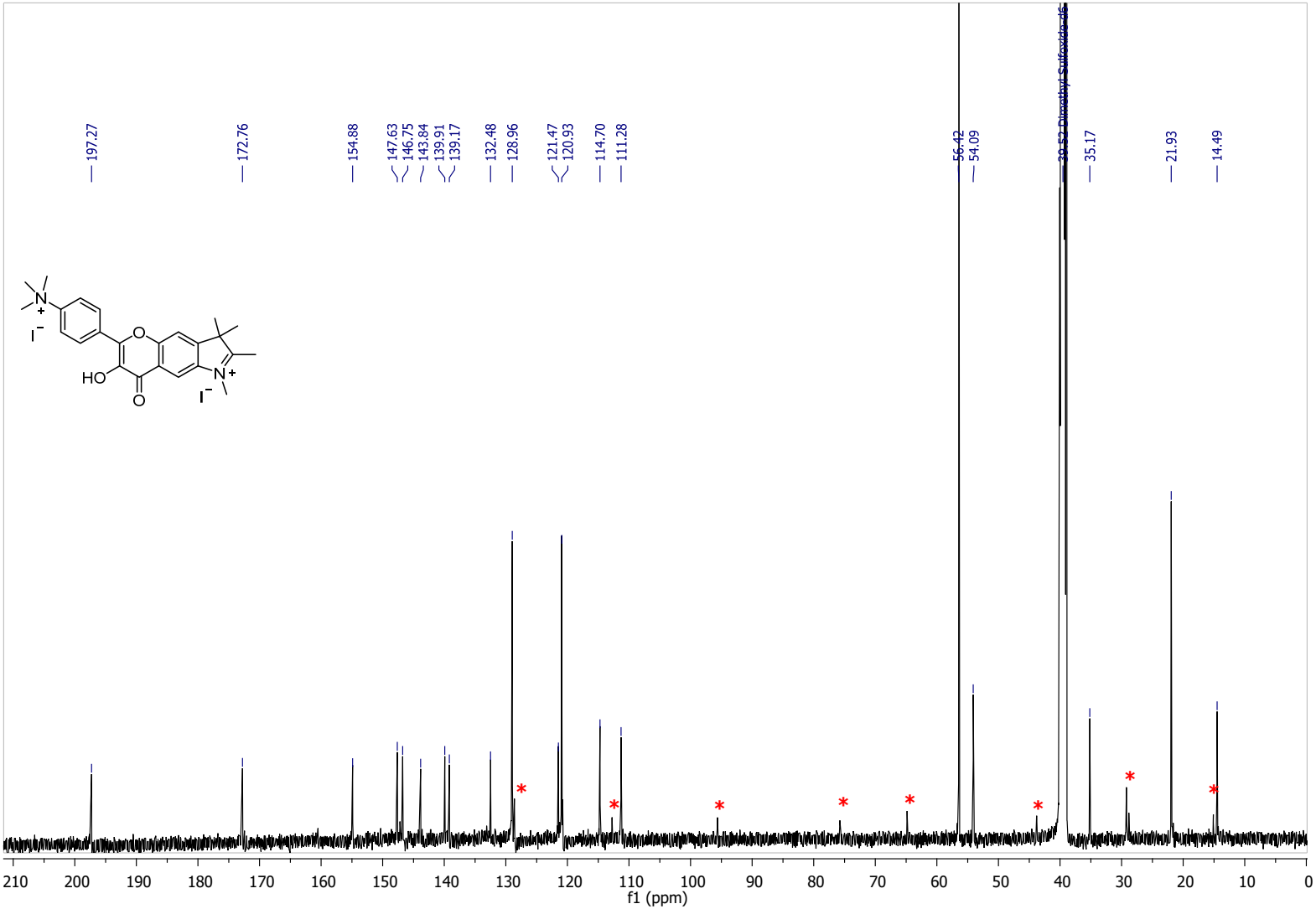

Figure S7. ^{13}C NMR (125 MHz, d_6–DMSO): **10b** and its tautomer (red asterisk).

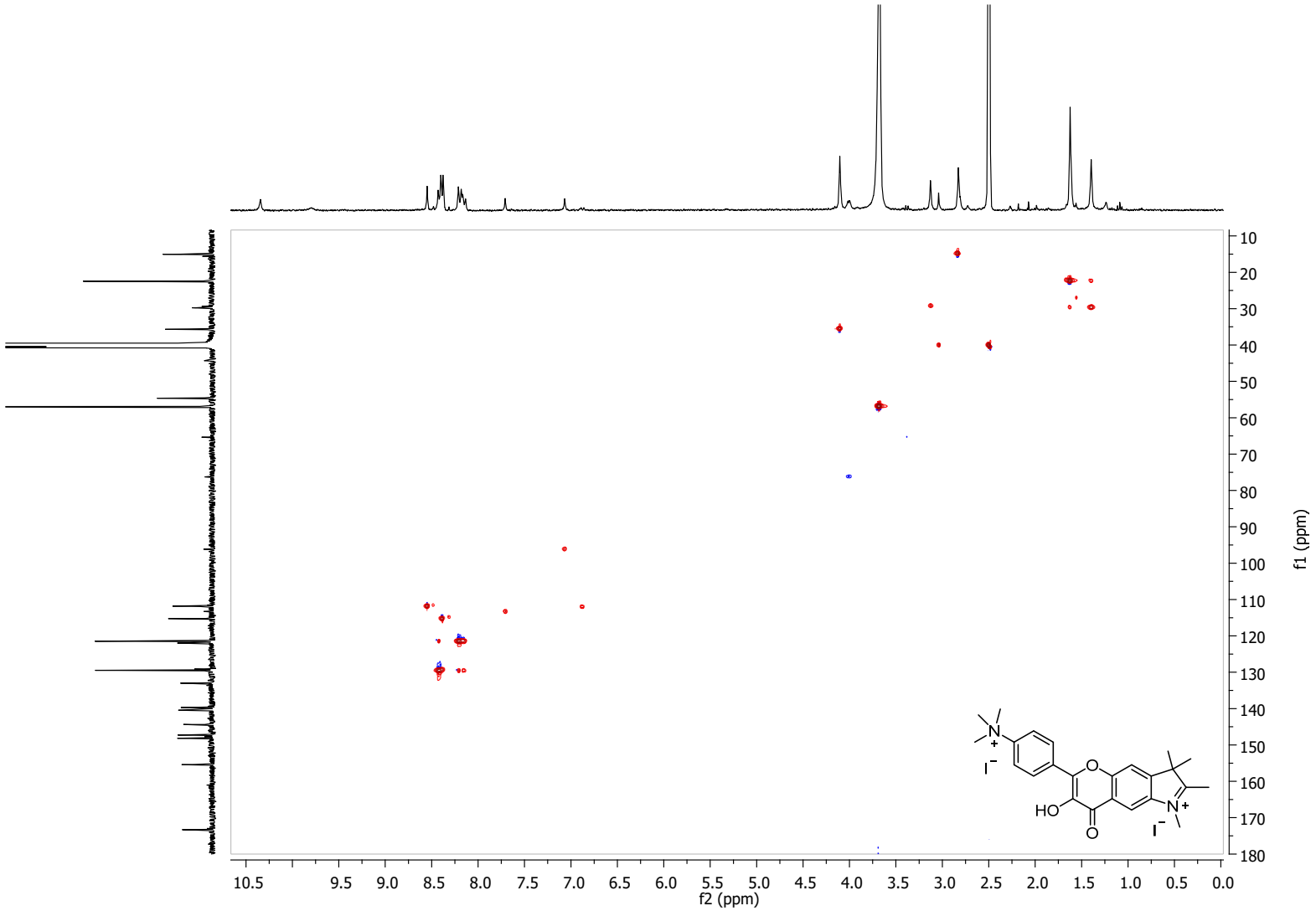

Figure S8. $^{1}H–^{13}C$ HSQC (500 MHz, d_6–DMSO): **10b** and its tautomer.

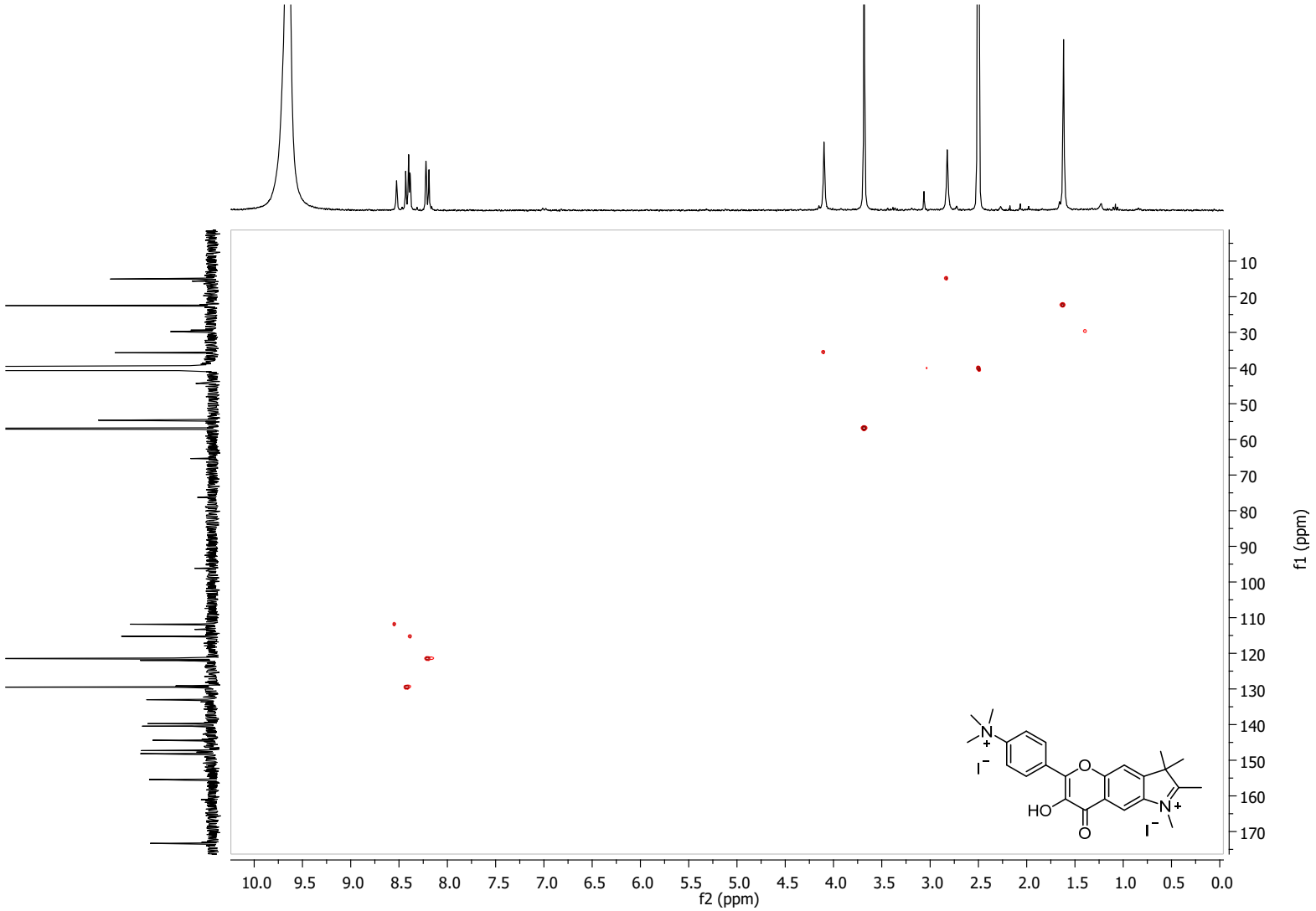

Figure S9. $^{1}H–^{13}C$ HSQC (500 MHz, d_6–DMSO): **10b**.

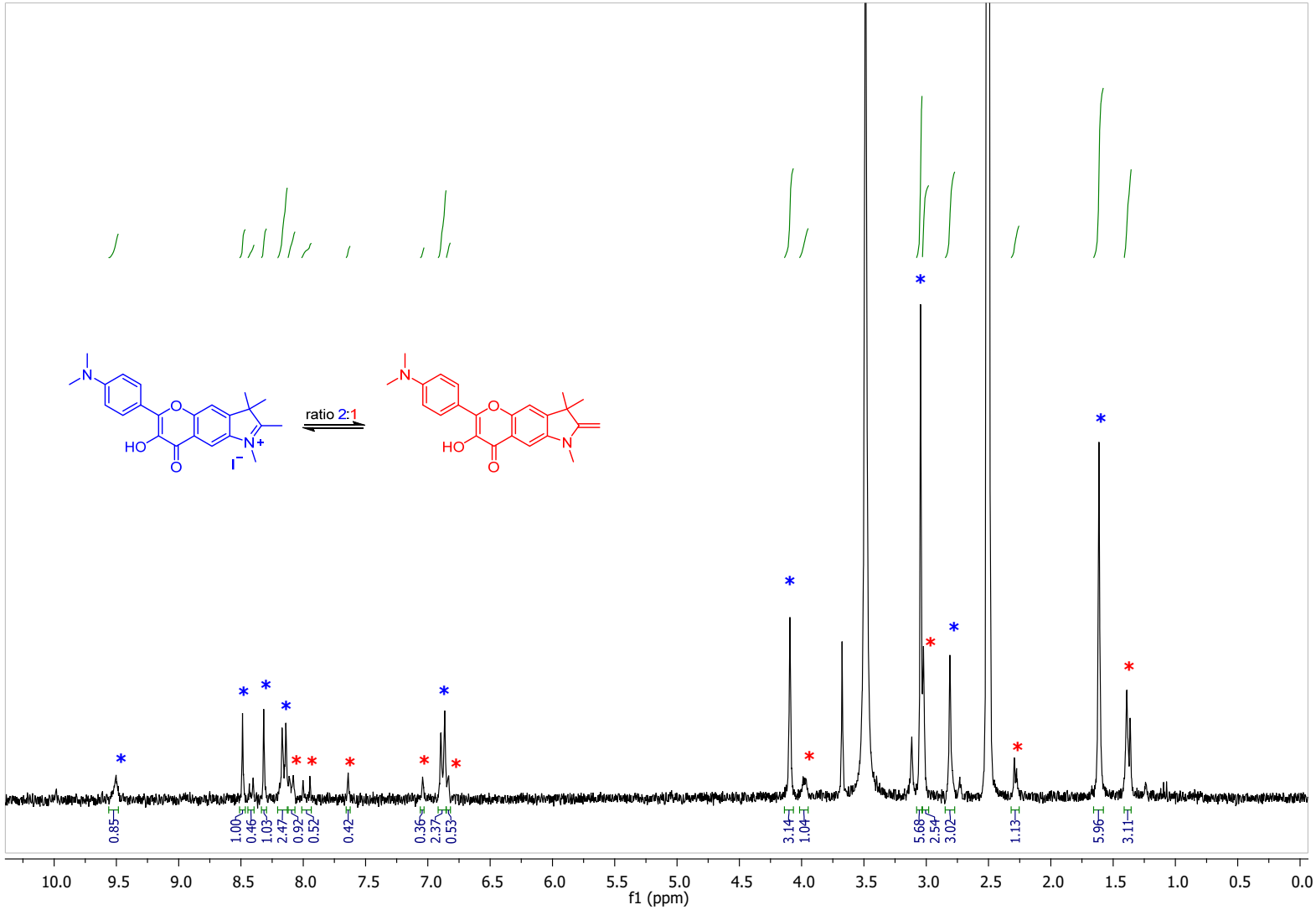

Figure S10. ^{1}H NMR (300 MHz, d_6–DMSO): **10c** (blue) and its tautomer (red).

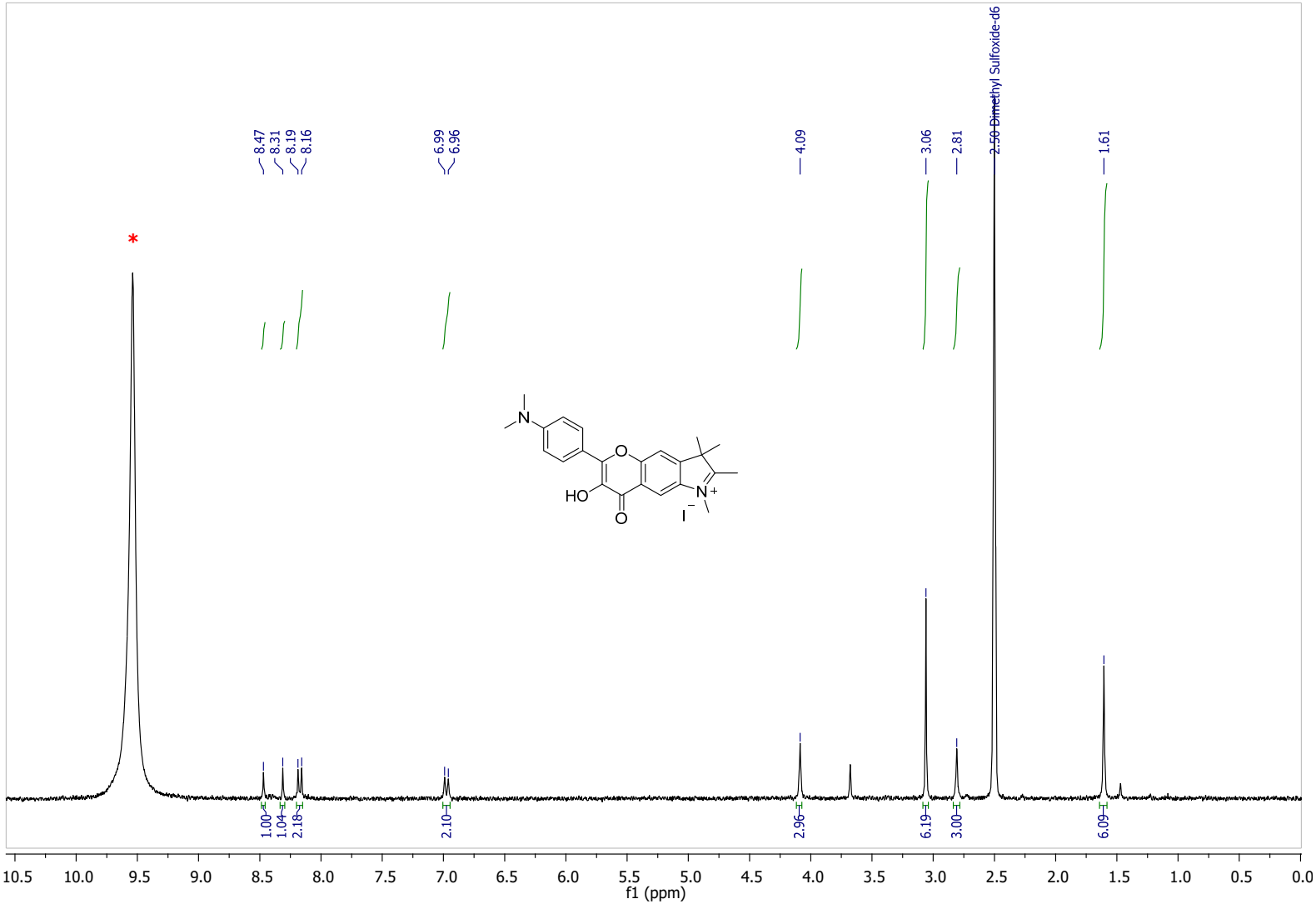

Figure S11. ^{1}H NMR (300 MHz, d_6–DMSO + 2µL H_2SO_4): **10c**. Asterisk denotes H_2SO_4.

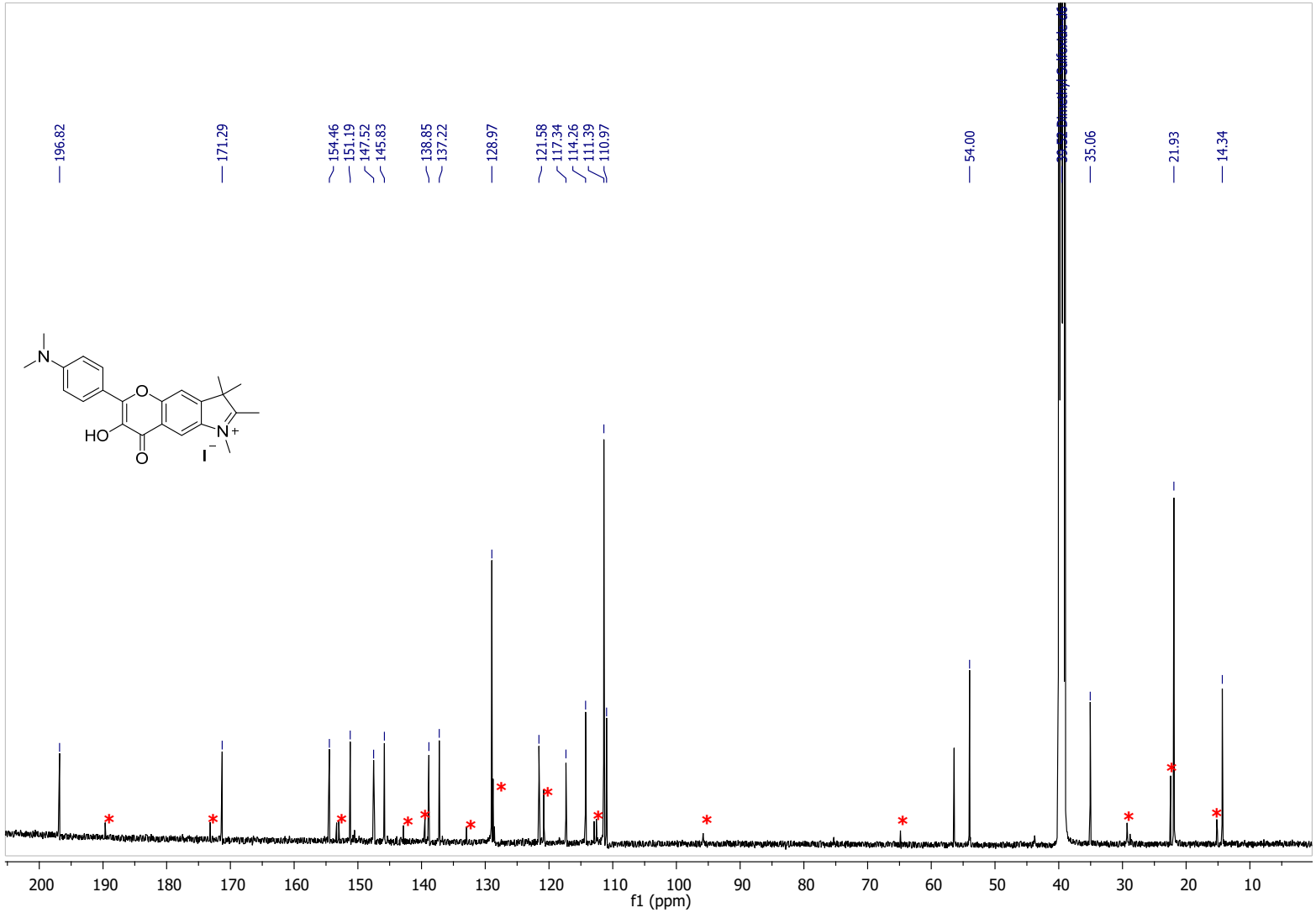

Figure S12. ^{13}C NMR (125 MHz, d_6–DMSO): **10c** and its tautomer (red asterisk).

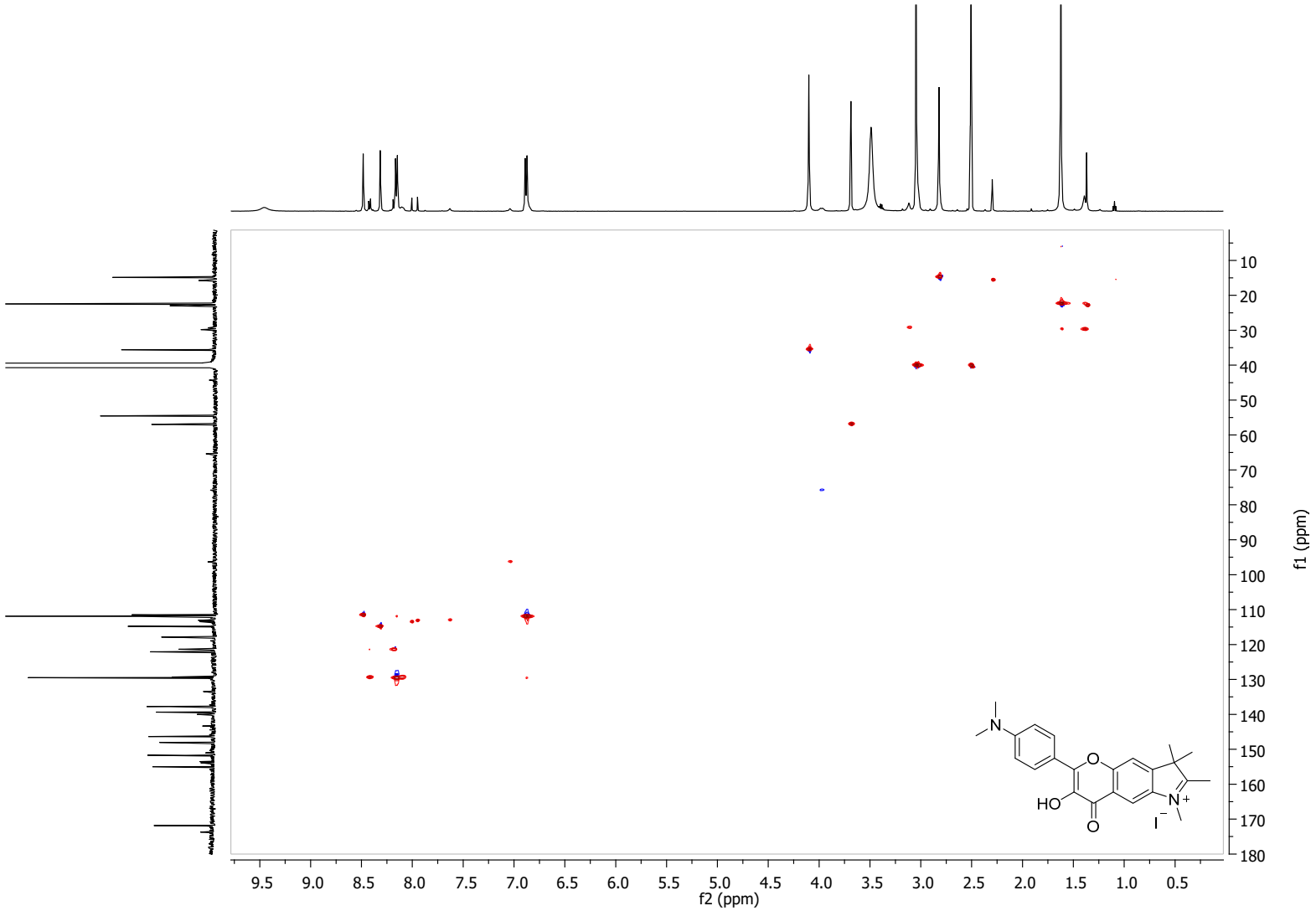

Figure S13. $^{1}H–^{13}C$ HSQC (500 MHz, d_6–DMSO): **10c** and its tautomer.

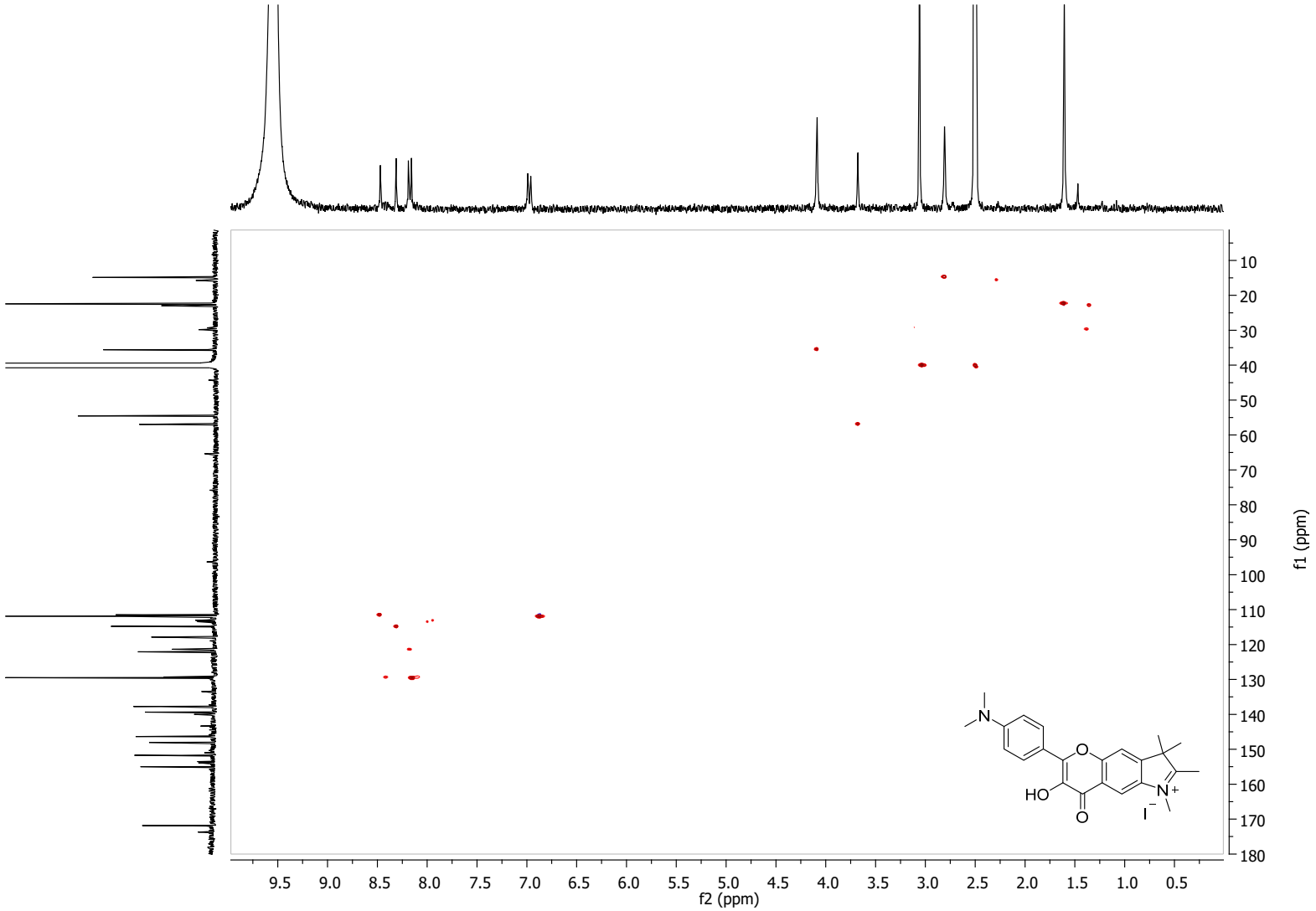

Figure S14. $^{1}H-^{13}C$ HSQC (500 MHz, d_6–DMSO): **10c**.

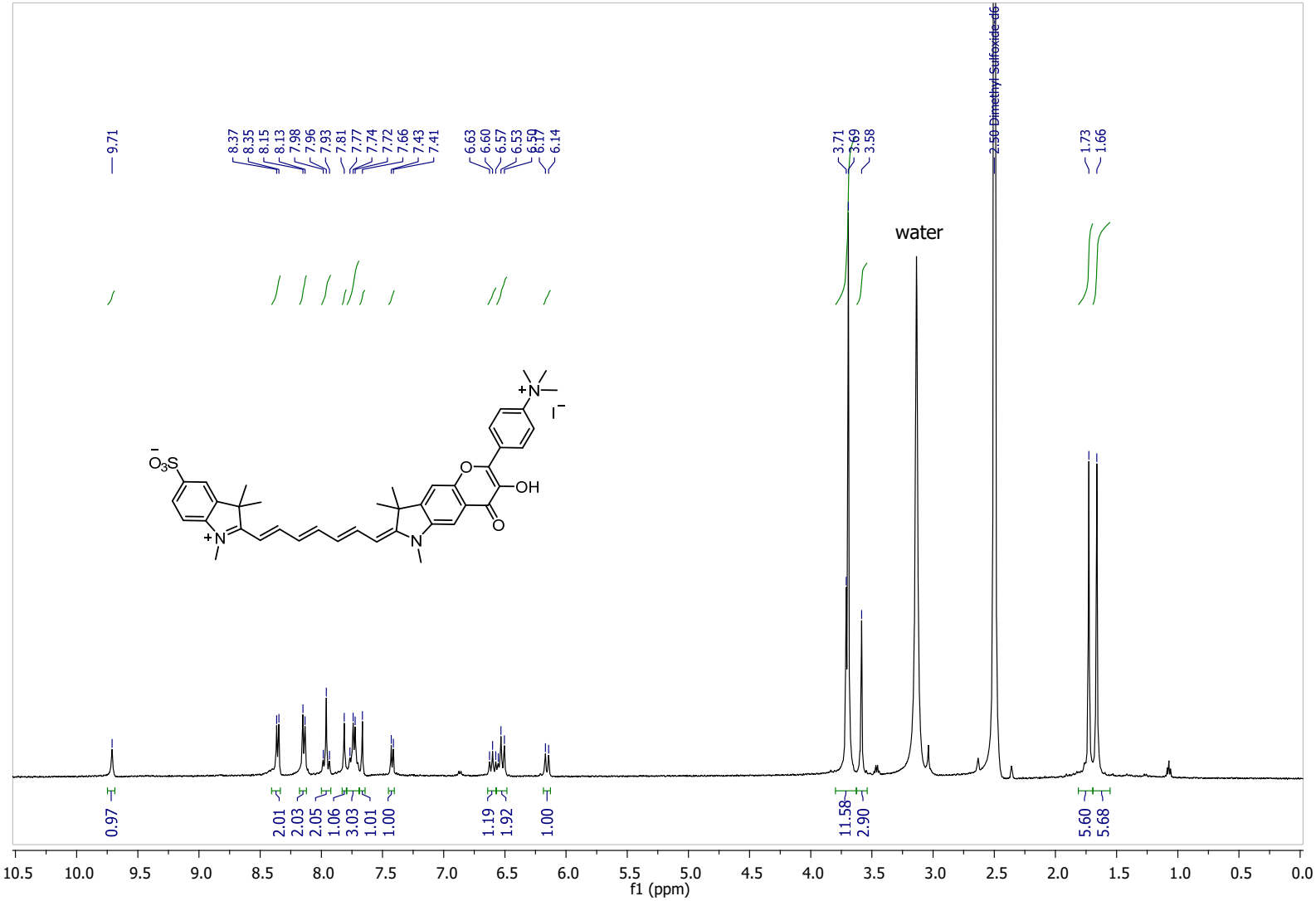

Figure S15. ^{1}H NMR (500 MHz, d_6–DMSO): **3**. Asterisk denotes residual water from d_6–DMSO.

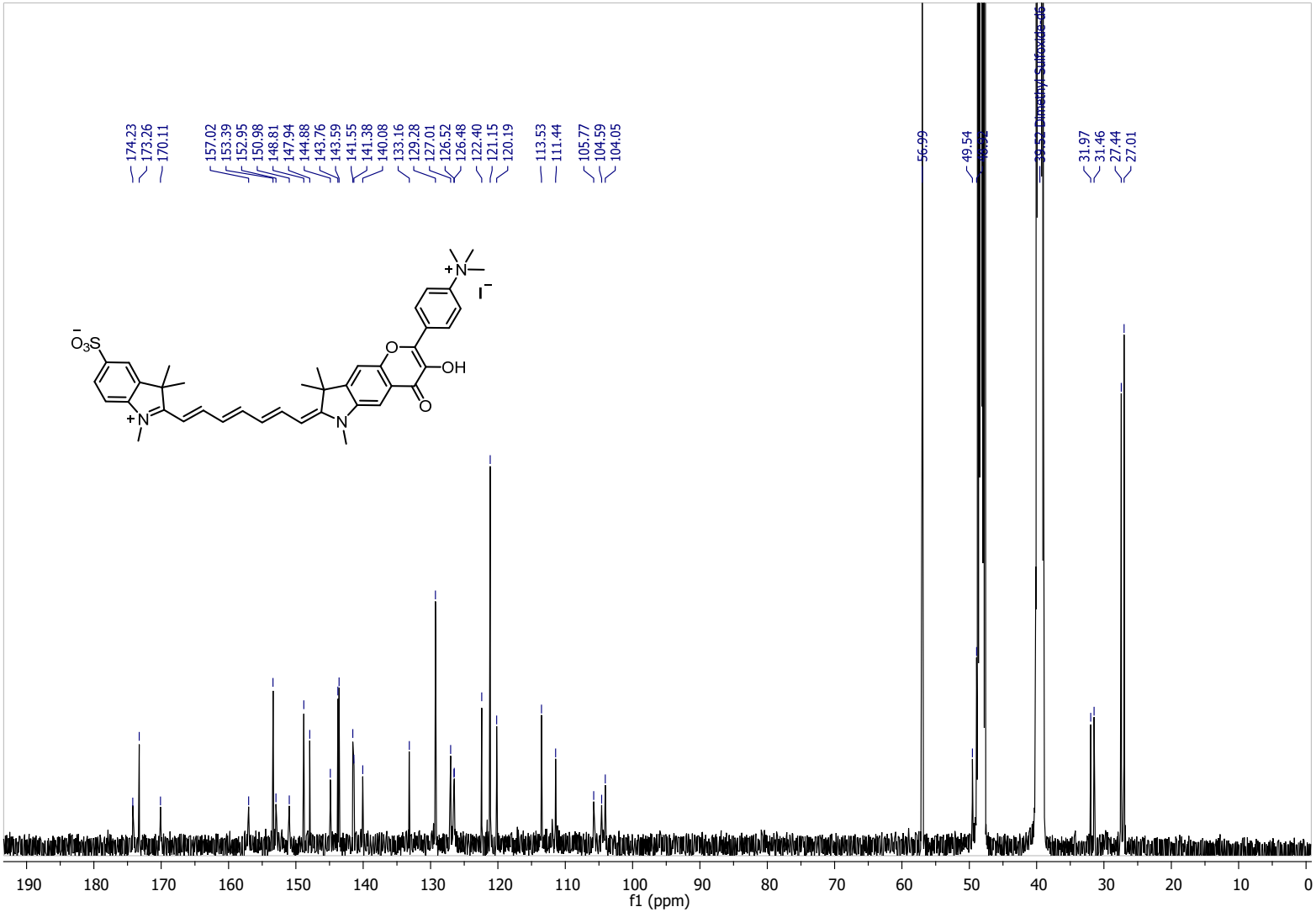

Figure S16. ^{13}C NMR (125 MHz, d_6–DMSO/d_4–MeOD (1:1)): **3**.

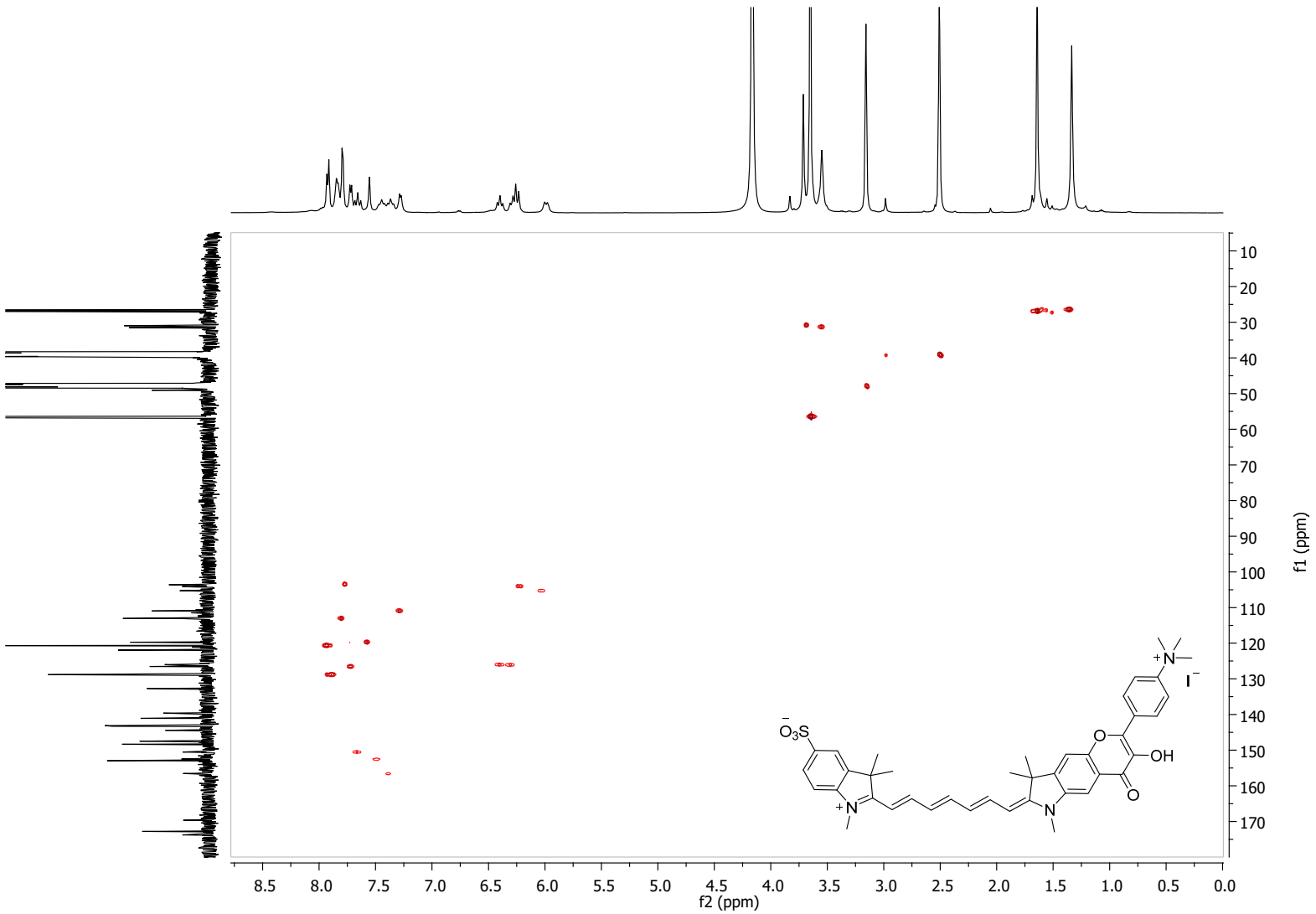

Figure S17. $^{1}H-^{13}C$ HSQC (500 MHz, d_6–DMSO/d_4–MeOD (1:1)): **3**.

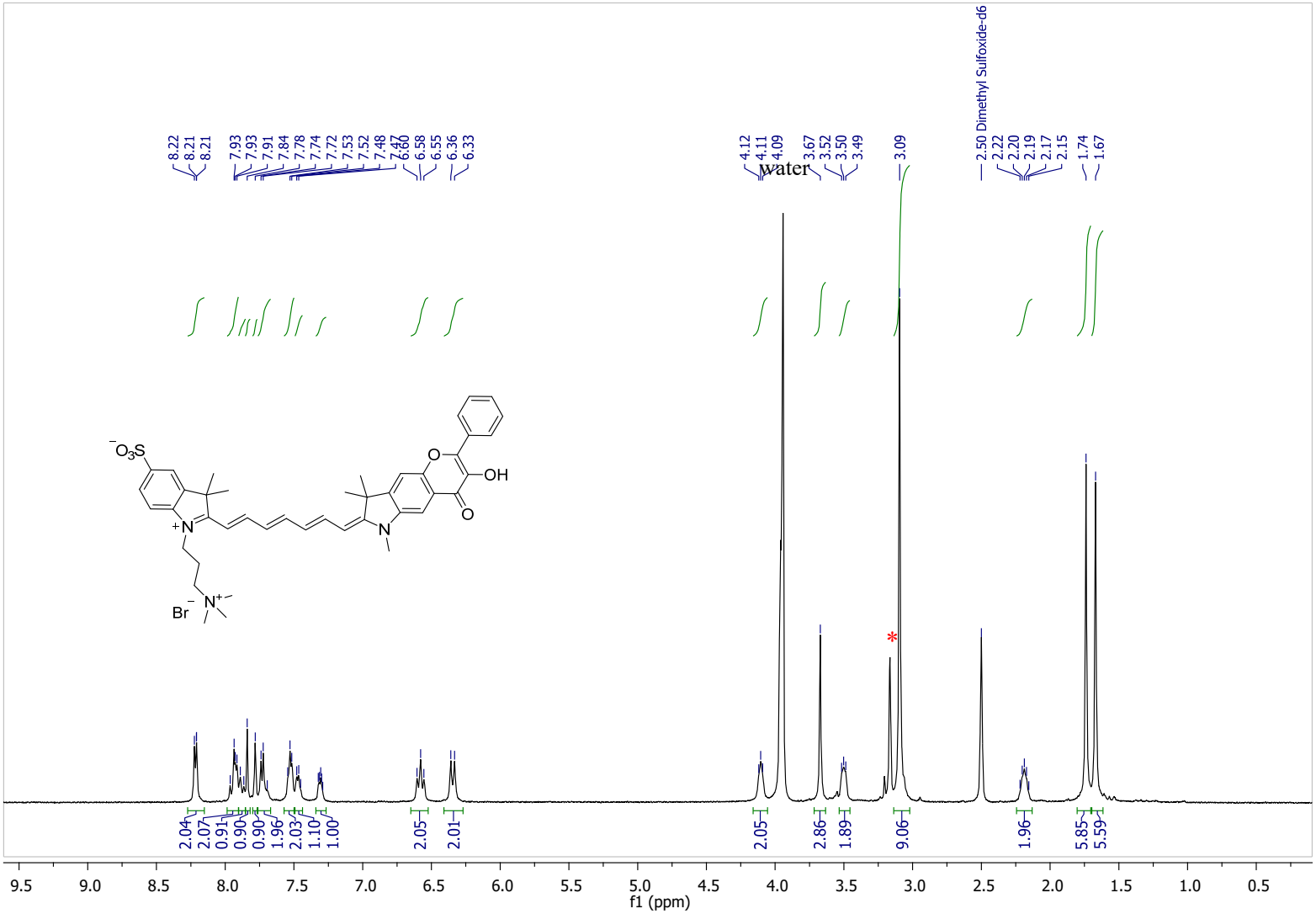

Figure S18. ^{1}H NMR (500 MHz, d_6–DMSO/d_4–MeOD (1:1)): **4**. Asterisk denotes d_4–MeOD.

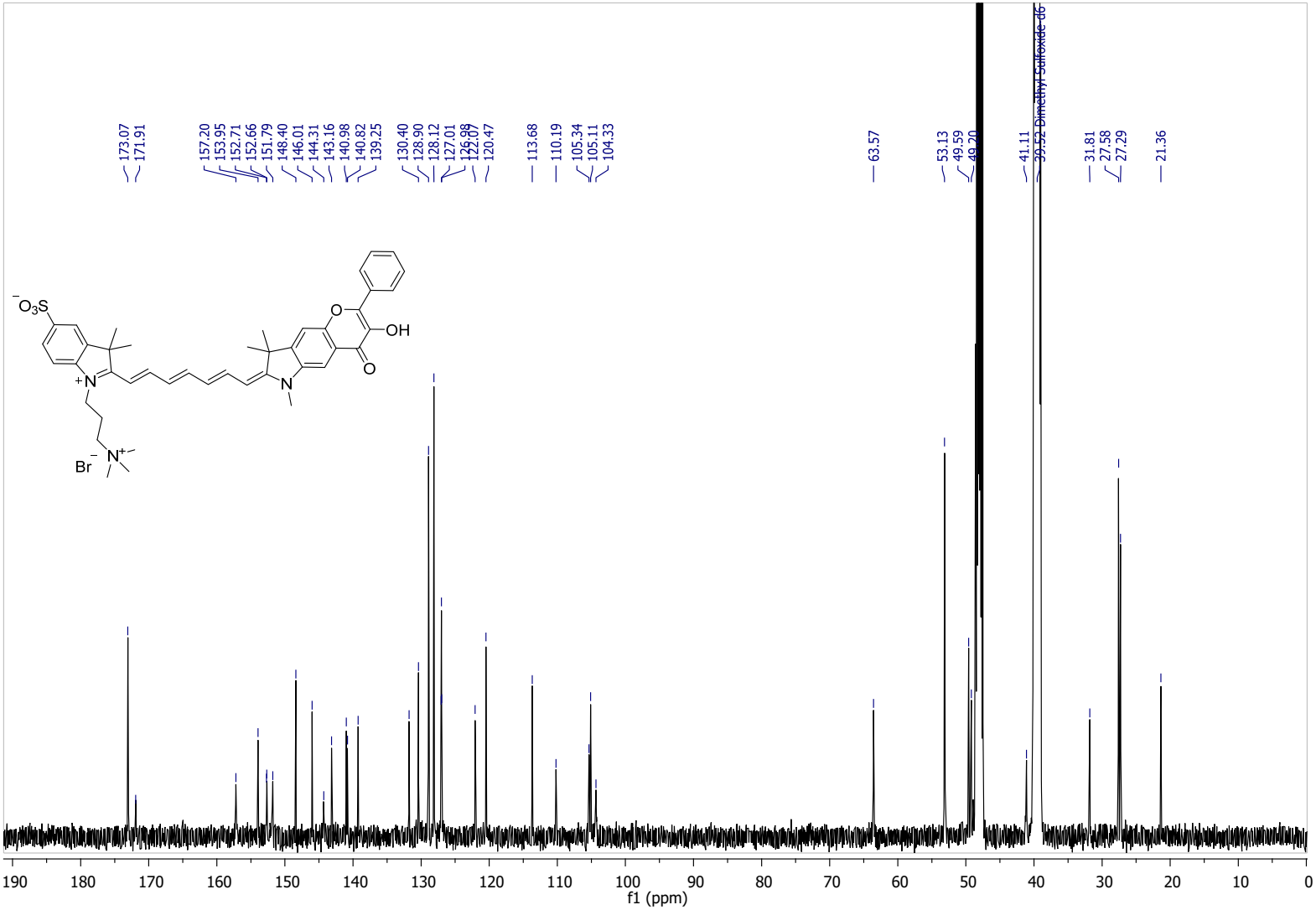

Figure S19. ^{13}C NMR (125 MHz, d_6–DMSO/d_4–MeOD (1:1)): **4**.

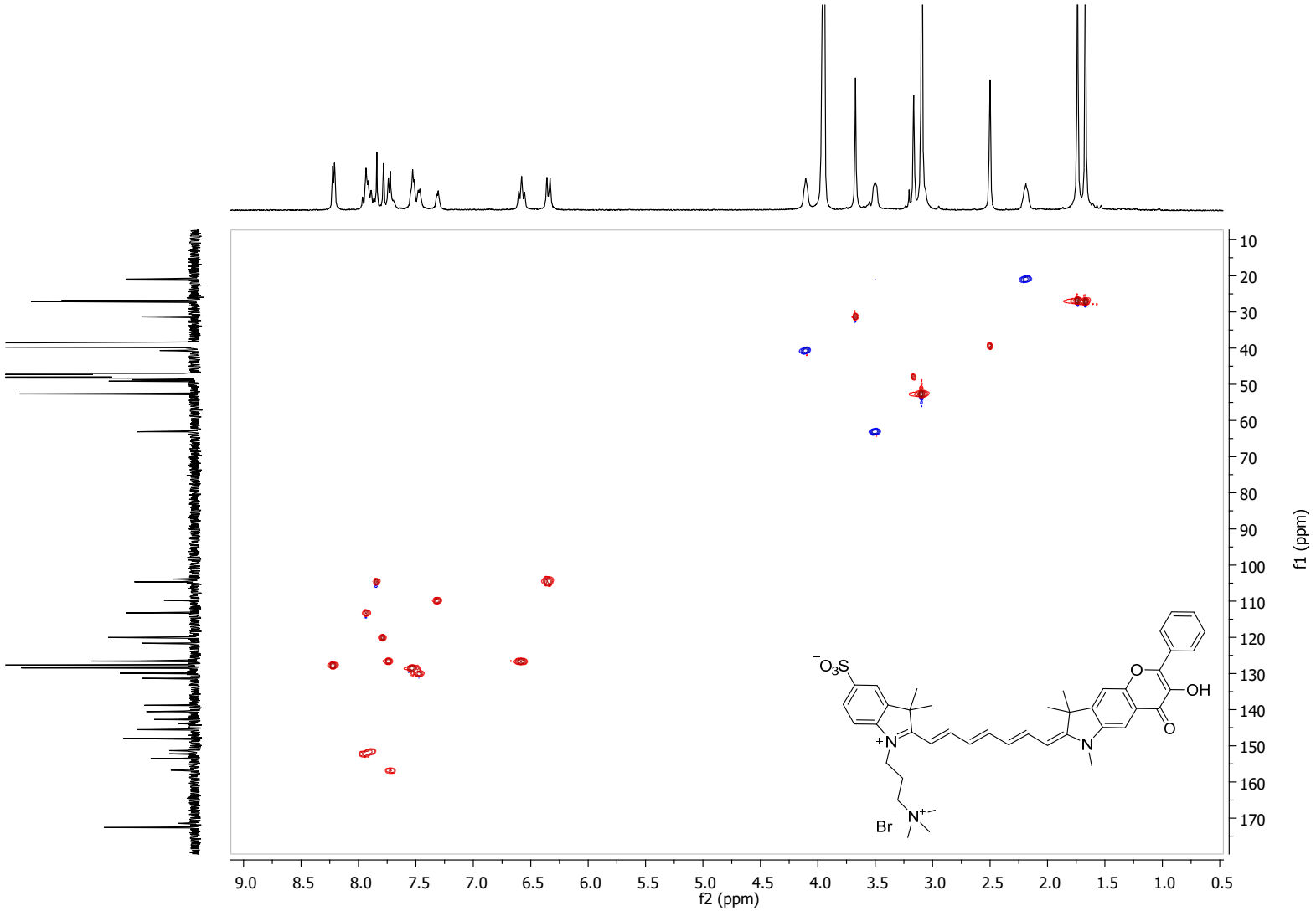

Figure S20. $^{1}H–^{13}C$ HSQC (500 MHz, d_6–DMSO/d_4–MeOD (1:1)): **4**.

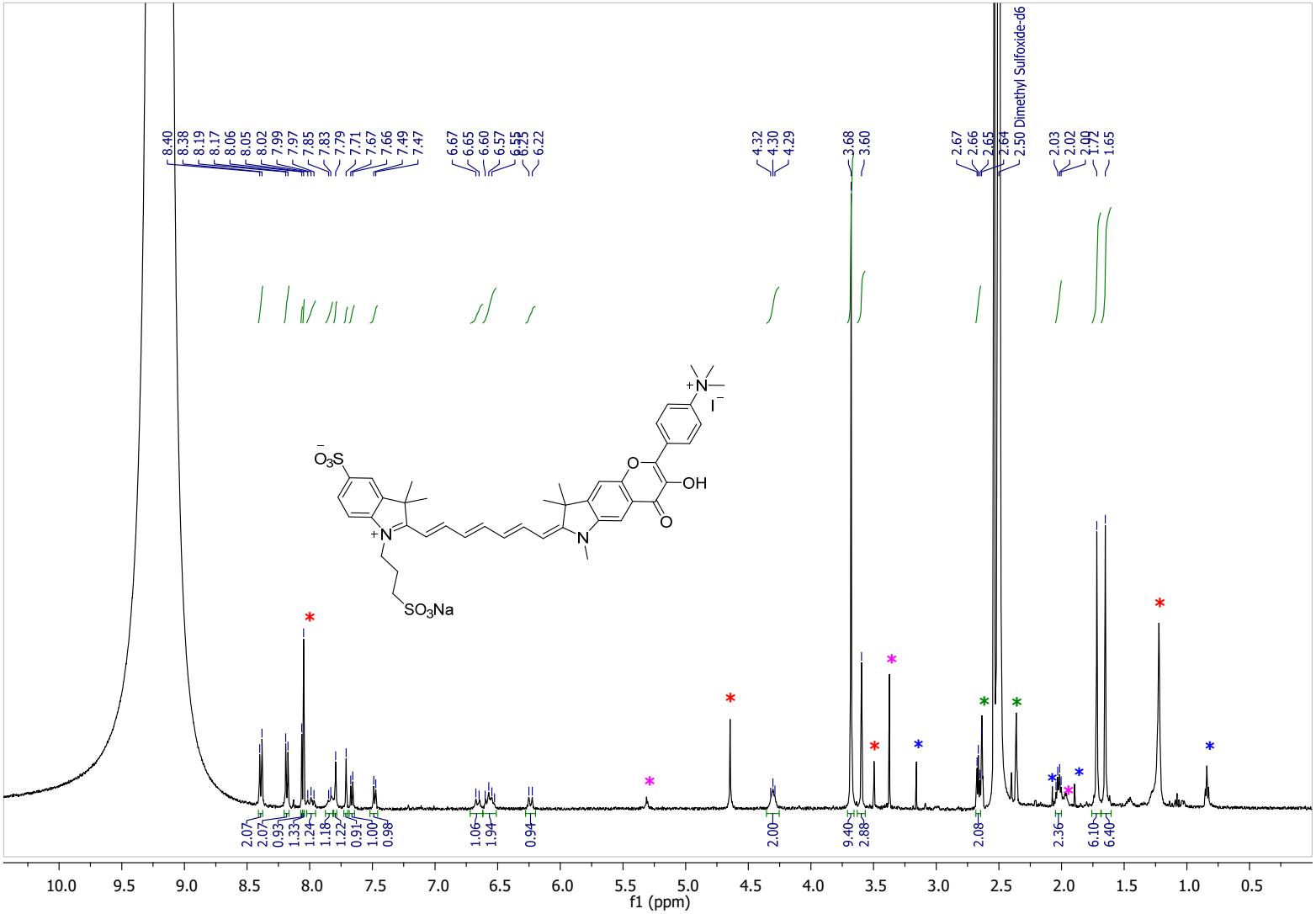

Figure S21. [1]H NMR (500 MHz, d_6–DMSO): **5**. The compound was very poorly soluble in any solvent. Asterisks denote impurities from the syringe filter (red), solvents (blue), satellite peaks of d_6–DMSO (green), and unknown impurities (magenta).

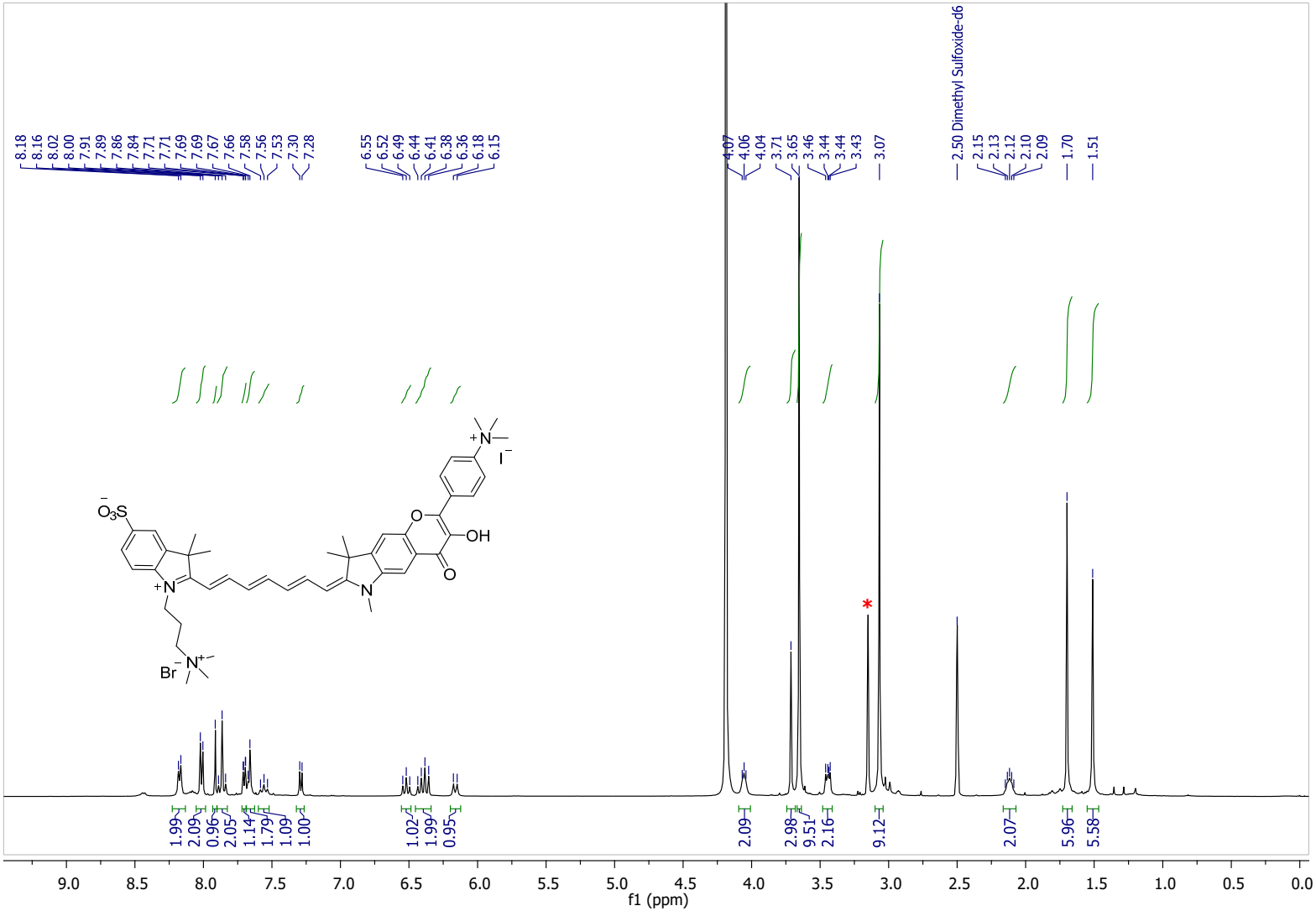

Figure S22. ^{1}H NMR (500 MHz, d_6–DMSO/d_4–MeOD (1:1)): **6**. Asterisk denotes d_4–MeOD.

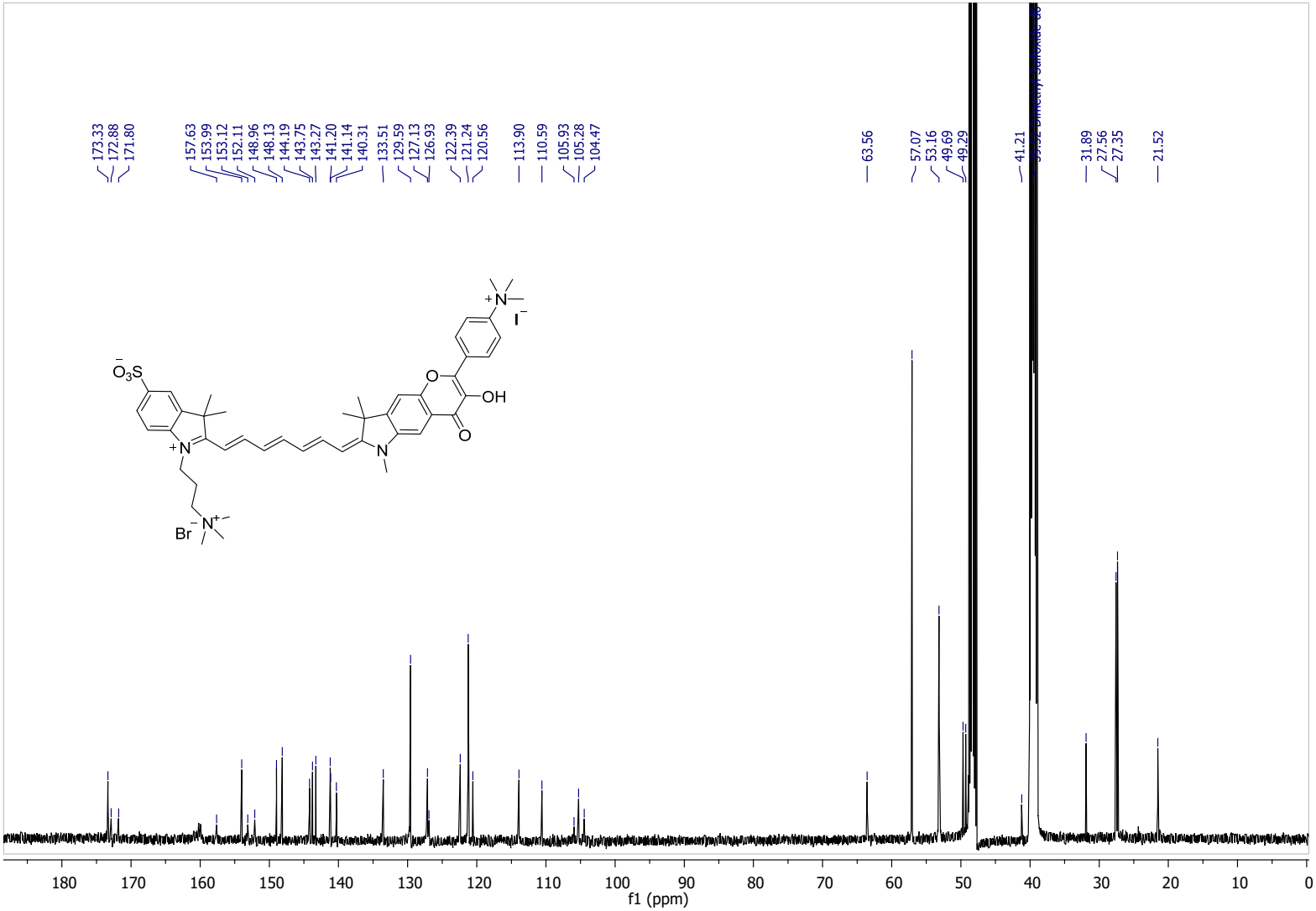

Figure S23. ^{13}C NMR (125 MHz, d_6–DMSO/d_4–MeOD (1:1)): **6**.

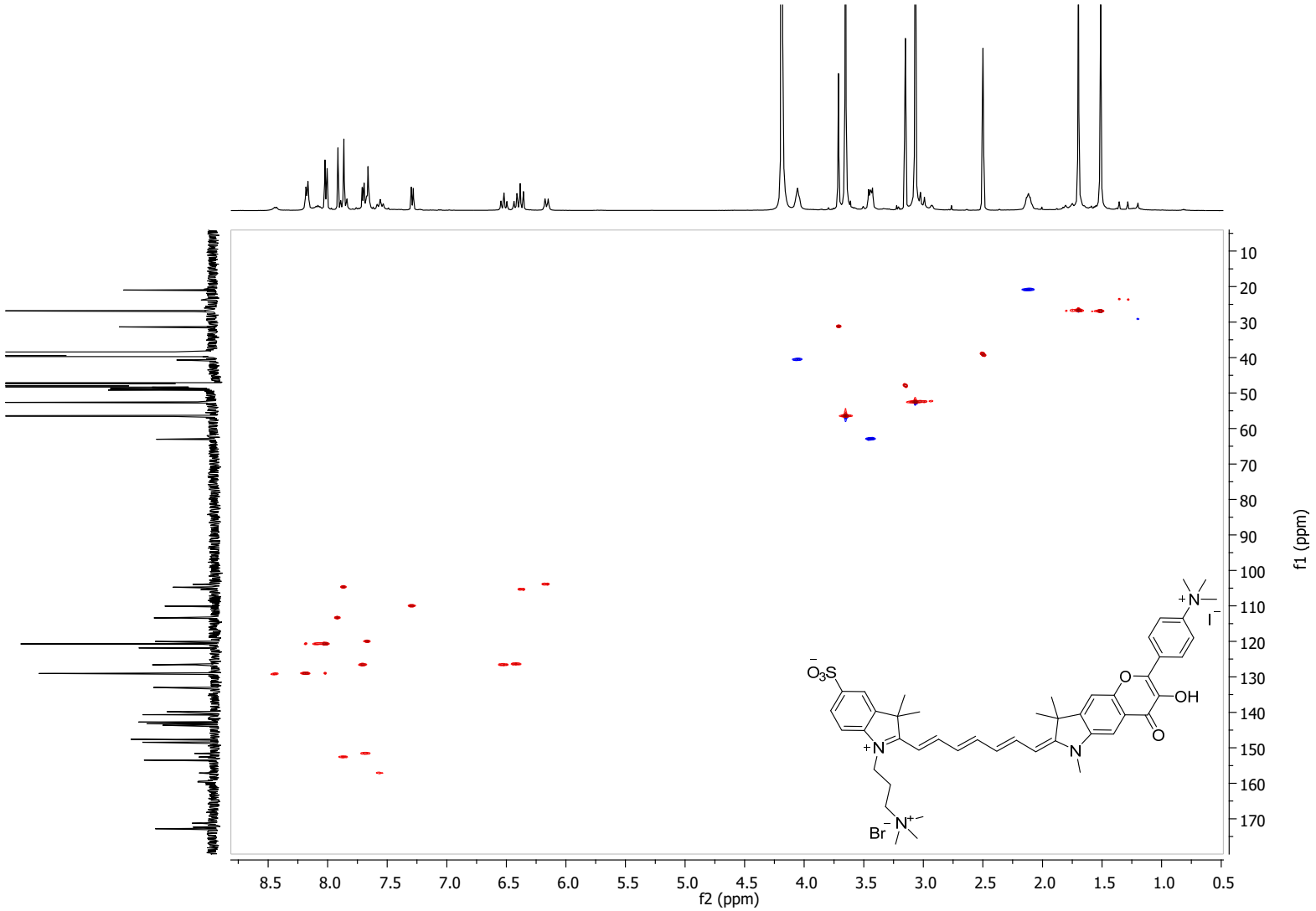

Figure S24. $^{1}H–^{13}C$ HSQC (500 MHz, d_6–DMSO/d_4–MeOD (1:1)): **6**.

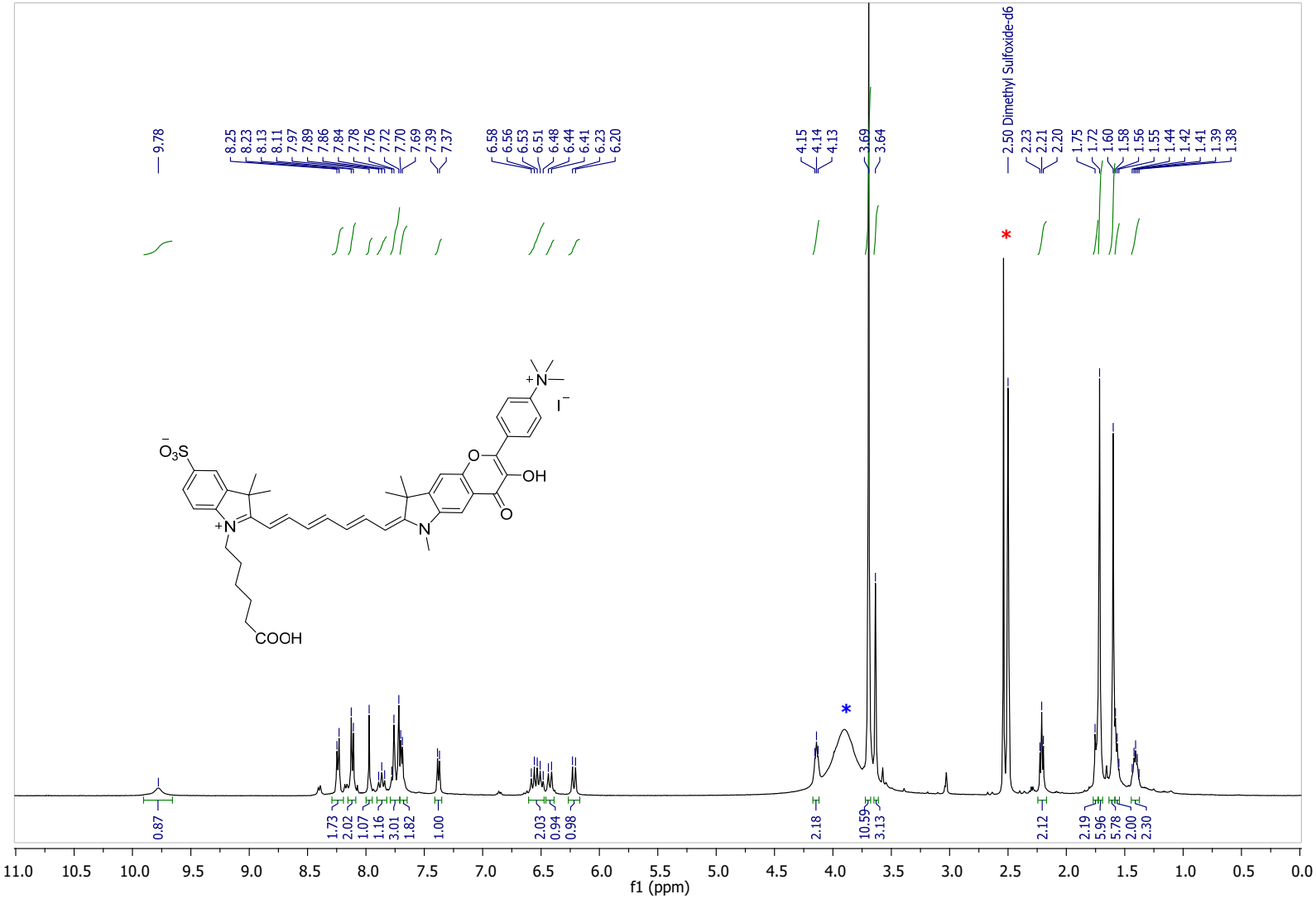

Figure S25. ^{1}H NMR (500 MHz, d_6–DMSO): **7**. Asterisks denote residual DMSO (red) from purification and water (blue).

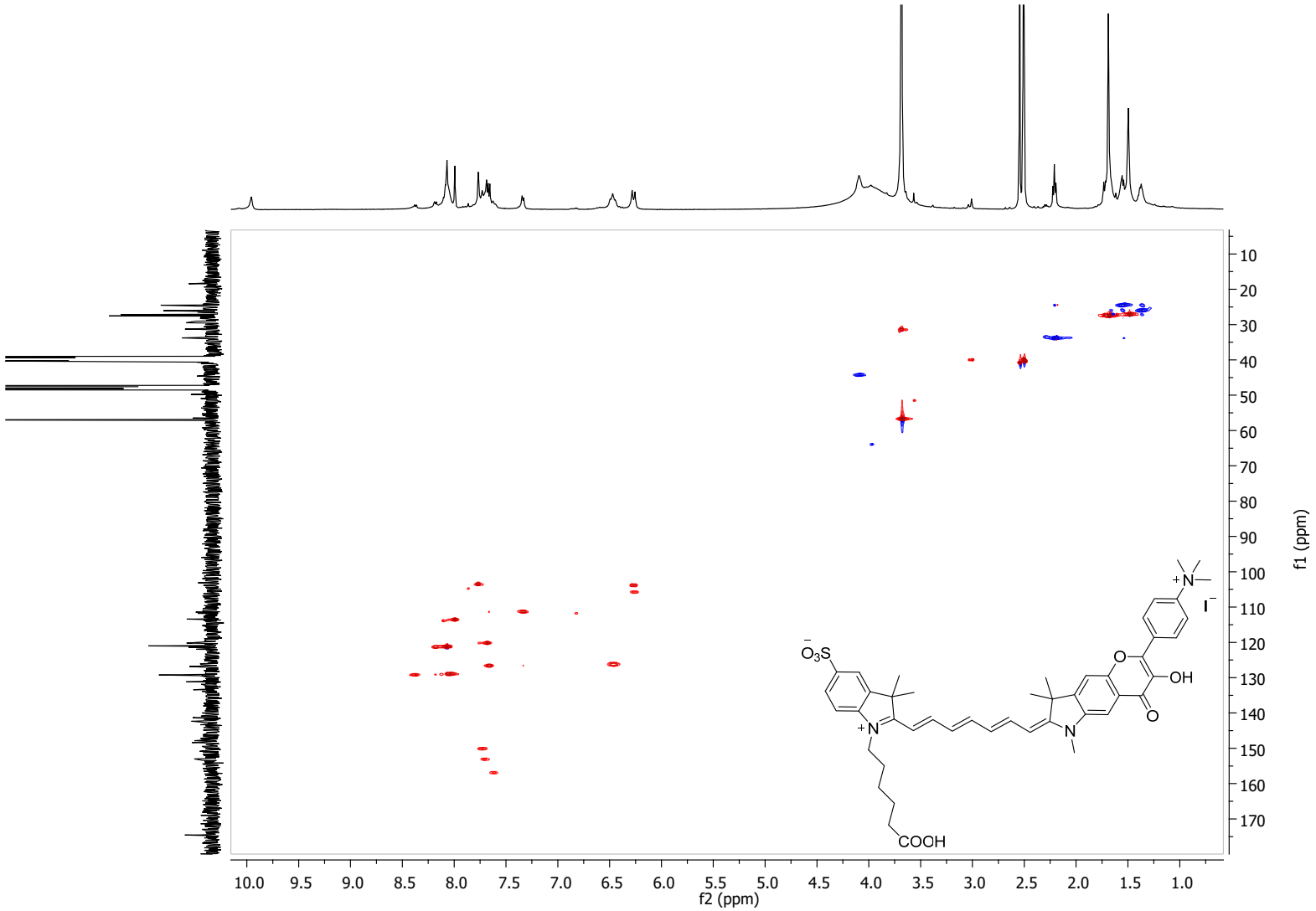

Figure S26. $^{1}H–^{13}C$ HSQC (500 MHz, d_6–DMSO): **7**.

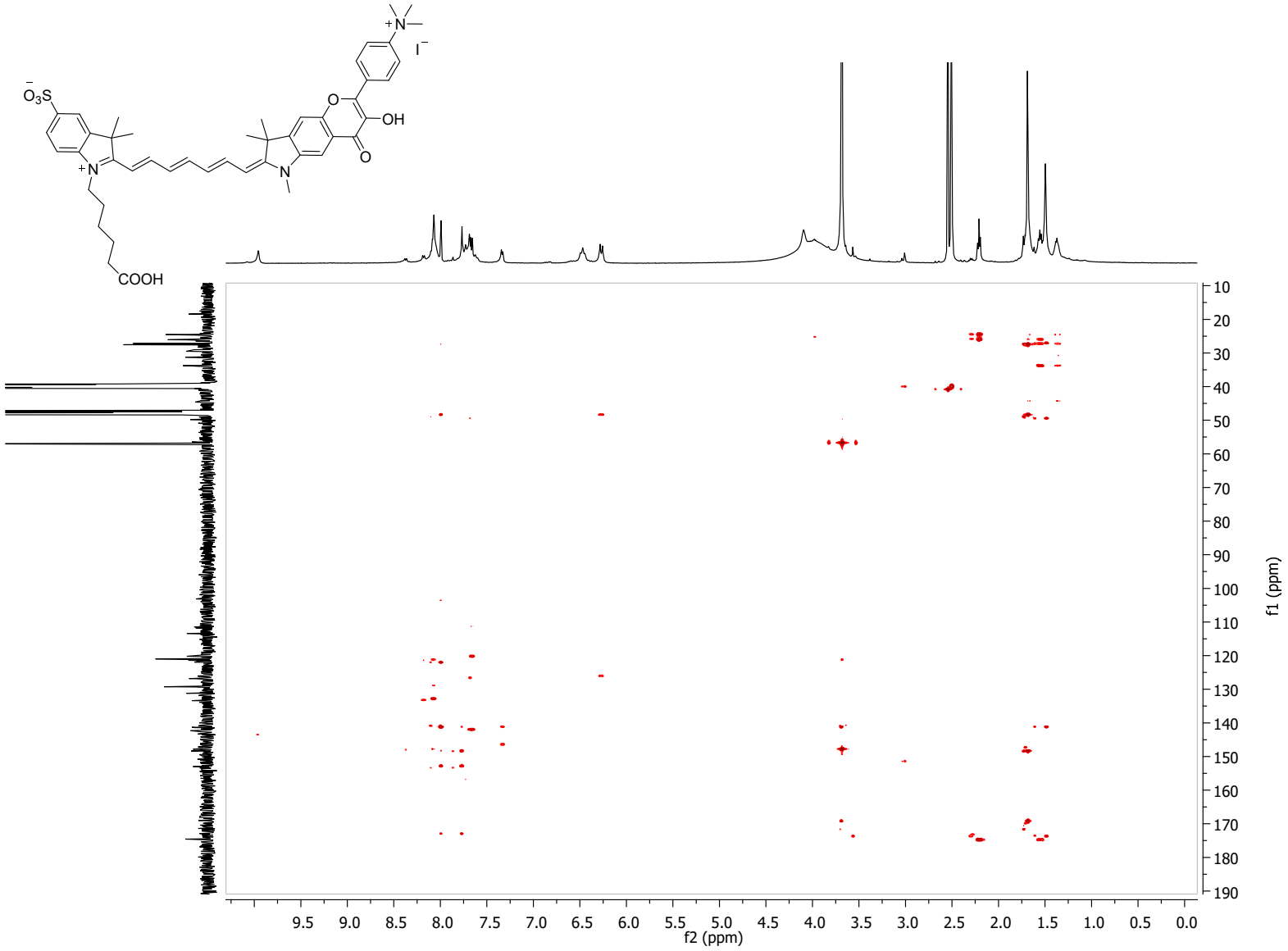

Figure S27. $^{1}H–^{13}C$ HMBC (500 MHz, d_6–DMSO): **7**.

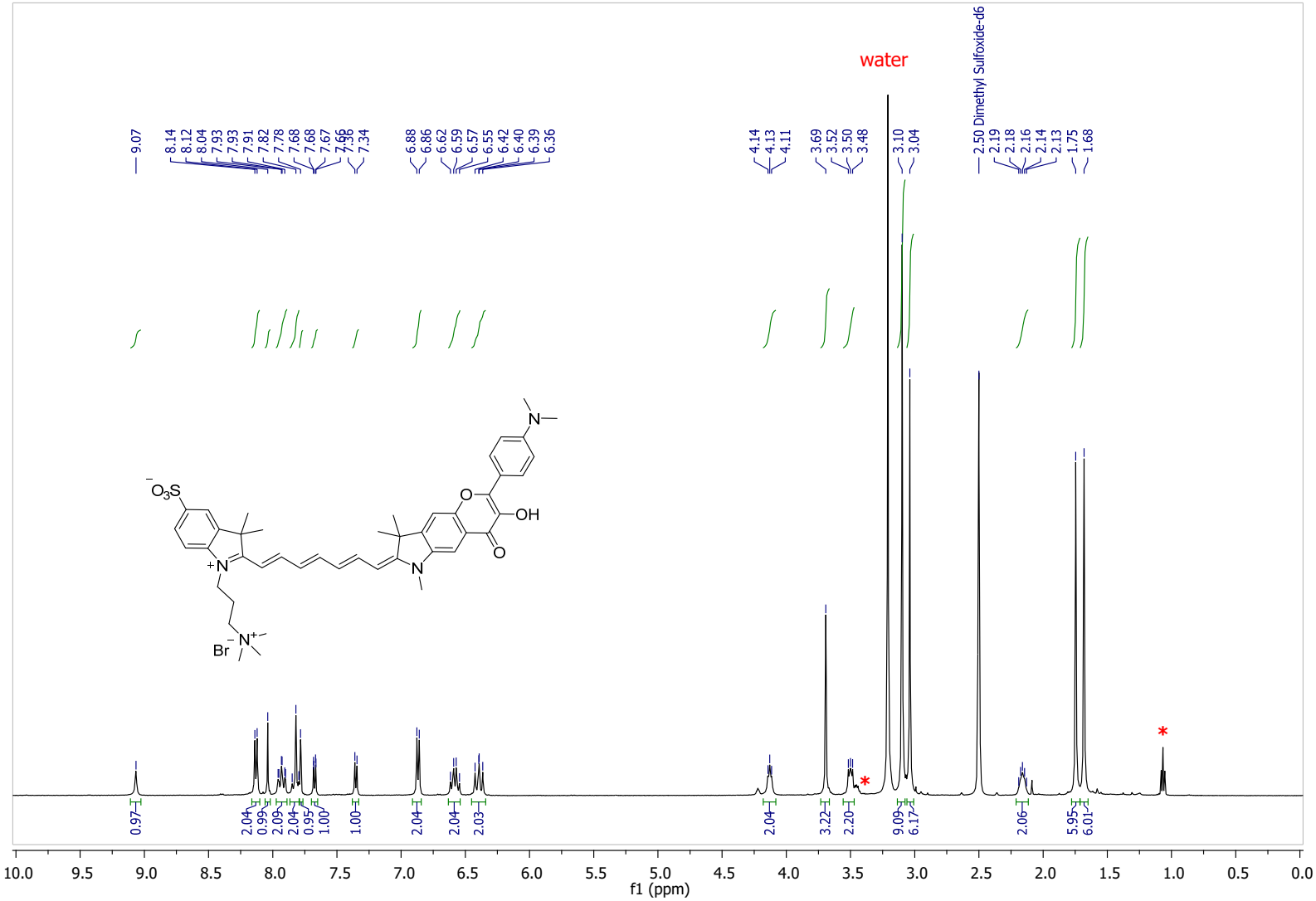

Figure S28. ^{1}H NMR (500 MHz, d_6–DMSO): **8**. Asterisk denotes residual ethanol from purification.

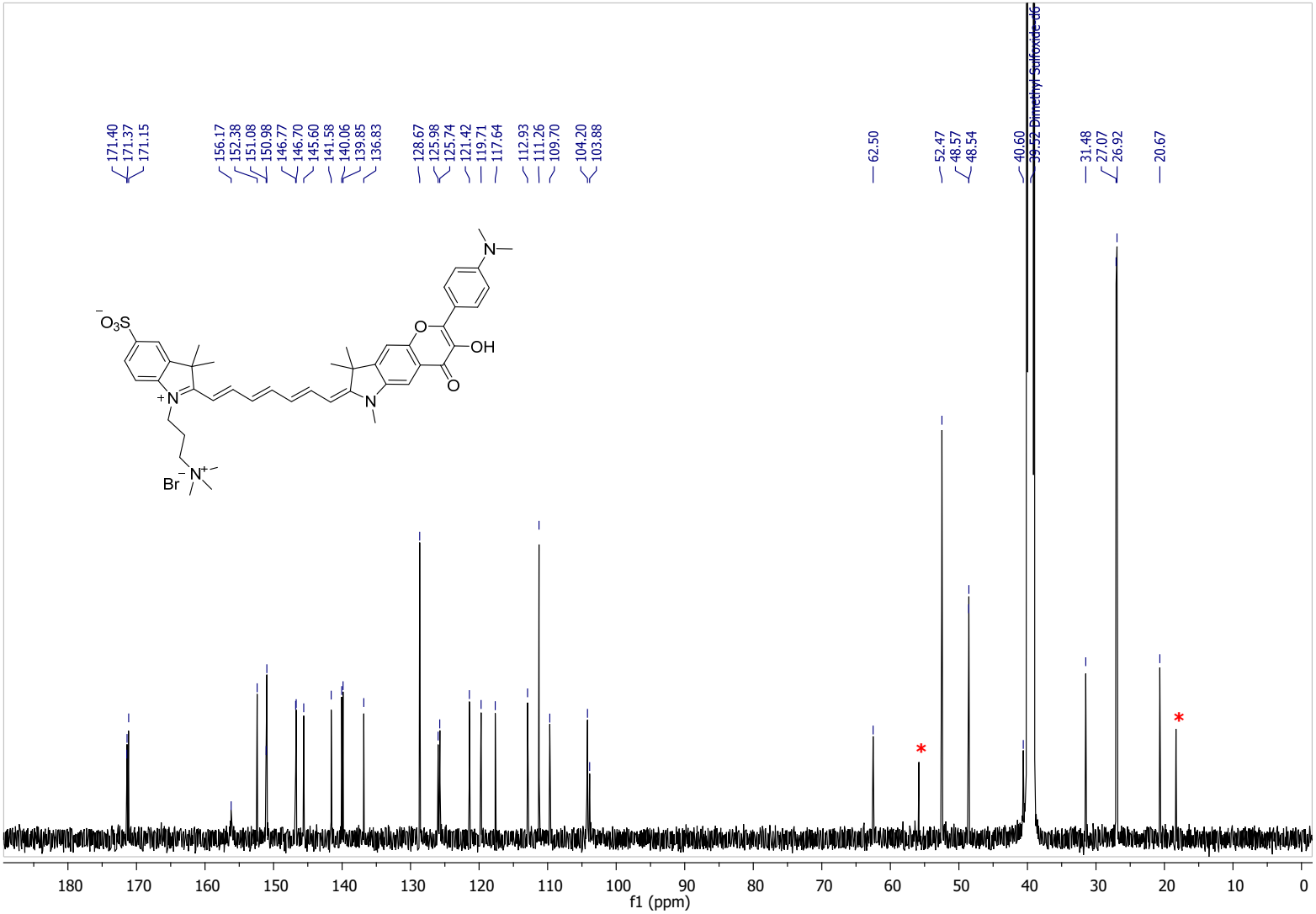

Figure S29. ^{13}C NMR (125 MHz, d_6–DMSO): **8**. Asterisk denotes residual ethanol from purification.

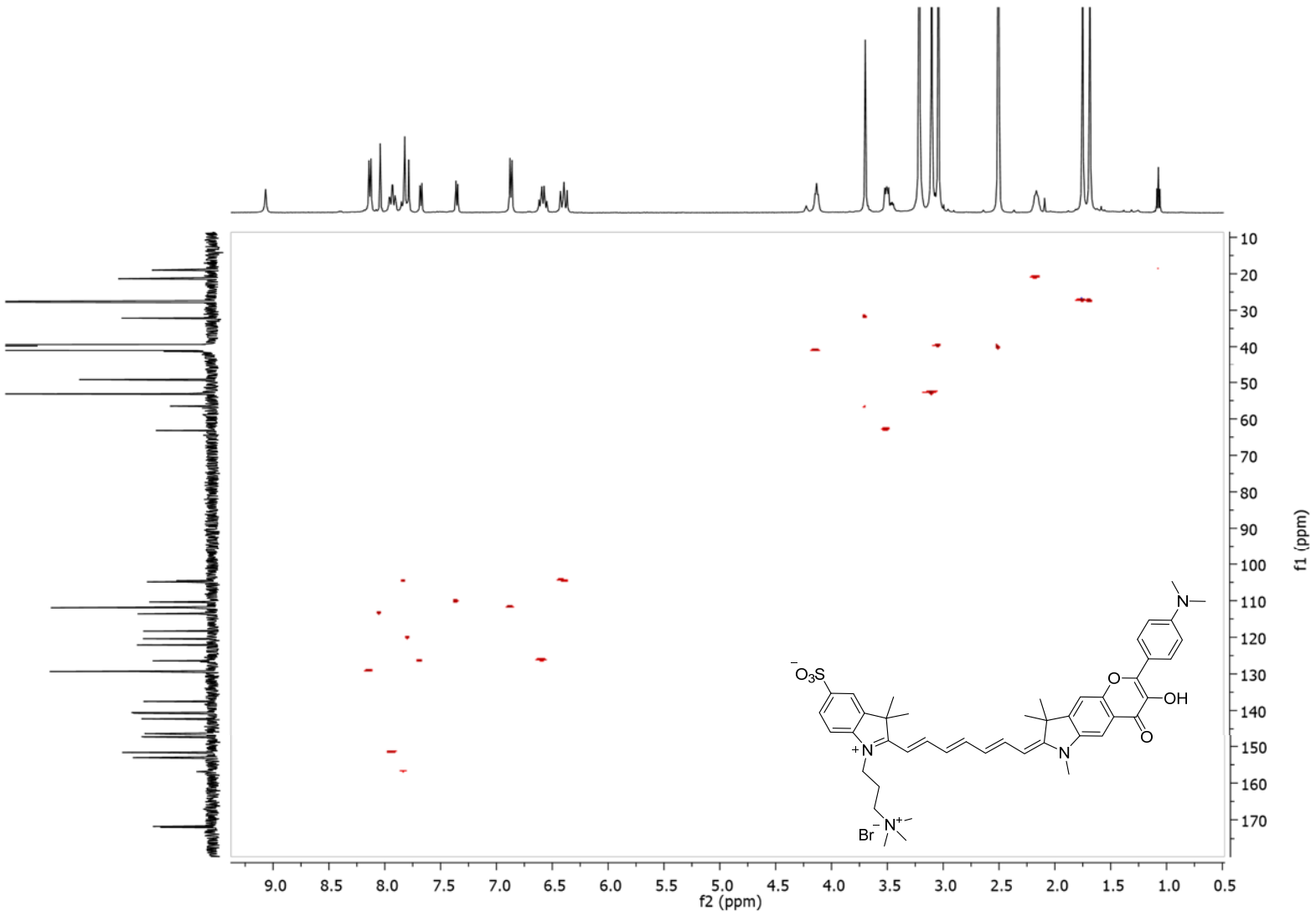

Figure S30. $^{1}H–^{13}C$ HSQC (500 MHz, d_6–DMSO): **8**.

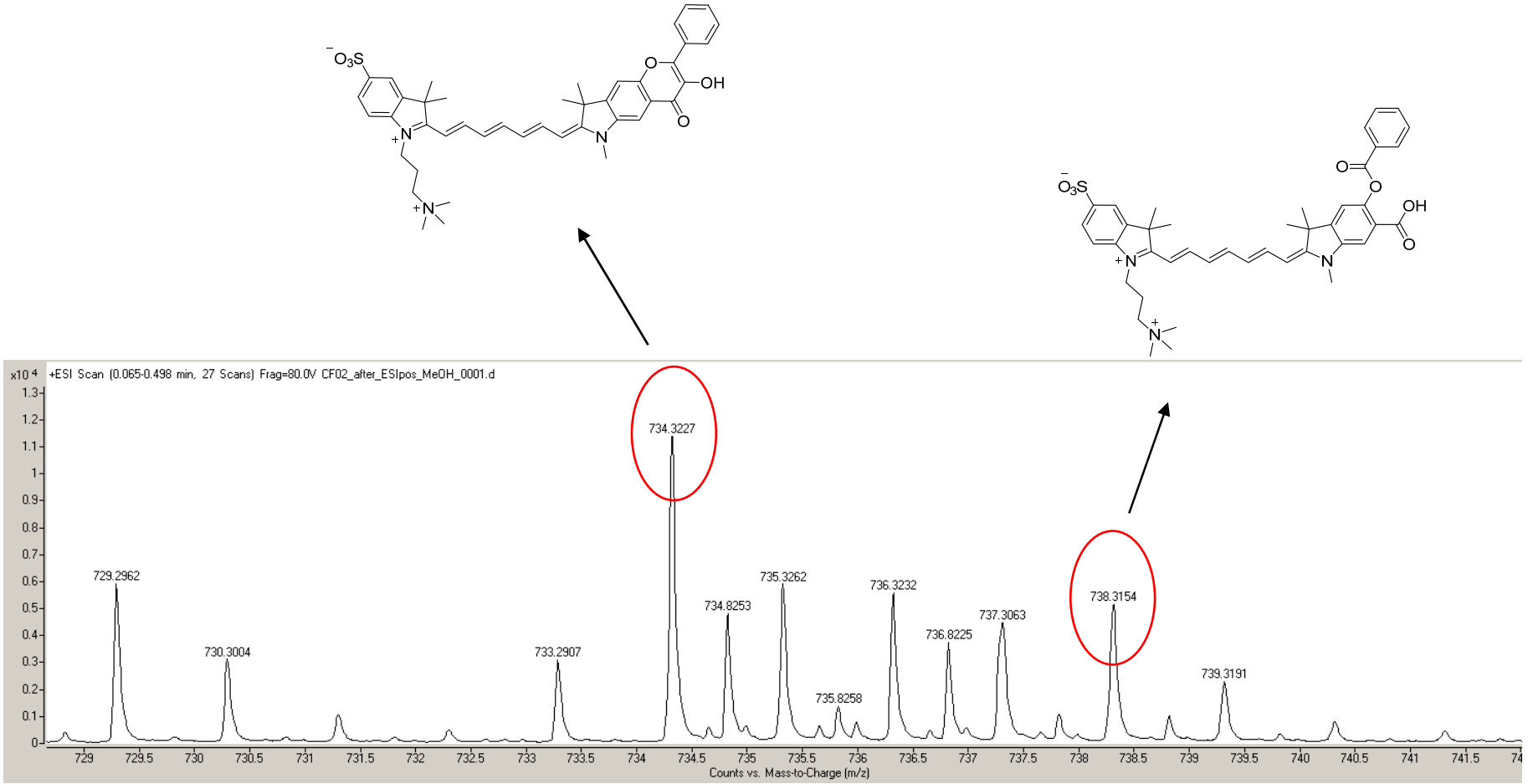

Figure S31. HRMS (ESI^+) of **4** in aerated methanol irradiated at 770 nm.

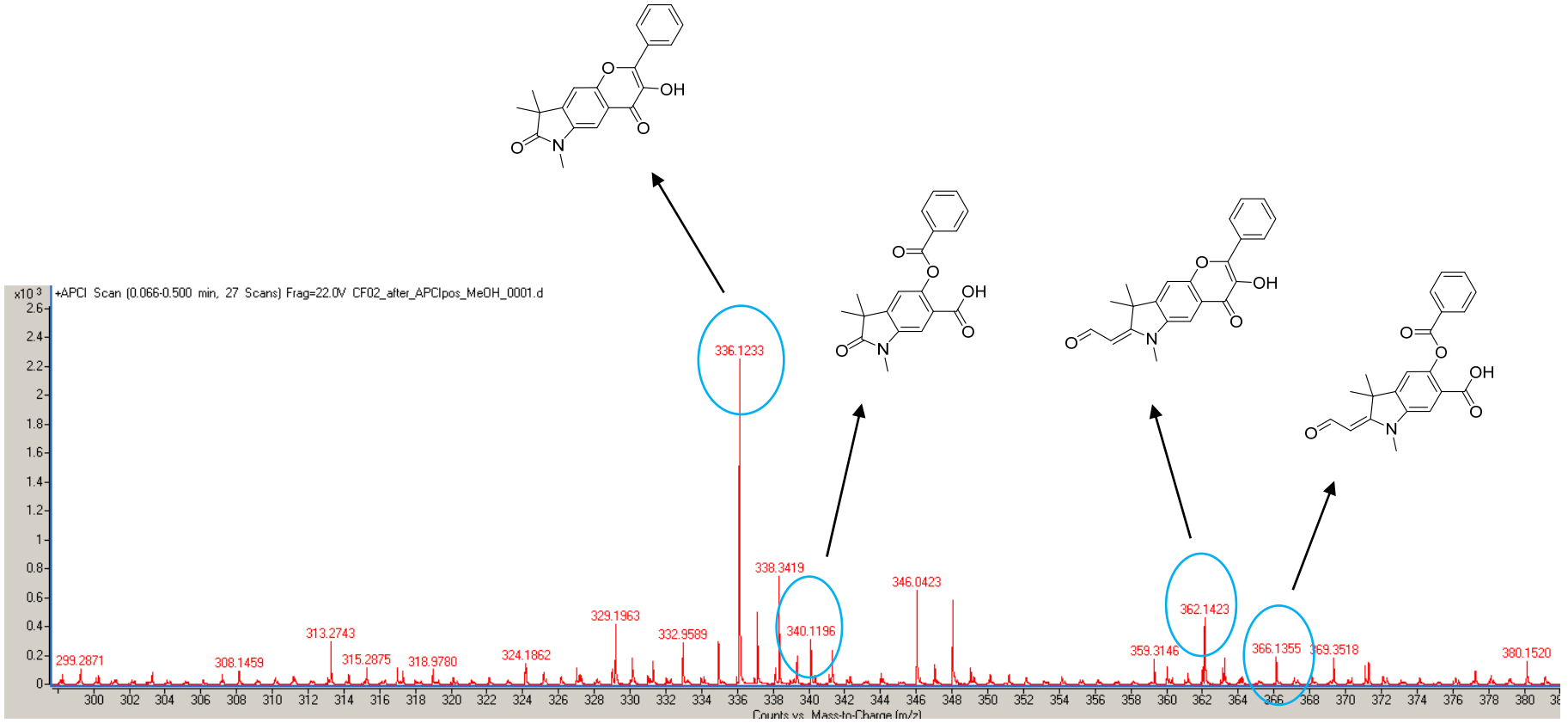

Figure S32. HRMS (ESI^+) of **4** in aerated methanol irradiated at 770 nm.

Absorption and Emission Spectra in Methanol

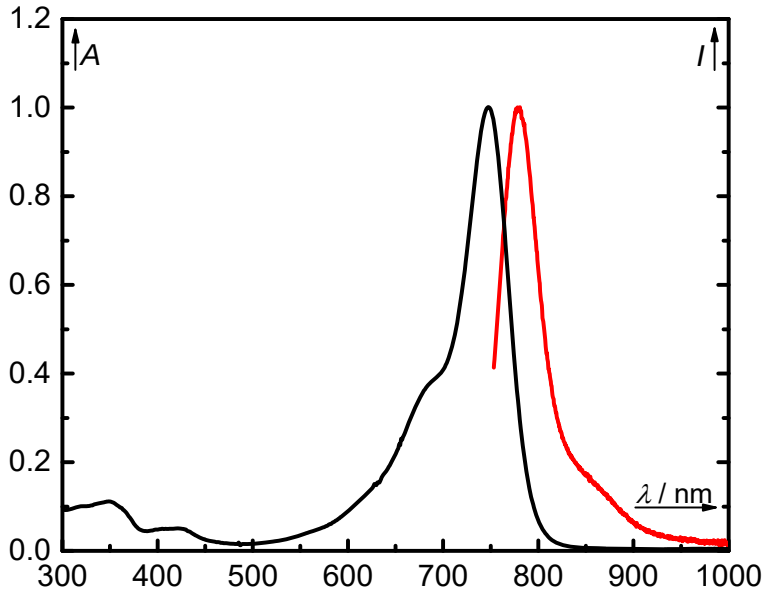

Figure S33. Normalized absorption (black) and emission (red) spectra of **3** in methanol.

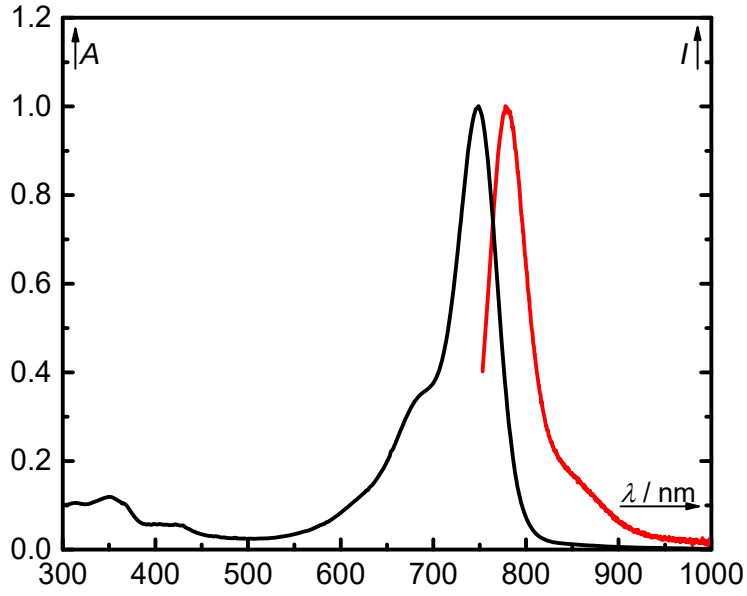

Figure S34. Normalized absorption (black) and emission (red) spectra of **4** in methanol.

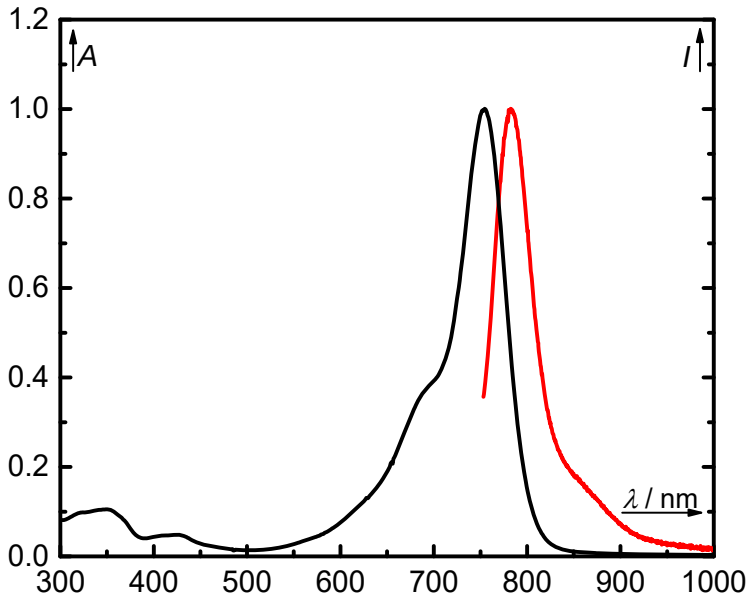

Figure S35. Normalized absorption (black) and emission (red) spectra of **5** in methanol.

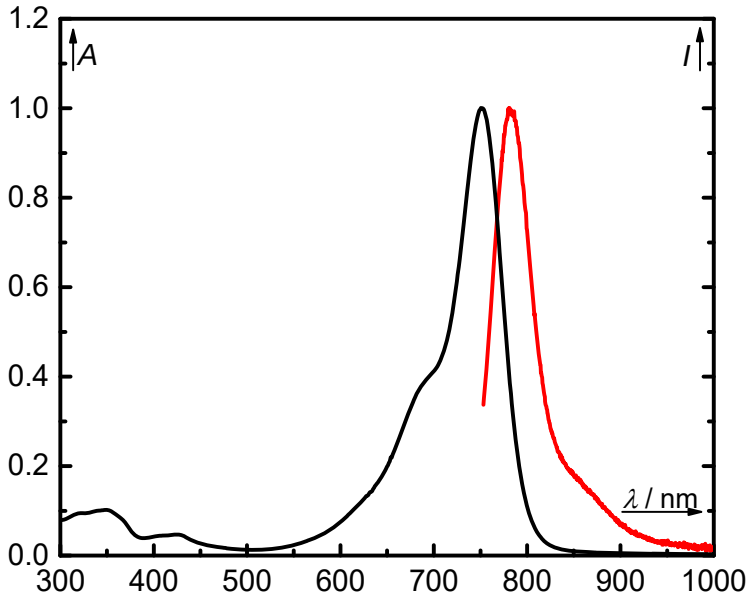

Figure S36. Normalized absorption (black) and emission (red) spectra of **7** in methanol.

Photochemistry in Methanol

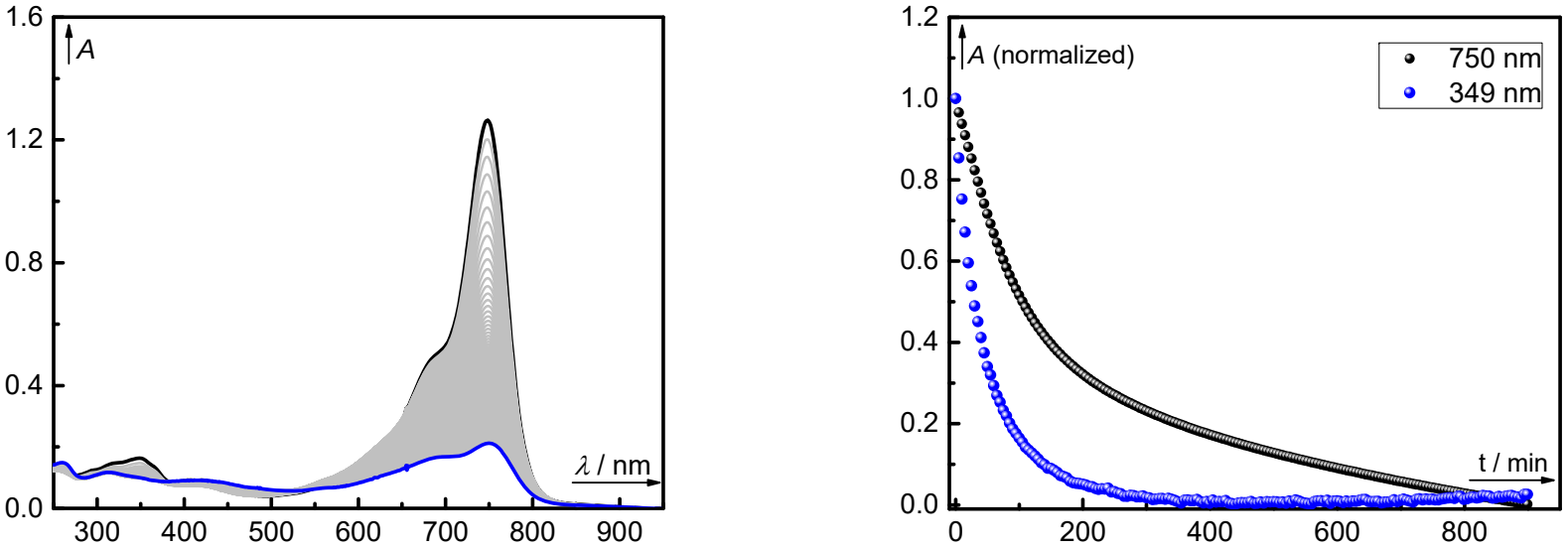

Figure S37. Left: irradiation of **3** (c ~1.0 × 10^{-5} M) at 770 nm in methanol monitored by UV-vis spectroscopy in 10-min intervals (black to blue). Right: kinetic traces of **3** at 750 nm (black, normalized) and 349 nm (blue, normalized).

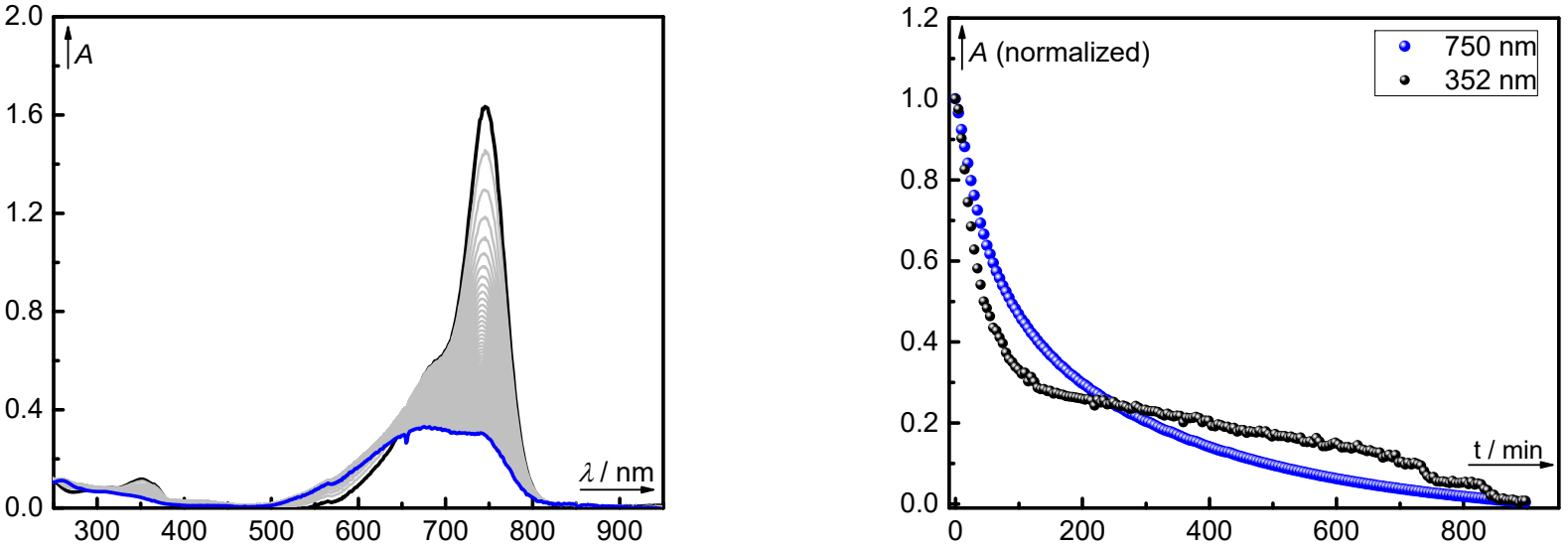

Figure S38. Left: irradiation of **4** (c ~1.0×10^{-5} M) at 770 nm in methanol monitored by UV-vis spectroscopy in 10-min intervals (black to blue). Right: kinetic traces of **4** at 750 nm (black, normalized) and 352 nm (blue, normalized).

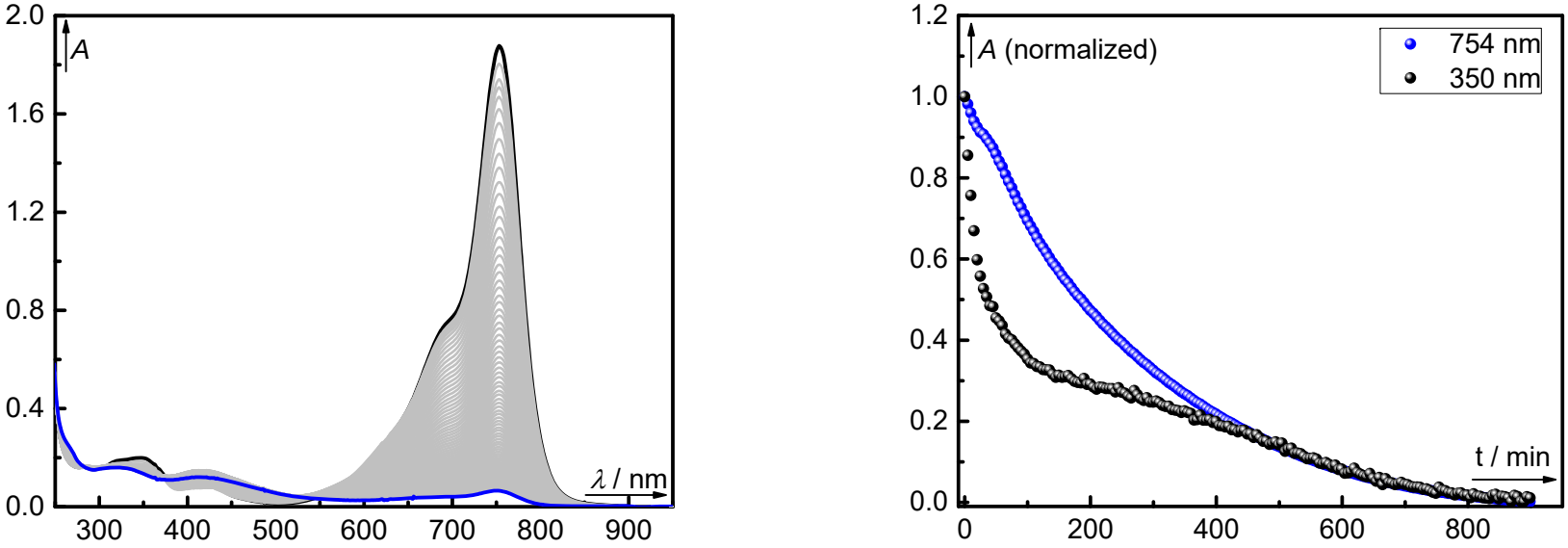

Figure S39. Left: irradiation of **5** (c ~1.0 × 10^{-5} M) at 770 nm in methanol (10% DMSO) monitored by UV-vis spectroscopy in 10-min intervals (black to blue). Right: kinetic traces of **5** at 754 nm (black, normalized) and 350 nm (blue, normalized).

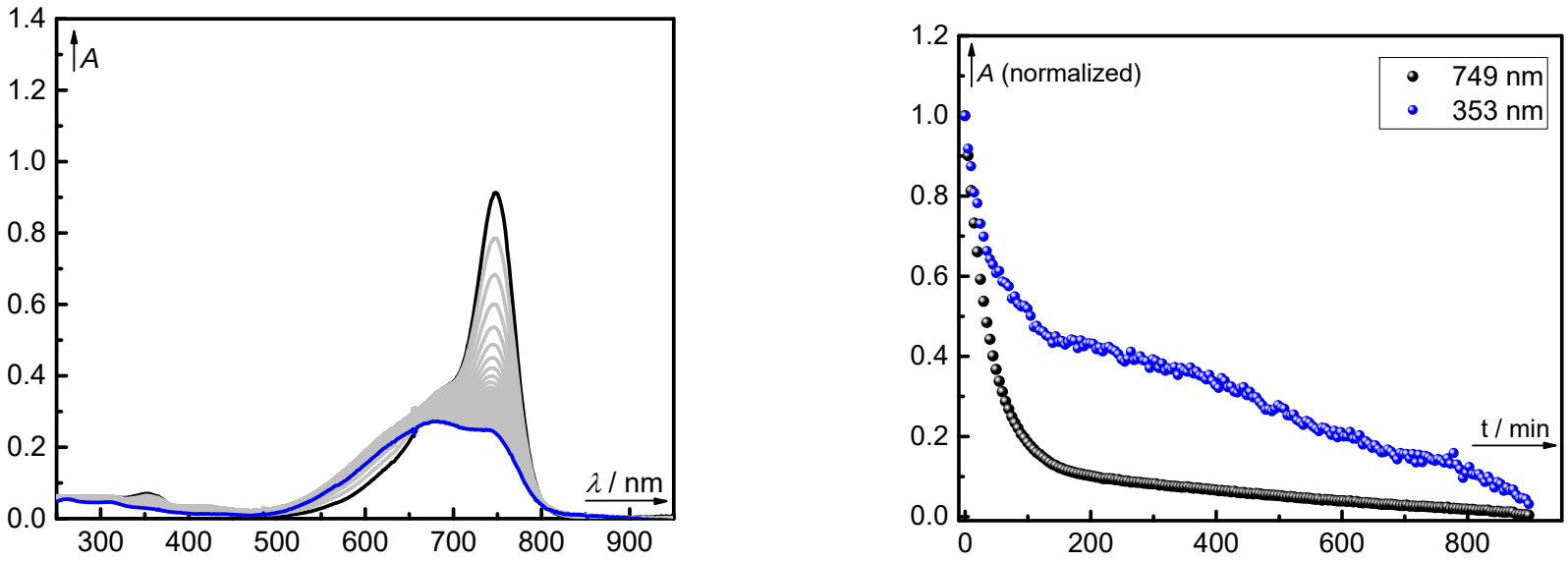

Figure S40. Left: irradiation of **6** (c ~1.0 × 10^{-5} M) at 770 nm in methanol monitored by UV-vis spectroscopy in 10-min intervals (black to blue). Right: kinetic traces of **6** at 749 nm (black, normalized) and 353 nm (blue, normalized).

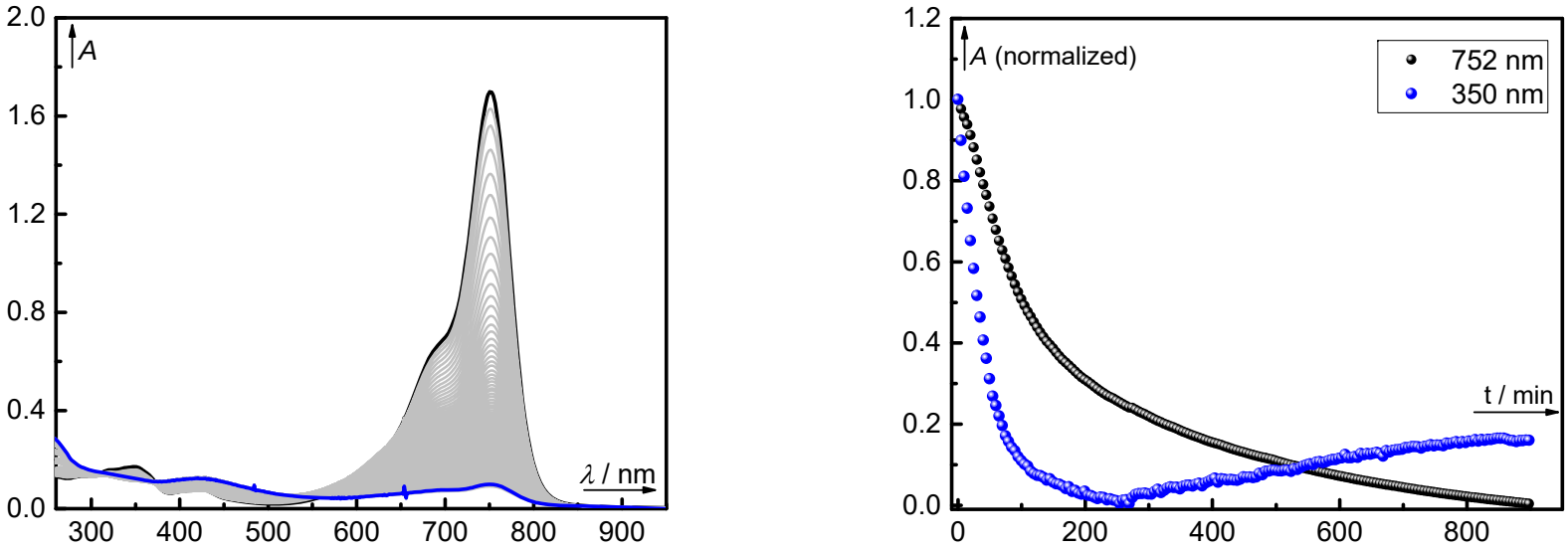

Figure S41. Left: irradiation of **7** (c ~1.0 × 10^{-5} M) at 770 nm in methanol (10% DMSO) monitored by UV-vis spectroscopy in 10-min intervals (black to blue). Right: kinetic traces of **7** at 752 nm (black, normalized) and 350 nm (blue, normalized).

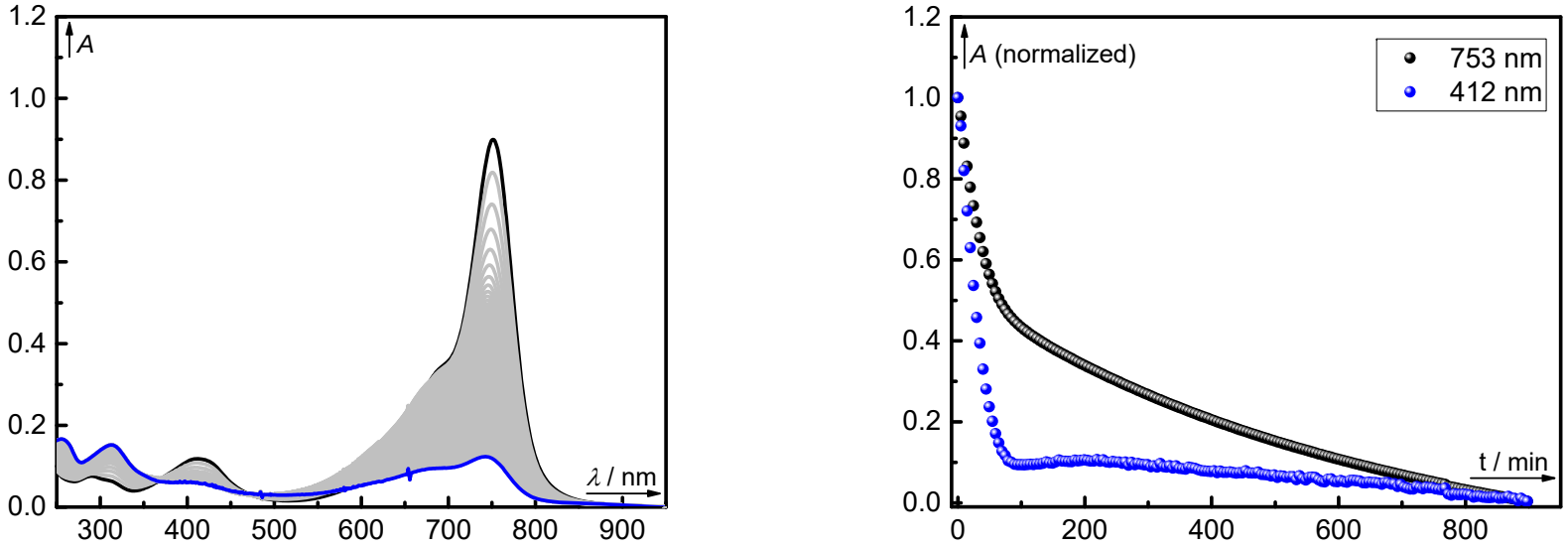

Figure S42. Left: Irradiation of **8** (c ~1.0 × 10^{-5} M) at 770 nm in methanol (5% DMSO) monitored by UV-vis spectroscopy in 10-min intervals (black to blue). Right: kinetic traces of **8** at 753 nm (black, normalized) and 412 nm (blue, normalized).

Kinetic Traces in Aerated and Degassed Methanol

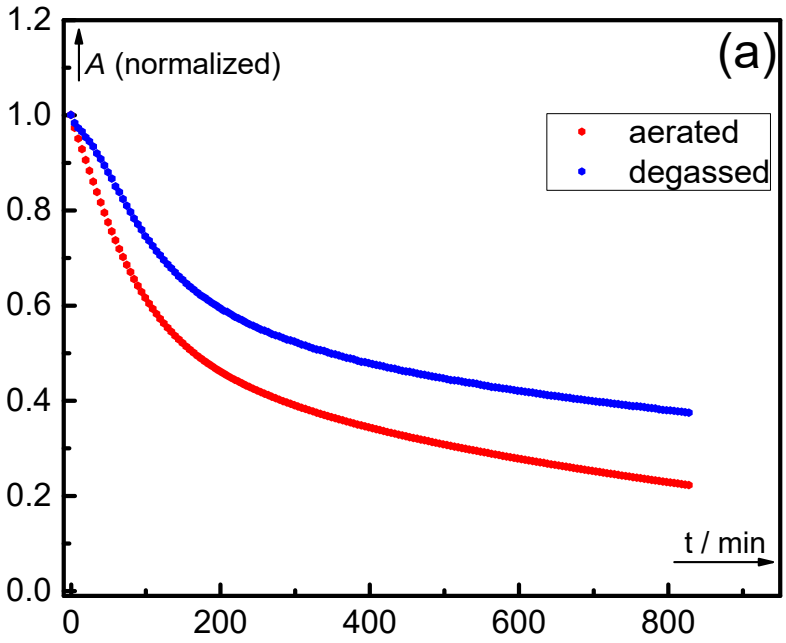

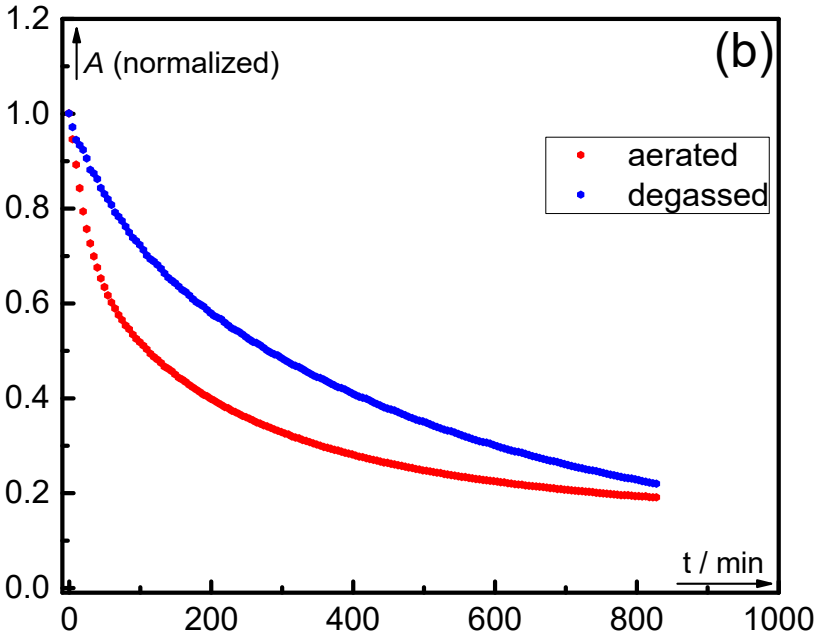

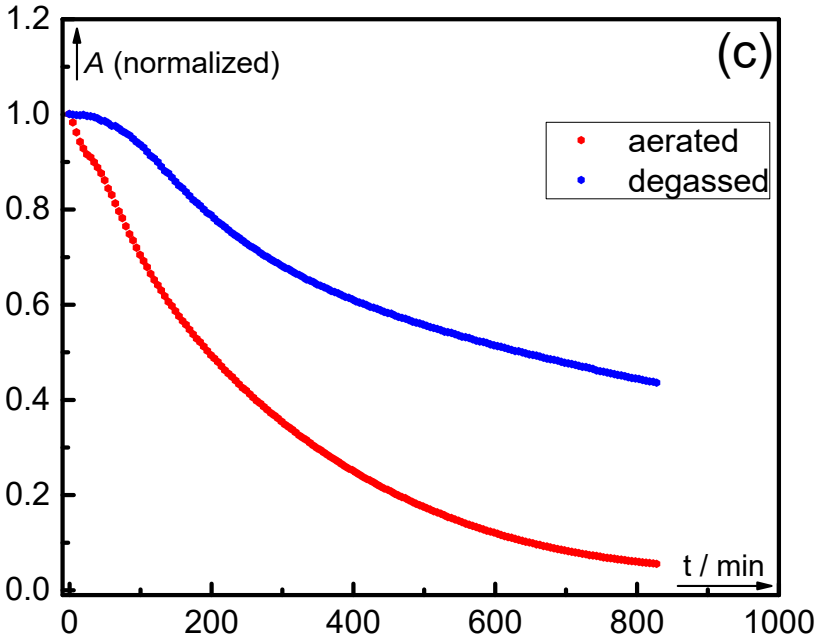
(c)
A (normalized)
aerated
degassed
t / min
1.2
1.0
0.8
0.6
0.4
0.2
0.0
0
200
400
600
800
1000

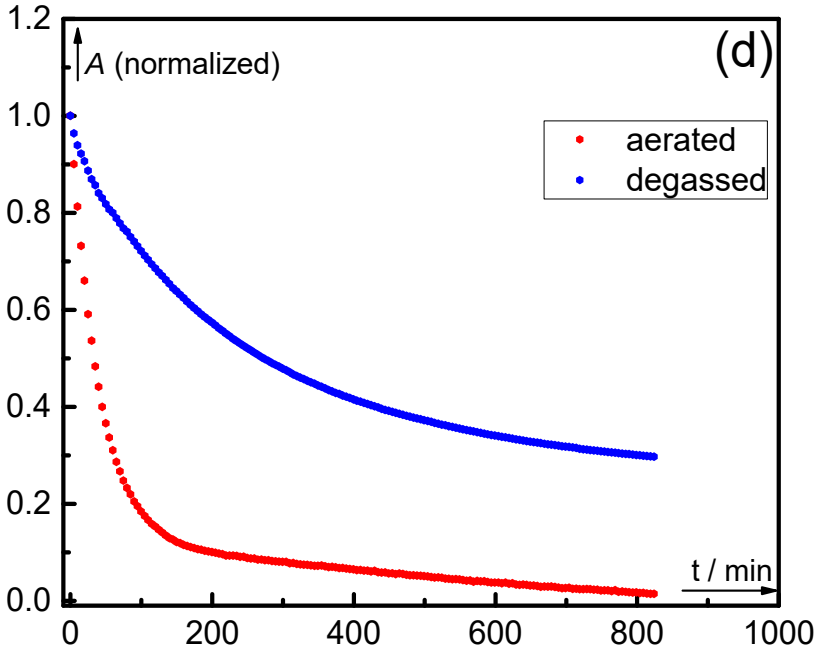
(d)
A (normalized)
aerated
degassed
t / min
1.2
1.0
0.8
0.6
0.4
0.2
0.0
0
200
400
600
800
1000

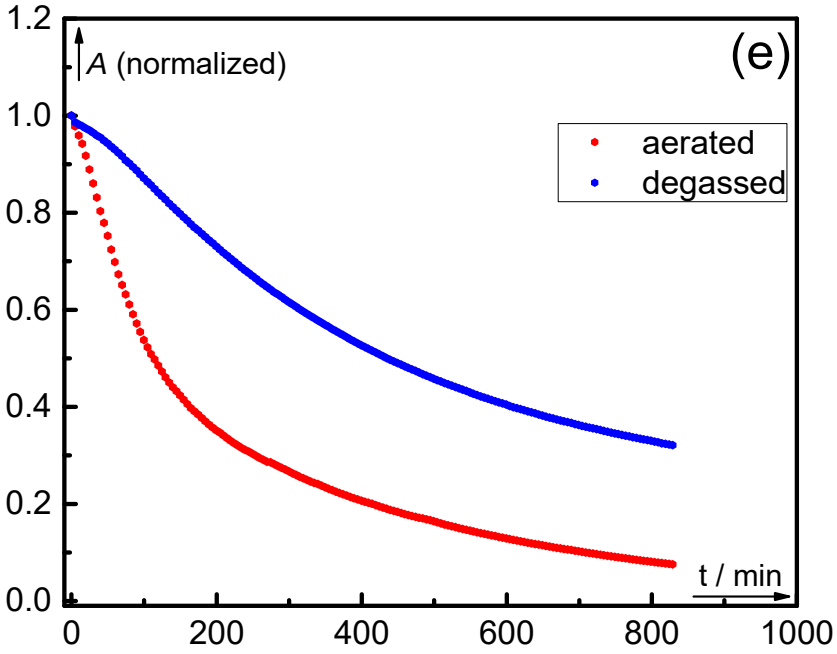

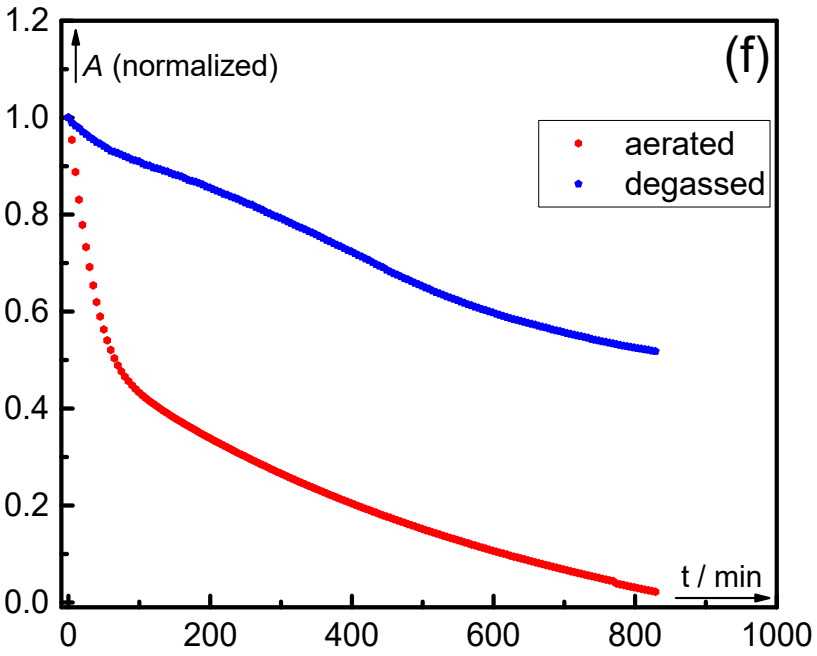

Figure S43. Kinetic traces monitored at the absorption maxima for (a) **3**, (b) **4**, (c) **5**, (d) **6**, (e) **7**, and (f) **8** in aerated (red) and degassed (blue, Ar bubbling) methanol irradiated at 770 nm. Normalized to $A = 1.0$ at $t = 0$ min.

Stability in the Dark

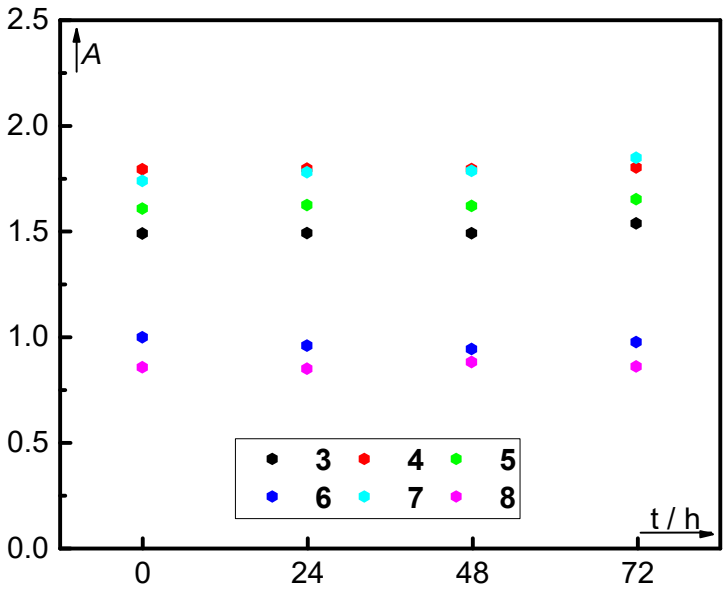

Figure S44. Stability in the dark at room temperature for compounds **3** (black), **4** (red), **5** (green), **6** (blue), **7** (cyan), and **8** (magenta) in methanol. Monitored by absorption spectrometer.

Absorption Spectra in PBS with Different Amounts of DMSO

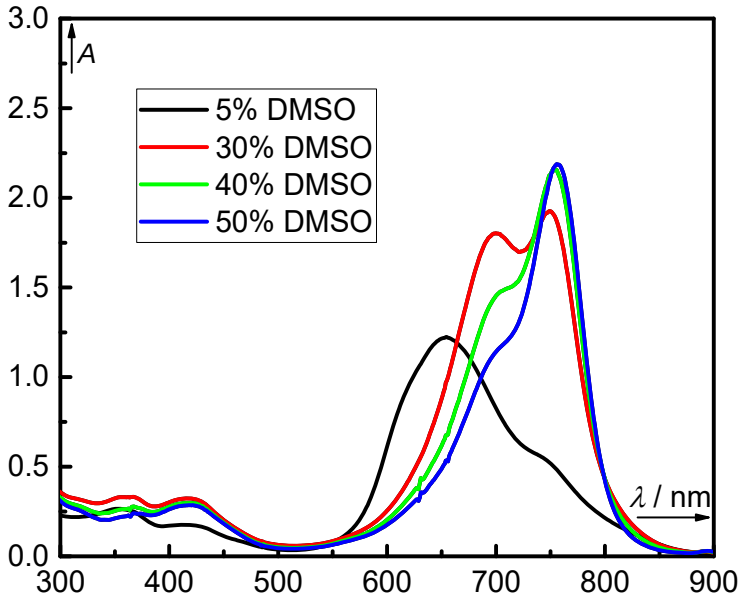

Figure S45. Absorption spectra of **3** in the DMSO/PBS with different amounts of DMSO.

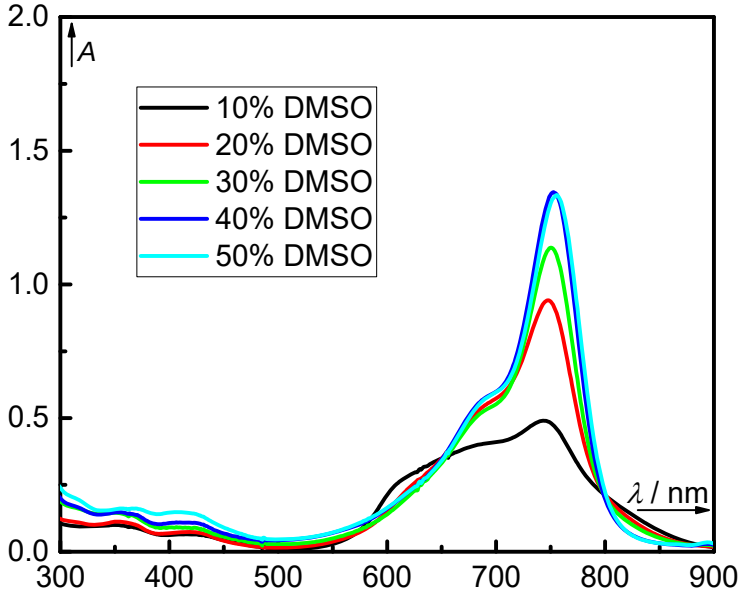

Figure S46. Absorption spectra of **4** in the DMSO/PBS with different amounts of DMSO.

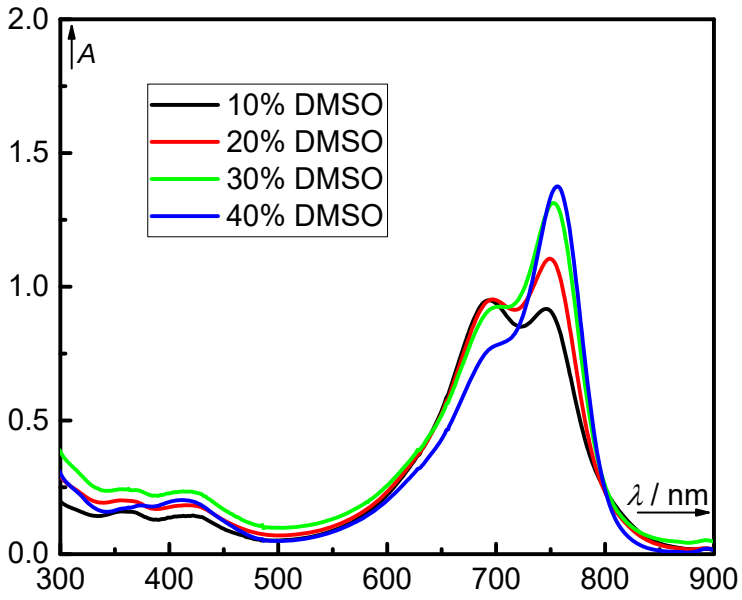

Figure S47. Absorption spectra of **6** in the DMSO/PBS with different amounts of DMSO.

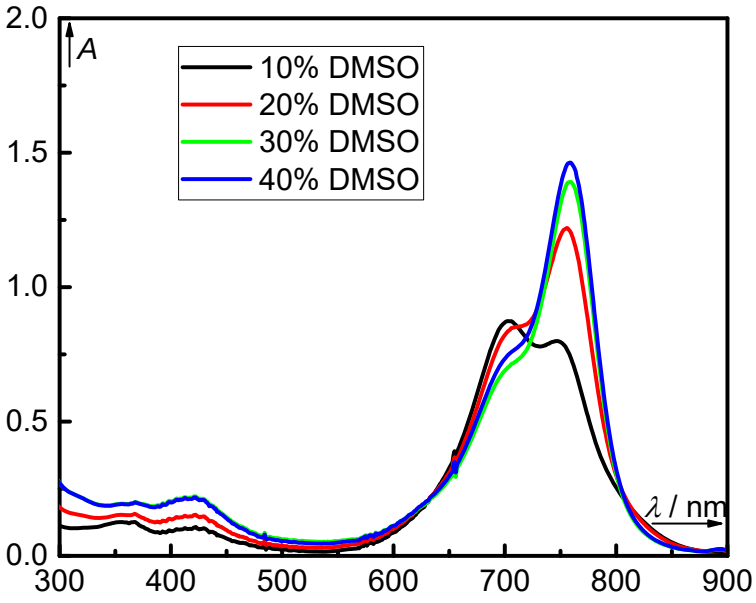

Figure S48. Absorption spectra of **7** in the DMSO/PBS with different amounts of DMSO.

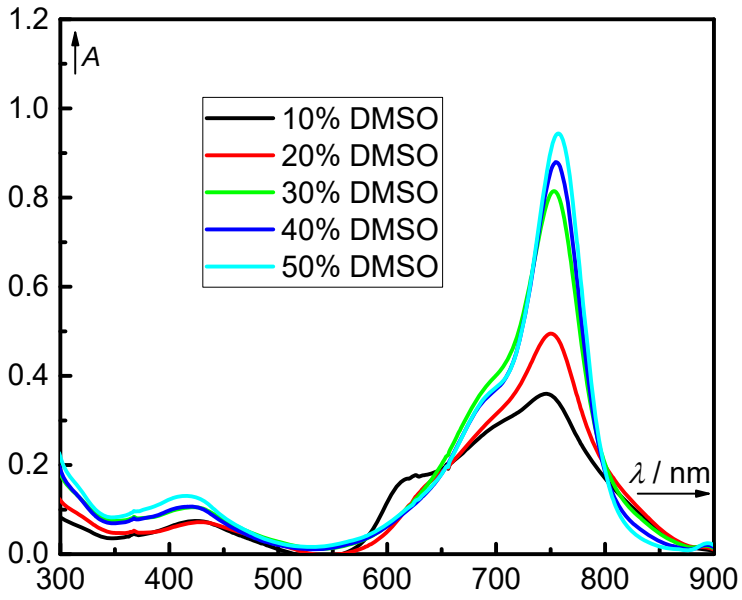

Figure S49. Absorption spectra of **8** in the DMSO/PBS with different amounts of DMSO.

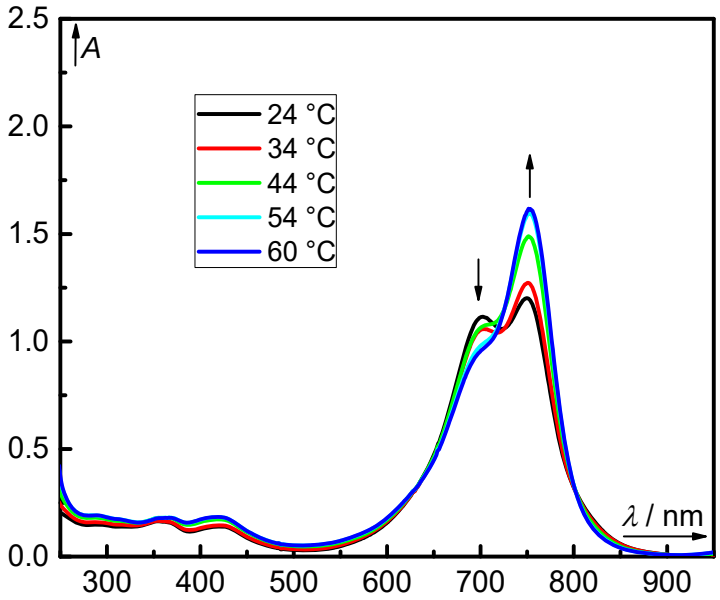

Figure S50. Absorption spectra of **5** in 20% DMSO/PBS at different temperatures.

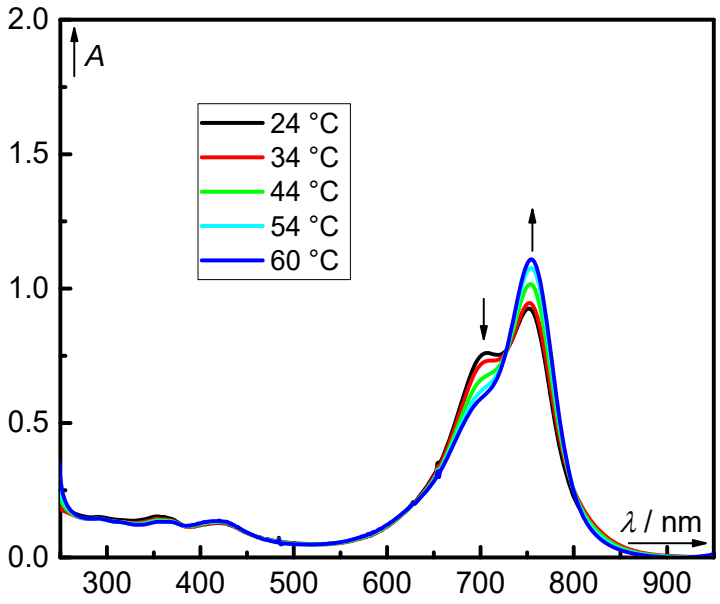

Figure S51. Absorption spectra of **7** in 20% DMSO/PBS at different temperatures.

HPLC Chromatography

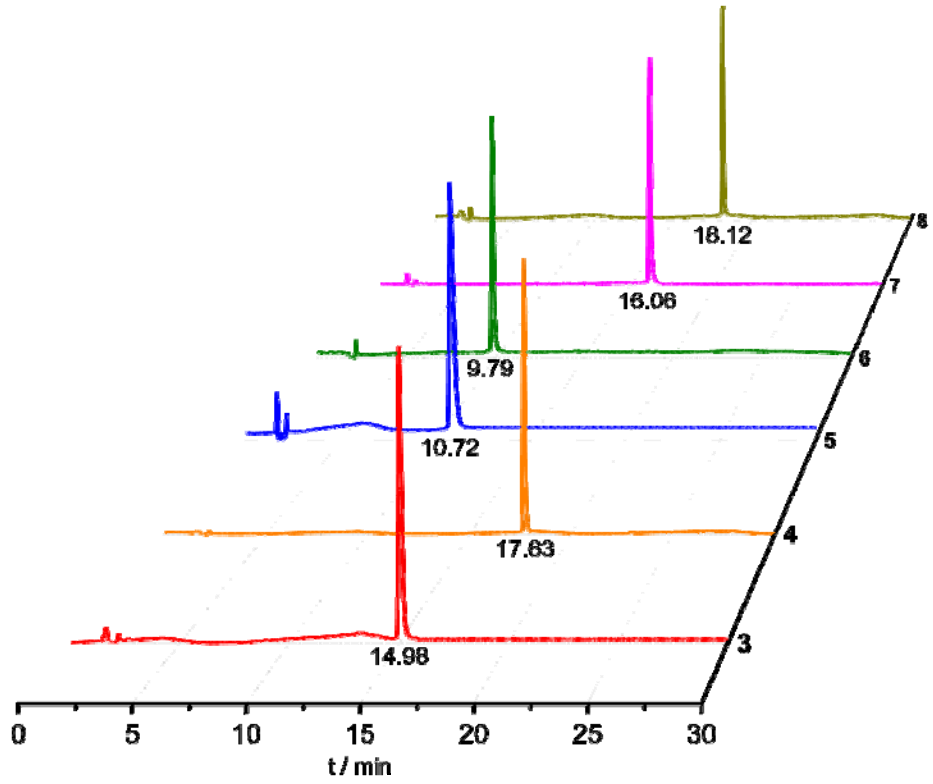

Figure S52. HPLC spectra of **3**–**8**. An HPLC method: a reversed-phase column, a mixture of acetonitrile and water (with 0.1% trifluoroacetic acid; from 20:80 to 80:20 in 30 min) was used as an eluent (1 mL min^{-1}).

Host-Guest Complex of 6 and Cucurbit[7]uril

A solution of **6** (10 μM, 3 mL) was prepared in a matched 1.0 cm quartz cuvette. The spectra were recorded after every titration with CB7 (0−4 equiv.) by UV−vis spectroscopy. The addition of CB7 results in a significant absorbance increase at 750 nm and a decrease at 690 nm. However, the absorbance at 750 nm was still increasing after the addition of 1.0 equivalent of CB7 and nearly stopped upon the addition of 2.0 equivalents of CB7 (Figure 2 and S53). The data were fitted (global analysis) with a 2 : 1 host−guest complex binding model[7] with the equations (3) and (4) (Figure S53).

The complex model of CB7 (H) with **6** (G) was calculated according to:

$$H + G \overset{K_1}{\rightleftharpoons} HG \qquad (1)$$

$$H + HG \overset{K_2}{\rightleftharpoons} H_2G \qquad (2)$$

$$[G_0] = [G] + [HG] + [H_2G] \qquad (3)$$

$$[H_0] = [H] + [HG] + 2[H_2G] \qquad (4)$$

where K_1 and K_2 are the association constants, $[G_0]$ is the total concentration of a guest (**6**); $[H_0]$ is the total concentration of a host (CB7), [G] is the concentration of a free guest, [HG] is the concentration of a complex HG; $[H_2G]$ is the concentration of a complex H_2G, and [H] is the concentration of a free host.

The association constants K_1 and K_2 were determined to be $(2.87 \pm 0.03) \times 10^7$ M^{-1} and $(8.26 \pm 0.05) \times 10^5$ M^{-1}, respectively. However, due to the existence of aggregate (dimer) of **6**, the binding mechanism is complex. Our fitting was carried out by considering that **6** exists as a monomer.

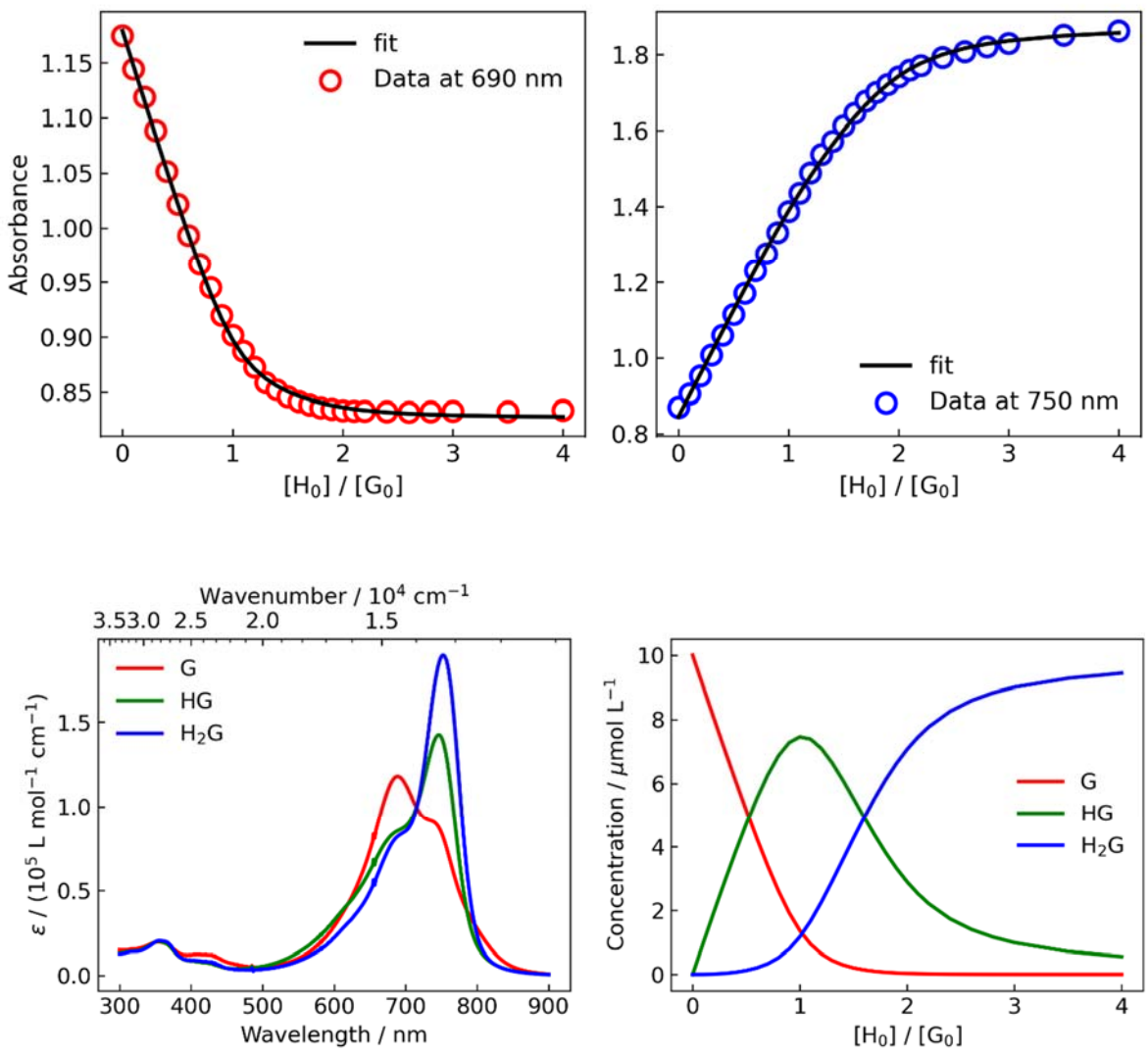

Figure S53. Top: plot of the absorbance at 690 nm (left) and 750 nm (right) as a function of the amount of CB7 added. The solid line represents the fit of the data to a 2 : 1 binding model. Bottom: simulated molar absorption coefficients of **6** (G) and host-guest complexes (HG and H_2G, left) and a plot of the concentrations for G, HG, and H_2G (Eqs. 1–4) as a function of the amount of CB7 added.

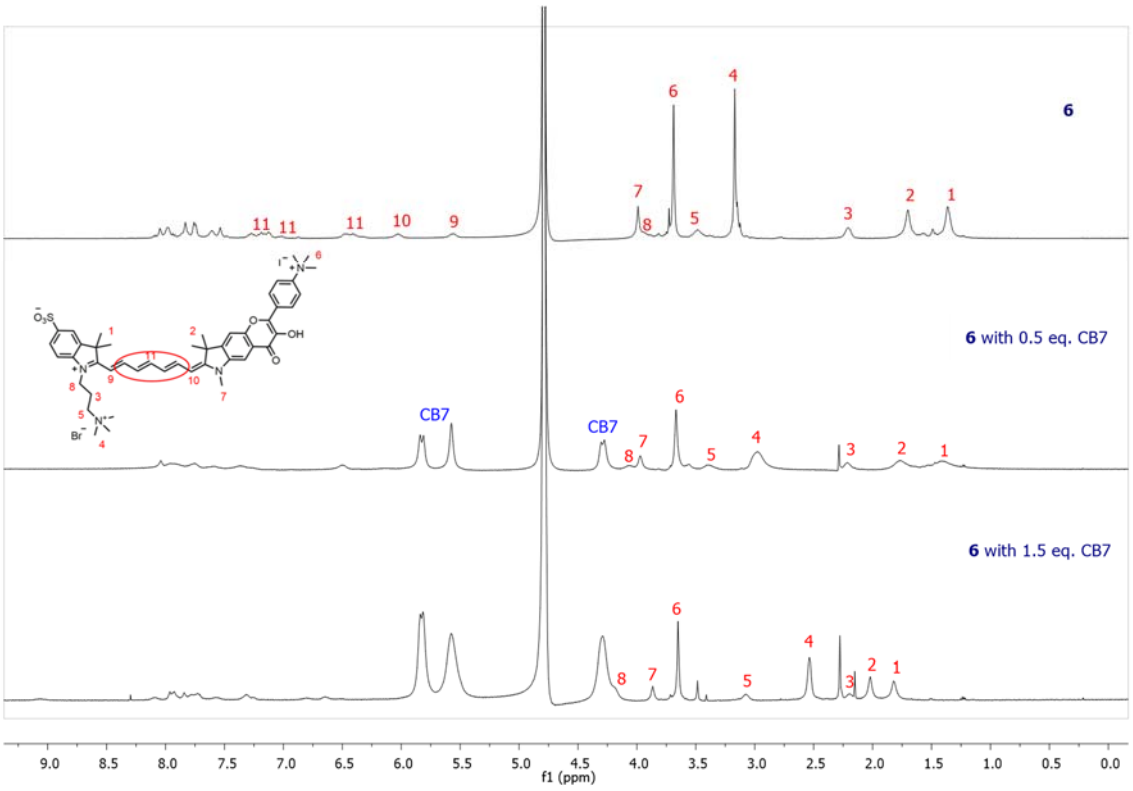

Figure S54. ^{1}H NMR (500 MHz, D_2O) spectra of **6** ($c = 1.4 \times 10^{-3}$ M) in the presence of 0, 0.5, and 1.5 equiv. of CB7.

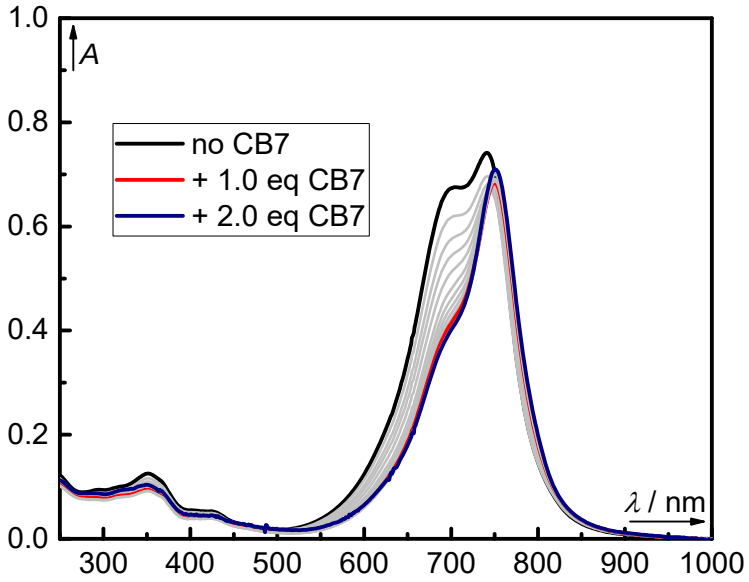

Figure S55. Effects of the addition of CB7 on the UV−vis absorption spectra of **4** in water.

Cytotoxicity of 3–8

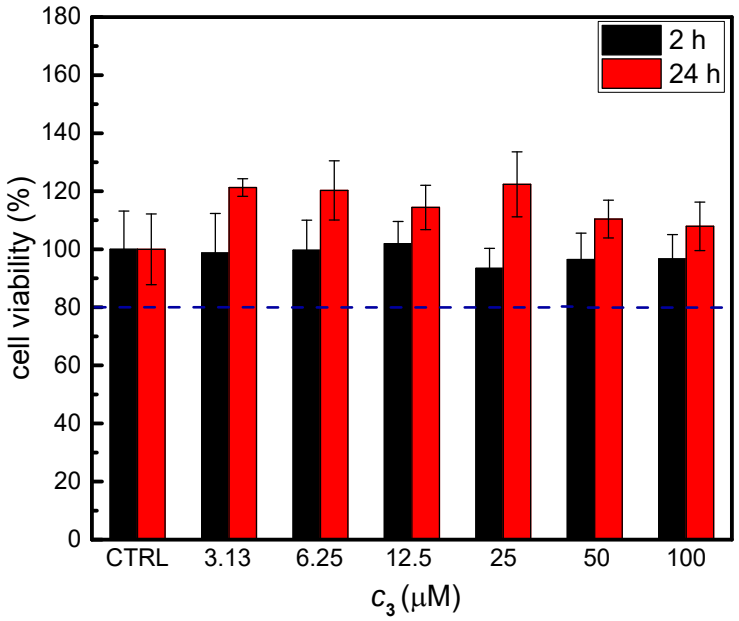

Figure S56. The effect of **3** on the viability of HepG2 cells. Cytotoxicity of individual compounds was assessed by an MTT test after treatment of HepG2 cells with solutions of flavonol hybrids in MEM media for 2 (black column) or 24 h (red column). A dashed line at 80% viability represents a start point for the cytotoxicity assessment. The values are expressed as % of untreated controls (CTRL).

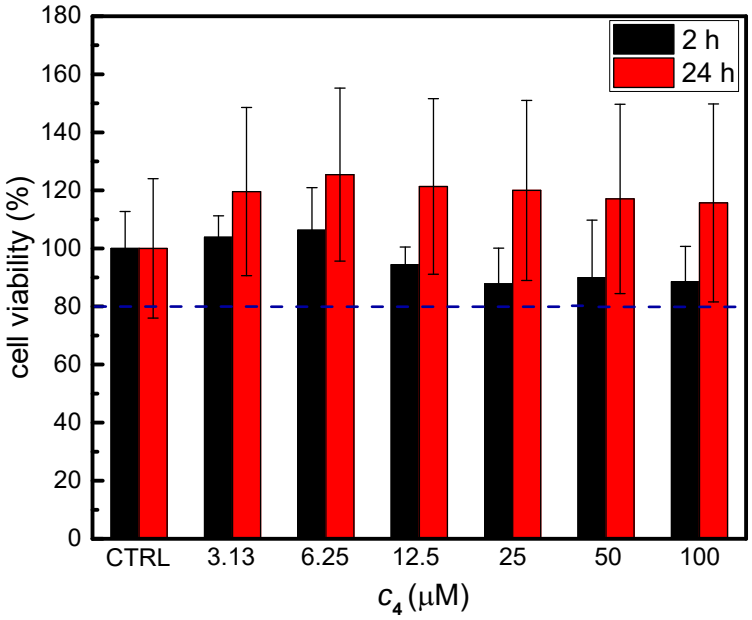

Figure S57. The effect of **4** on the viability of HepG2 cells. Cytotoxicity of the individual compounds was assessed by an MTT test after treatment of HepG2 cells with solutions of flavonol hybrids in MEM media for 2 (black column) or 24 h (red column). A dashed line at 80% viability represents a start point for the cytotoxicity assessment. The values are expressed as % of untreated controls (CTRL).

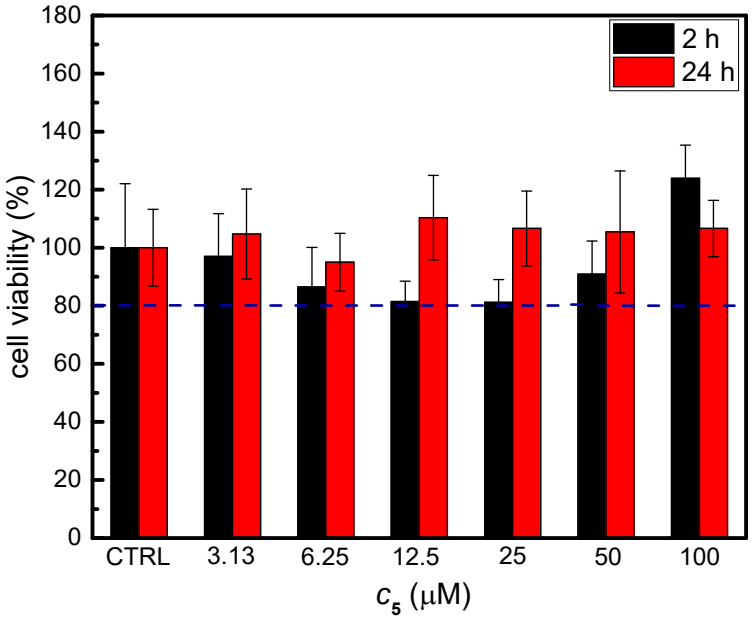

Figure S58. The effect of **5** on the viability of HepG2 cells. Cytotoxicity of the individual compounds was assessed by an MTT test after treatment of HepG2 cells with solutions of flavonol hybrids in MEM media for 2 (black column) or 24 h (red column). A dashed line at 80% viability represents a start point for the cytotoxicity assessment. The values are expressed as % of untreated controls (CTRL).

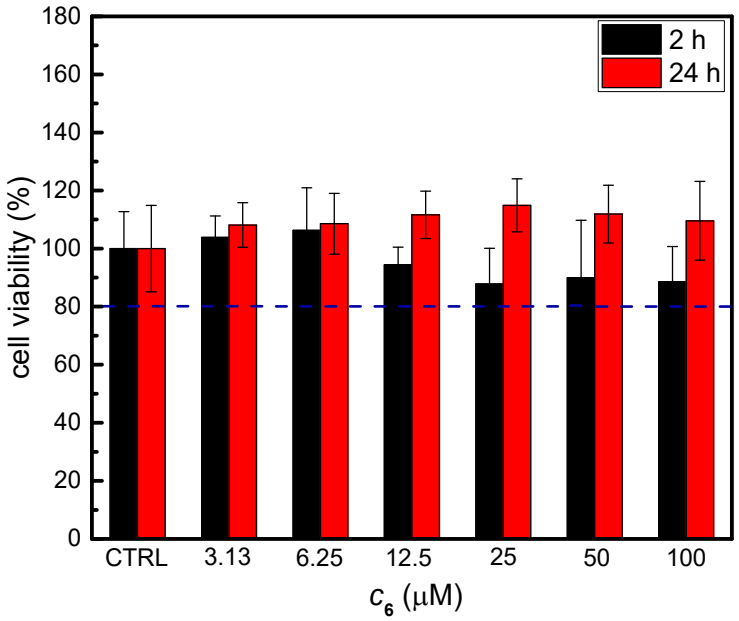

Figure S59. The effect of **6** on the viability of HepG2 cells. Cytotoxicity of the individual compounds was assessed by an MTT test after treatment of HepG2 cells with solutions of flavonol hybrids in MEM media for 2 (black column) or 24 h (red column). A dashed line at 80% viability represents a start point for the cytotoxicity assessment. The values are expressed as % of untreated controls (CTRL).

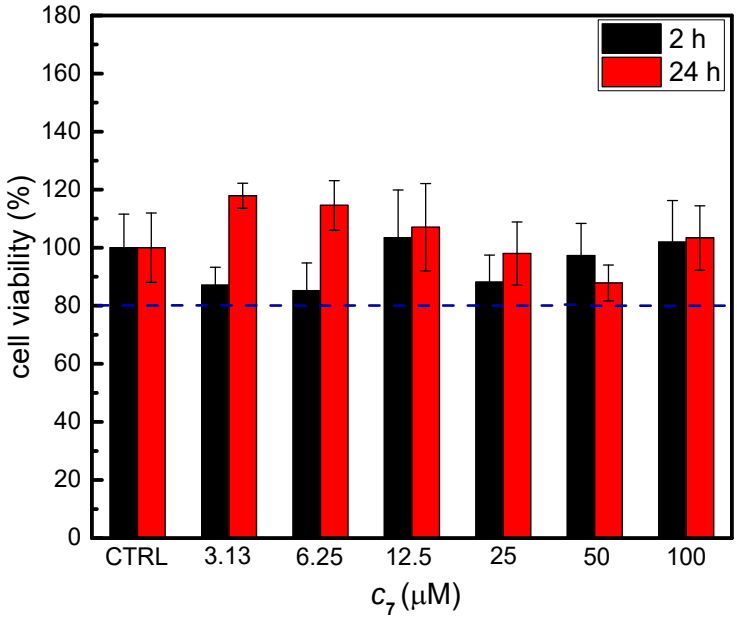

Figure S60. The effect of **7** on the viability of HepG2 cells. Cytotoxicity of the individual compounds was assessed by an MTT test after treatment of HepG2 cells with solutions of flavonol hybrids in MEM media for 2 (black column) or 24 h (red column). A dashed line at 80% viability represents a start point for the cytotoxicity assessment. The values are expressed as % of untreated controls (CTRL).

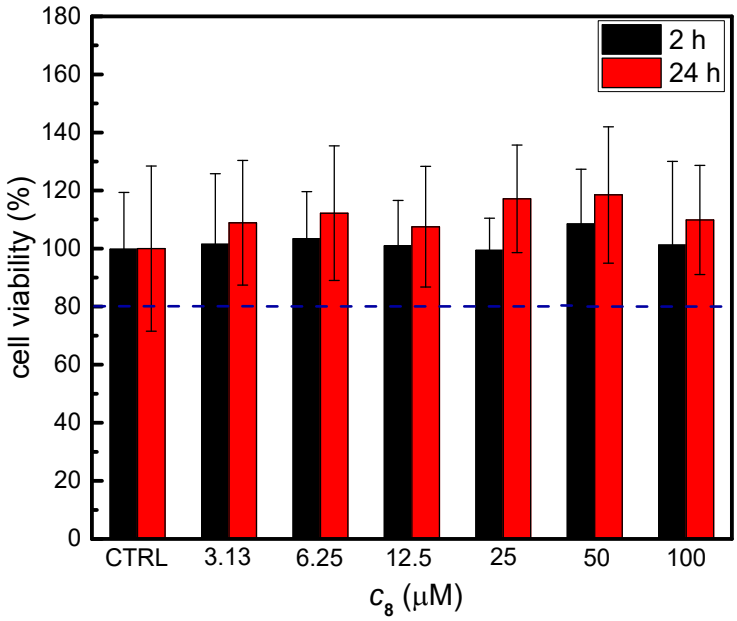

Figure S61. The effect of **8** on the viability of HepG2 cells. Cytotoxicity of the individual compounds was assessed by an MTT test after treatment of HepG2 cells with solutions of flavonol hybrids in MEM media for 2 (black column) or 24 h (red column). A dashed line at 80% viability represents a start point for the cytotoxicity assessment. The values are expressed as % of untreated controls (CTRL).

Fluoresence Measurements in Cells

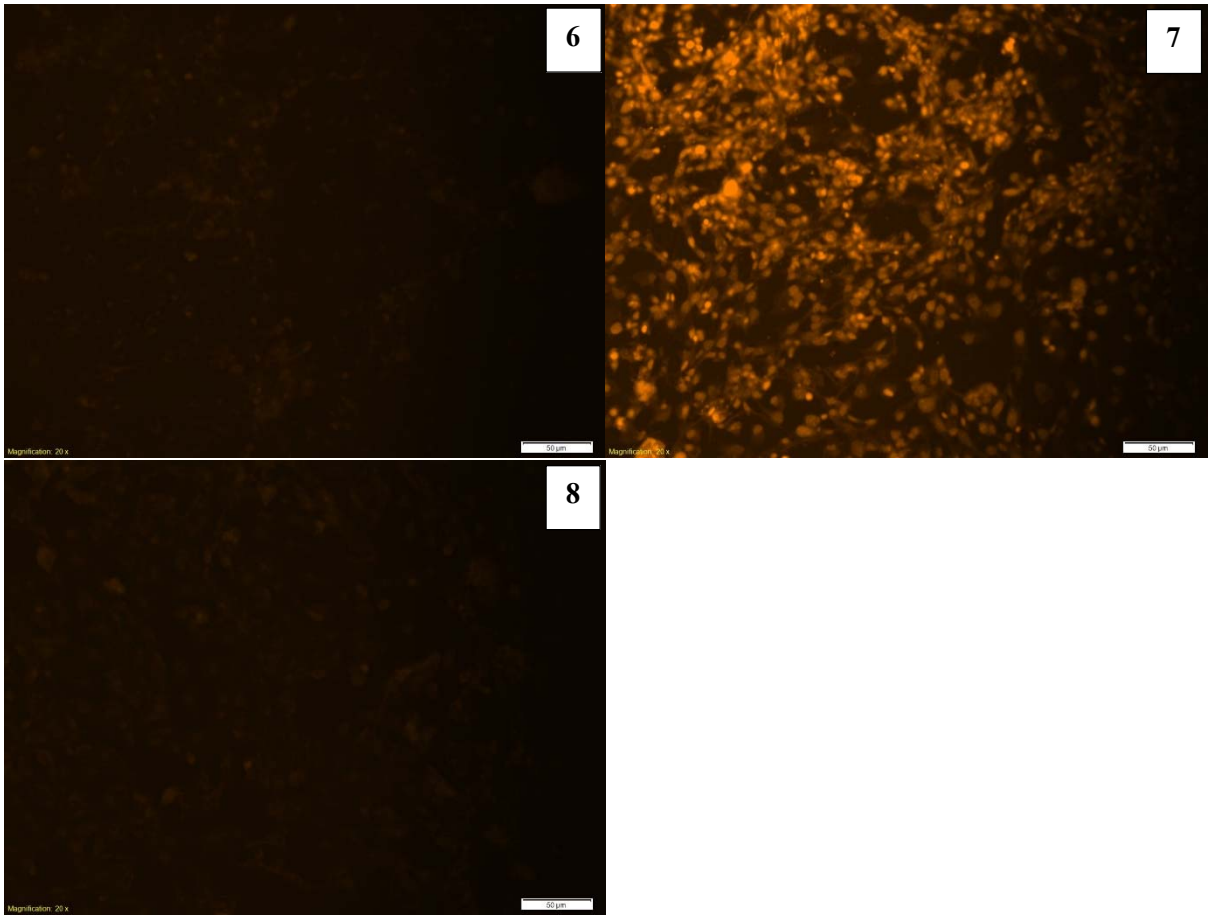

Figure S62. Fluorescent microscopy images of HepaRG cells treated with **6**, **7**, or **8** (c = 100 µmol/L) for 24 h. The scale bar represents 50 µm. The fixed exposure time was set for 500 ms to compare the fluorescence intensity of individual treatments. Clear cellular staining with intense fluorescence was observed for treatment with **7**, whereas a very weak fluorescence was detected for **6** and **8**.

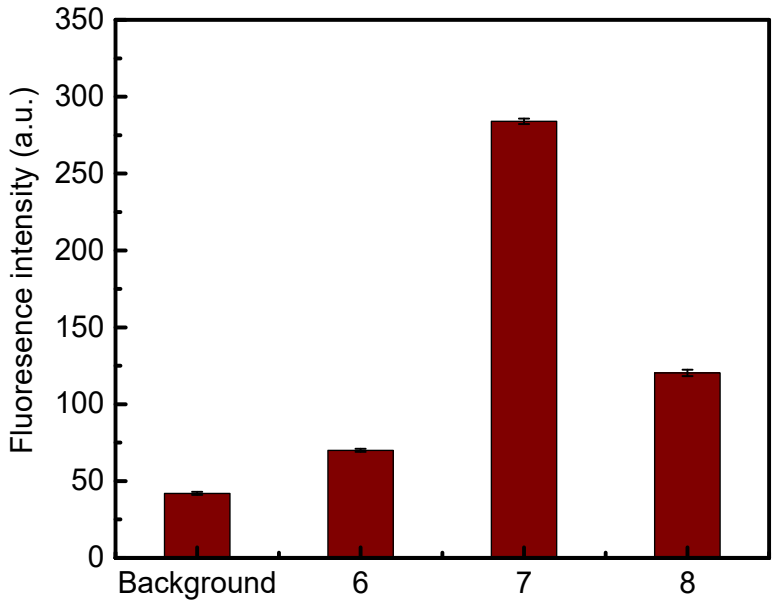

Figure S63. Comparison of fluorescence intensity of **6**, **7**, and **8** in cell culture media. **6**, **7**, or **8** were dissolved in colorless MEM medium (c = 100 µmol/L) and the fluorescence intensity (λ_{ex} = 530 nm, λ_{em} = 590 nm) was measured using a microplate reader. Fluorescence of MEM served as a negative control (background). The values represent the mean ± SD (n = 3).

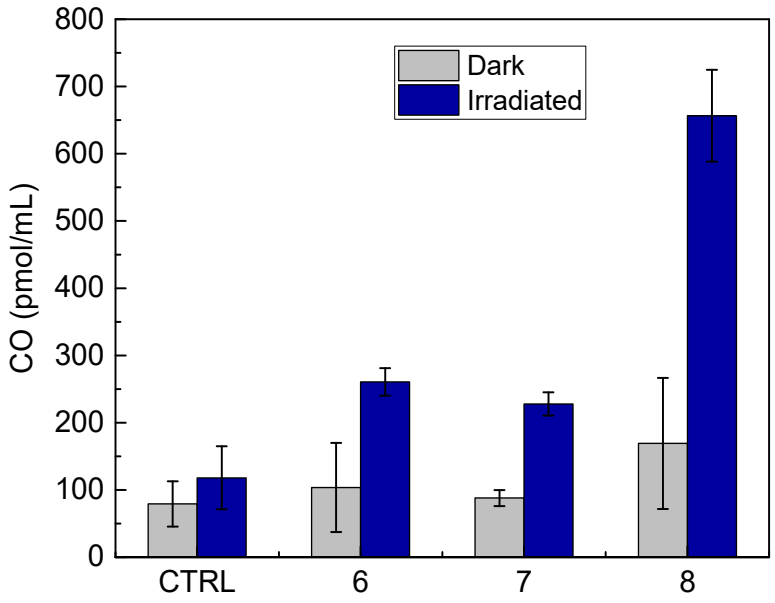

Figure S64. The CO content in medium. HepaRG cells were incubated with **6**, **7**, or **8** (c = 50 µmol L^{-1} in colorless MEM medium) in 10-cm Petri dishes. Cells were either kept in the dark or irradiated with white light (I = 600 mW cm^{-2}). After 30 min, the CO content in the medium was measured using GC/RGA. The medium without active compound was used as a control (CTRL).

References

1. M. Martínek, L. Filipová, J. Galeta, L. Ludvíková and P. Klán, *Org. Lett.*, 2016, **18**, 4892-4895.
2. N. S. James, Y. Chen, P. Joshi, T. Y. Ohulchanskyy, M. Ethirajan, M. Henary, L. Strekowsk and R. K. Pandey, *Theranostics*, 2013, **3**, 692-702.
3. L. Stackova, M. Russo, L. Muchová, V. Orel, L. Vitek, P. Stacko and P. Klan, *Chem. Eur. J.*, 2020, **26**, 13184-13190.
4. M. Russo, V. Orel, P. Stacko, M. Sranková, L. Muchová, L. Vitek and P. Klan, *J. Org. Chem.*, 2022, **87**, 4750–4763.
5. H. J. Vreman and D. K. Stevenson, *Anal. Biochem.*, 1988, **168**, 31-38.
6. A. Bunschoten, D. M. van Willigen, T. Buckle, N. S. van den Berg, M. M. Welling, S. J. Spa, H.-J. Wester and F. W. B. van Leeuwen, *Bioconjugate Chem.*, 2016, **27**, 1253-1258.
7. P. Thordarson, *Chem. Soc. Rev.*, 2011, **40**, 1305-1323.